JEFFREY NEAL AGAR
Biological Iron-Sulfur Cluster Assembly
(Under the direction of MICHAEL K. JOHNSON)

Fe-S clusters are one of the most ancient and ubiquitous prosthetic groups in biology. The range of their biological functions makes them one of the most versatile prosthetic groups as well. While the last twenty years have provided a wealth of information on the functional aspects of Fe-S clusters, very little is known about how organisms deal with the delivery of iron and sulfide, or the manufacture and insertion of Fe-S clusters into apoproteins. Recent studies have shown that the movement of metals into and through cells is a tightly regulated process, and many aspects of this metal homeostasis are conserved throughout the three kingdoms of life. One of the most conserved process in metal homeostasis in particular and in biology in general, is the assembly of iron-sulfur clusters. Research in this thesis centers around two proteins, NifU and NifS, and their more general homologues, IscU and IscS. A combination of molecular biology, biochemistry, and spectroscopy detail a process in which NifS or IscS direct the assembly of transient iron-sulfur clusters upon NifU or IscU. The spectroscopic and biochemical properties of NifU and IscU are consistent with a role in providing a scaffold for the assembly of transient iron-sulfur clusters that are transferred intact to different apoproteins. In a complementary study, NifEN, which is implicated as a scaffold for the assembly of the heterometallic Mo-Fe-S cluster that constitutes the active site of nitrogenase, has also been characterized.

INDEX WORDS: Iron-Sulfur Cluster Assembly, Iron Homeostasis, Magnetic Circular Dichroism, Electron Paramagnetic Resonance, Resonance Raman

BIOLOGICAL IRON-SULFUR CLUSTER ASSEMBLY

by

JEFFREY NEAL AGAR

B.S., University of Michigan, Flint, 1995

Ph.D. The University of Georgia, 2000

A Dissertation Submitted to the Graduate Faculty of

The University of Georgia in Partial Fulfillment

of the Requirements for the Degree

DOCTOR OF PHILOSOPHY

ATHENS, GEORGIA

2000

BIOLOGICAL IRON-SULFUR CLUSTER ASSEMBLY

by

JEFFREY NEAL AGAR

Approved:

Major Professor: Michael Johnson

Committee: Robert Scott
Robert Phillips
Donald Kurtz
Michael Adams

Electronic Version Approved:

Gordan L. Patel
Dean of the Graduate School
The University of Georgia
July 2000

To Nathalie, who has endured two years at too long a distance; aux filles, Alexandrine and Noémie; to my brothers and sisters, DeAnna, Charlie, Veronica, Winston, Michelle, Evan, Elizabeth, Michael, Joshua, and Erik; to my parents, Cliff, Mom, Dad, and Jill; and to Grandma Herbert, the great matriarch.

ACKNOWLEDGMENTS

I wish to express my deepest gratitude to my major Professor, Dr. Michael K. Johnson, for his guidance, support, and loyalty during the course of my studies.

I wish to extend my sincere gratitude to Dennis Dean, for the opportunity to work on such an exciting project, for his mentoring, and for graciously opening his home and laboratory to me.

I thank my reading and examining committee, Dr. Donald M. Kurtz, Jr., Dr. Robert A. Scott, Dr. Michael W. W. Adams, and Dr. Robert S. Phillips, for their effort and for insightful discussion.

I thank Dr. David O'Keeffe for teaching me about research, and for helping me to choose the right graduate school, and Dr. Robert Kren for defending me from the great bureaucracy.

I thank Rodger Wells, my boss at DuPont, for teaching me how to be a chemist, for showing me how to prosper in an industrial environment, and most of all for his unwavering support.

I thank my father Cliff for driving with me to the University of Georgia and helping me choose the right graduate school.

TABLE OF CONTENTS

LIST OF TABLES

TABLE

LIST OF FIGURES

FIGURE

Chapter I

Introduction

1.1 Summary

The movement of metals into and through cells is a tightly regulated process (1-3), and many aspects of this metal homeostasis are conserved throughout the three kingdoms of life (4). One of the most conserved process in metal homeostasis in particular and in biology in general (5), is the assembly of iron-sulfur clusters. In fact, a search of thirty four complete genomes reveals twenty eight contain an iron-sulfur cluster assembly, or *isc* gene. Research in this thesis centers around two of these proteins, NifU and NifS, and their more general homologues, IscU and IscS. A combination of molecular biology, biochemistry, and spectroscopy detail a process in which NifS or IscS direct the assembly of transient iron-sulfur clusters upon NifU or IscU. *The spectroscopic and biochemical properties of NifU and IscU are consistent with a role in providing a scaffold for the assembly of transient iron-sulfur clusters that are transferred intact to different apoproteins*. In a complementary study, NifEN, which is implicated as a scaffold for the assembly of the heterometallic Mo-Fe-S cluster (6, 7) that constitutes the active site of nitrogenase, has also been characterized.

1.2 Iron-Sulfur Proteins: Background

Fe-S clusters are one of the most ancient and ubiquitous prosthetic groups in biology (8-10). Iron-sulfur cluster containing ferredoxins were first isolated in the 1950's (11), although the chemical nature of the Fe-S prosthetic group was not understood until 1962 (12). Soon thereafter, Shethna (13-15) and Rieske (16) discovered the ferredoxins that to this day bear their names, and by 1963 rubredoxin (17), [Fe_2S_2] (12), and [Fe_4S_4] (18) containing proteins were characterized. The advances continued, and by 1972, 1.5-Å and 2.8-Å resolution crystal structures for rubredoxin (19) and [Fe_4S_4] cluster containing proteins (20) were solved. These Fe-S clusters were involved in electron transport, and

until 1980 when the (de)hydratase function of the cluster in aconitase was discovered (21), this remained their only reported biological function. A look at the mitochondrial respiratory chain, perhaps the most studied area in biology, supports the conclusion that Fe-S clusters are adept electron carriers. Mitochondrial electron transport using electrons derived from succinate, nicotinamide adenine dinucleotide (NADH), or the β-oxidation of fatty acids, involves thirteen iron-sulfur clusters, see Figure 1 (10). Loss of function in any of these clusters would result in immediate death to an obligate aerobe. Anaerobes wouldn't fair any better without Fe-S clusters, for although the types of anaerobic respiration are diverse, there is not a major respiratory pathway devoid of Fe-S clusters.

Beginning in 1980, nearly thirty years after their discovery, entirely new functions for iron-sulfur clusters began to emerge. It is now clear that iron-sulfur clusters can do much more than carry electrons. One-hundred and twenty different types of Fe-S cluster proteins and enzymes have been characterized (8, 10). These enzymes and proteins differ in either cluster nuclearity, function, or in the spacing of ligating cysteines. For instance, within [Fe_2 S_2] cluster containing proteins, there are twenty-four functionally distinct proteins (10, 22-27). Iron-sulfur clusters are now known to act in purely structural roles, as in the DNA repair enzymes, endonuclease III and MutY (28); to generate and stabilize one electron intermediates in two electron processes, as in ferrodoxin thioredoxin reductase (29, 30); to catalyze hydration or dehydration reactions as in aconitase (31, 32); to be involved in iron storage as in the polyferredoxins (33, 34); to act as sensors to regulate enzyme activity as in glutamine phosphoribosylpyrophosphate amidotransferase (35); to act as sensors which turn on or off transcriptional regulators as in fumarate nitrate reductase (FNR) or the iron-responsive protein (IRP), which respond to O_2 and iron respectively (31, 36, 37); to serve as substrates as in biotin synthase (38, 39); to generate radicals as in pyruvate-formate lyase-activating enzyme (27); to act as redox dependent transcriptional regulators as in SoxR (40); to couple proton and electron transfer as in Rieske and nitrogenase P-cluster (67-70); and to act as O_2 protective clusters as with the

nitrogenase-associated FeSII protein (41). The range of functions carried out by Fe-S proteins makes them one of the most versatile prosthetic groups in biology.

1.3 Iron-Sulfur Proteins: Properties

Both structurally and electronically Fe-S clusters can be considered as being composed of $[Fe_2S_2]$ rhombs. It has been established experimentally that $[Fe_2S_2]$ cluster will couple reductively to form their thermodynamic sink, $[Fe_4S_4]$ clusters (42, 43). As this has been the observed mechanism for $[Fe_4S_4]$ cluster formation, it is useful to consider $[Fe_4S_4]$ clusters as being composed of two, $[Fe_2S_2]$ rhombs. In terms of electronic structure, Fe-S clusters are best thought of as being composed of $[Fe_2S_2]^{2+,1+,0}$ units (44, 45), see Figure 2. The mixed-valance form, $[Fe_2S_2]^{1+}$, can be valance localized with the high spin Fe(III) and Fe(II) sites coupled antiferromagnetically to yield S=1/2 ground state, or valance delocalized with the spins coupled ferromagnetically to yield S=9/2 ground state. While the former is generally observed for biological $[Fe_2S_2]^{1+}$ clusters, Mössbauer studies indicate that the latter is generally present in higher nuclearity [3Fe-4S]^0 and $[Fe_4S_4]^{3+,2+,1+,0}$ clusters. Moreover, as illustrated in Figure 2, S=9/2 spin state for the valance delocalized $[Fe_2S_2]$ cluster is required to explain the spin states of the higher nuclearity clusters. The experimentally observed core oxidation states and ground spin states which result from magnetic coupling between $[Fe_2S_2]$ units or $[Fe_2S_2]$ units and Fe units are detailed in Figure 3, for each of the crystallographically defined biological Fe-S clusters.

In each of the five chapters, Fe-S clusters are characterized spectroscopically using a range of complementary techniques. These include magnetic circular dichroism (MCD), which can probe the ground and excited state electronic structure of paramagnetic species (46-48); electron paramagnetic resonance (EPR) which is a sensitive probe of the electronic ground state in paramagnetic species (49-53); resonance Raman, which probes the ground vibrational states in a chromophoric species (54-58); Mössbauer, a probe of ground state electronic information (59-61); and finally by UV-visible spectroscopy, a

probe of electronic excited states. There has been a considerable amount of characterization of both native and mutant Fe-S clusters (29, 62, 63, 63-66). By comparison of the spectra that were observed for the different Fe-S species in this thesis to previously characterized mutant and wildtype Fe-S proteins, it was possible to draw conclusions about the coordination environment and nuclearity of the Fe-S species observed. Much work has also been done with model systems, where clusters have been stabilized in both protic and aprotic solvents (42, 71-80). Both are pertinent, as biological Fe-S clusters are exposed to a mixture of aprotic and protic environments.

1.4 Iron Homeostasis

In accord with the model chemistry, there have been a number of cases in which it has been possible to remove an iron-sulfur cluster from a protein, separate the protein from the exogenous iron and sulfur, and then reassemble a functional, iron-sulfur cluster back into the protein using only Fe(II) or Fe(III), S^{2-}, and dithiothreitol (DTT) (80-83). However, such "spontaneous self assembly" of biological iron-sulfur clusters is unlikely to occur *in vivo* for two main reasons: 1) iron has a well established cytotoxicity, linked to the ability to generate hydroxyl radicals via Fenton chemistry (84, 85) and accordingly is not free in the cytosol; and 2) there have been a number of genes characterized that are absolutely necessary for iron homeostasis and iron-sulfur cluster assembly.

The clearest picture that has emerged regarding iron homeostasis is in the yeast, *Saccharomyces cerevisiae*. As most of the research in this field has been done in the last few years, a comprehensive review does not exist. A pictorial view of those genes with published phenotypes is therefore presented. Figure 4 illustrates the forty characterized genes that are directly involved in iron-homeostasis, a number nearing one percent of the total genes in this yeast. If the recent rate of discovery in *S. cerevisiae* continues, there will be many more iron-homeostasis genes discovered and characterized in the years to come. In accord with iron-homeostasis being an indispensable process, there are also at least four separate pathways for iron to enter the cell.

Yeast are able to uptake insoluble Fe(III) using either a siderophore uptake pathways, or a strategy involving cell surface reductases which release iron from its insoluble ferric forms. Depending on the iron availability, *S. cerevisiae* can switch on three different high-affinity or one low-affinity iron uptake pathway (86-88). In one high-affinity pathway, iron is reduced at the cell surface by Fre1 (89) or Fre2, oxidized by Fet3 (90, 91) and then passes through the membrane permease, Ftr1 (90). In the second and third high-affinity iron-uptake pathways, siderophores are used to extract Fe(III), rather than using the reductive strategy employed by the first high affinity pathway. The current dogma is that *S. cerevisiae* does not excrete its own siderophores, but instead use the siderophores secreted by both prokaryotes and other eukaryotes (86, 88, 92, 93). The siderophore transport proteins Arn1, Arn2, Arn3 (also known as Sit1) (86), Taf1, Enb1, Arn4 (94), and Fet3 are responsible for the import of ferrioxamines, ferrichromes, and fusarinine related siderophores. In the low affinity pathway, iron is reduced by Fre1 (89) or Fre2 and transported across the membrane by Fet4 (95, 96).

Once inside the cell, Fe(III) homeostasis is controlled by the sequestration of iron in vacuoles (97). Fth1p and Fet5, which are homologous to Ftr1 and Fet3, form a membrane-permease complex (98) which is most likely vacuolar. Ccc1, a general divalent metal permease (99, 100) can adjust cytosolic iron levels through an unknown mechanism that does not involve excretion, and so is most likely also vacuolar (90) Vsp41, one of many vacuolar trafficking proteins (101) is responsible for the post Golgi processing of Fet3. Ctr1 and Atx1 (102-104) deliver copper to Fet3, and provide the long missing link between copper and iron homeostasis. The remaining iron-homeostasis genes are all in the mitochondria, and with the exception of Yfh1, the homologue of the human frataxin gene, (105, 106) are involved in iron-sulfur cluster assembly. For the most part, the *S. cerevisiae* iron-sulfur cluster assembly research has been derivative of the original *A. vinelandii* studies, in that it has established phenotypes for yeast genes which have high homology to characterized genes in *Azotobacter vinelandii*, see Figure 5 (105). In this

sense, it is best to summarize the iron-sulfur cluster assembly genes in their original context, and refer to those times when yeast studies provide insight that prokaryotic studies cannot. One such example is the observation by Lill and coworkers that in *S. cerevisiae* the iron-sulfur clusters of cytosolic proteins are somehow formed in the mitochondria and then transferred to the cytosol where they are incorporated (107-110).

1.5 Iron-Sulfur Cluster Assembly Genes

After sequencing *nif* specific genes from *A. vinelandii* (111, 112), and systematically creating knockout strains for six of the individual genes (113), Dean and coworkers found a number of genes which are essential for optimal diazotrophic growth. Further studies showed that for the *nifU* and *nifS* genes, the lack of diazotrophic growth resulted from an inability to make functional iron-sulfur clusters in the nitrogenase component proteins (114). As there was still a small amount of functional nitrogenase produced, Dean and coworkers looked for and found a set of housekeeping iron-sulfur cluster assembly genes. These genes were termed the iron-sulfur cluster assembly, or *isc* genes (115). The identification of the *isc* genes showed that unlike the *in vitro* assembly of iron-sulfur clusters, the biological assembly of iron-sulfur clusters involves a number of different proteins that serve to transfer iron, sulfur, apoproteins, and electrons to the same place at the same time.

In the simplest sense, the Isc proteins replace Fe(II), S^{2-}, and DTT in the common *in vitro* cluster reconstitution. However, there are many proteins that have yet to be successfully reconstituted *in vitro*. In these cases, there may be a need for protein folding assistance which could be supplied by genes in the *isc* cluster. As with other biological processes, iron-sulfur cluster assembly must also be regulated, and at least one of the *isc* genes appears to be a regulatory protein. As a result of the work described in this thesis and the seminal and ongoing work in the Dean laboratory, it becomes possible to ascribe functions to many of the genes from the *isc* cluster along with their related *nif* specific genes from *A. vinelandii*, see Figure 5.

The gene products of *nifS* and *iscS* are cysteine desulfurases which catalyze the conversion of cysteine to alanine and either S^0 or S^{2-}, depending on the absence or presence of reducing equivalents (115, 116). The mechanism of NifS was described in 1993 (117) and involves the production of an enzyme bound cysteine persulfide using a pyridoxal phosphate cofactor. Interestingly, it would seem that iron-sulfur cluster assembly is dependent upon pyridoxal phosphate cofactor biosynthesis, although this link has never been experimentally addressed. Since NifS uses cysteine as a substrate, the process of iron-sulfur cluster assembly would deplete cellular cysteine levels. *CysE* genes, the product of which are O-acetylserine synthases that catalyze the rate limiting step in cysteine biosynthesis (118-120), presumably aid in supplying the excess cysteine needed for cluster biosynthesis (121). Both the *nif* specific cluster assembly pathway (111), and the *isc* pathway contain *cysE* genes, named *cysE1*, and *cysE2* respectively. The *hscA* and *hscB* genes in *A. vinelandii* bear homology to the *hscA* and *hscB* genes in *Escherichia coli* (122, 123). The *hscA* and *hscB* genes in *E. coli* are homologous to the *dnaJ* and *dnaK* genes, which code for molecular chaperones, and are likely to function in the folding of apoproteins for cluster insertion (124, 125). The gene product of *E. coli* and *A. vinelandii* *fdx* has been characterized, and is a $[Fe_2S_2]$ ferredoxin (123, 126, 127). As purified, it contains a $[Fe_2S_2]^{2+}$ cluster which can be reduced to a $[Fe_2S_2]^{1+}$ cluster without degradation and is therefore likely to participate in electron transfer.

Very little is known about *orf1 orf2*, and *orf3*, although the gene product for *orf2* contains a DNA binding sequence, and the requisite number of cysteines to assemble an Fe-S cluster, and hence may be a regulatory protein. The gene product of *orf1* bears homology to methyl transferases, but there has been no published work on this gene or its product that has established its function. Removal of *orf3* from a plasmid containing an extra copy of the *isc* cluster for the purpose of aiding in the overexpression of reporter ferredoxins in *E. coli*, did not effect Fe-S cluster production, except in the case of one reporter ferredoxin where production was impaired by the presence of excess iron.

Although the authors of this work ascribe to Orf3 a role as an iron chaperone (128), this is inconsistent with the observation that its function is impaired by excess iron. Further studies on *orf3* and its gene product will hopefully resolve these inconsistencies.

IscA and its *nif* homologue *orf6*, are particularly interesting, and code for proteins with three conserved cysteines, see Figure 6. A search of thirty four genomes showed that twenty eight contained an *iscU* homologue, while only fourteen contained an *iscA* homologue. One organism, *Synechocystis* does not contain an *iscU* gene, but does contain *iscA* gene (115). The absence of an *iscA* homologue in over half of the published genomes would suggest that its function, at least in organisms where it is absent, is not absolutely necessary for biological iron-sulfur cluster assembly. The lack of an *iscU* homologue in *Synechocystis*, where *iscA* is present, would suggest that IscA can complement the function of IscU. These observations, taken together with the findings presented in this thesis which show that IscU can serve as a scaffold for iron-sulfur cluster assembly, suggest a role for IscA as an alternate scaffold for iron-sulfur cluster assembly.

IscU and *nifU* are the two remaining iron-sulfur cluster assembly genes in Figure 4, and are the major focus of this thesis. In 1994 Fu *et al*., published an initial characterization of NifU, which described NifU as a homodimer of mass 66 kDa (129). NifU contains one $[Fe_2S_2]^{2+,1+}$ cluster per subunit, which like the Fdx cluster, is not labile, and therefore is not a good candidate for a transferable cluster. As described in chapter two, NifU has three domains. The N-terminal 15kDa is homologous to IscU and contain three highly conserved cysteine residues, see Figure 7. The middle 20kDa is homologous to bacterioferritin-associated ferredoxin (130), and the C-terminal 8kDa is similar to Nfu1p from yeast (131). Herein, the proteins IscU and NifU are shown to have the unique ability to assemble iron-sulfur clusters that are both oxidatively and reductively labile, an important quality for any cluster which is to be transferable. As these genes are so highly conserved throughout prokaryotes and eukaryotes, see Figure 7, the process described for *A. vinelandii* can serve as a model for biological iron-sulfur cluster assembly.

Exceptions to a universal mechanism of iron-sulfur cluster assembly occur in the thermophilic archaea, where *Pyrococcus horikoshi*, *Pyrococcus furiosis*, *Pyrococcus abyssi*, and *Methanococcus jannischii*, do not contain *iscU* or *iscA* homologues. This is not a general phenomenon with archaea, as *Archaeglobus fulgidus* contain a homologue with 65 % similarity to the *A. vinelandii* IscU, and is not a general phenomenon with anaerobes, as every other anaerobe with a completely sequenced genome was found to contain an *isc* homologue. While the experimental data on iron-sulfur cluster assembly is scant for these organisms, one striking feature that all four thermophilic archaea share is iron availability. As with all anaerobes, they have access to soluble ferrous iron, which is not present in aerobic environments. This fact may account for why anaerobes in general do not secrete siderophores. Unlike mesophilic anaerobes however, their hot oceanic environment also allows them access to soluble ferric iron. While the solubility of the two major forms of ferric hydroxide are 10^{-10} and 10^{-6} M at room temperature (132, 133), ferric chloride's solubility is reported at 15*M* at 25°C. At 100°C, Fe(III)Cl_3 is as soluble as $ZnCl_2$, with a reported solubility of 35*M* (134, 135). The laboratory conditions in which these solubilities were measured do not duplicate the more complex chemical environments found in nature, but do provide qualitative information that establish the following trends: 1) as chloride ion concentration increases, so does ferric iron solubility, and 2) as temperature increases, so does ferric iron solubility. In the thermophilic archaea's environment, many of the paradigms of mesophilic iron homeostasis, such as the cell surface ferric reductases, and siderophore production are superfluous. Inside the cell, iron must still be chaperoned, but the need for reduction to labilize iron is diminished by the increased temperature. The chemistry of iron is different at these temperatures, and it should be no surprise that the iron homeostasis genes are different as well. A few pathogens, including *Borrelia burgdorferi* and *Mycobacterium genetiallum* also lack *isc* homologues, although the significance of this exception is lessened by the fact that

pathogens rely on their host for the biosynthesis of a number of important cofactors (136) and are not free living.

NifEN is not an *isc* genes. Unlike the *isc* gene products, which have been shown to place functional iron-sulfur clusters into a vast array of proteins, NifEN has a very specific function. It's only role is in the maturation of the nitrogenase FeMoCofactor (137, 138). As *NifEN* knockout strains cannot assembly FeMo-cofactor, and based on the considerable homology that NifEN shares with the nitrogenase MoFe protein, a role for NifEN as a scaffold for the assembly and transfer of FeMo-cofactor has been proposed (6, 139).

1.6 Summary of Presented Work:

Chapter II is an initial characterization of NifEN. A strain of *A. vinelandii* was constructed which placed the *nifEN* gene under the control of the *nifHDK* promoter. This homologous overexpression system produced NifEN as 5-10% of the total soluble protein. NifEN was purified, and characterized by UV-vis, EPR, MCD, and resonance Raman spectroscopies. NifEN is shown to be an $\alpha_2\beta_2$ heterotetramer which contains two, $\alpha\beta$ subunit-bridging $[Fe_4S_4]^{2+,1+}$ clusters per heterotetramer.

Chapter III shows that NifU is a modular protein by producing and characterizing truncated forms of NifU which are still functional. The N-terminus of NifU, which bears homology to the IscU protein, is shown to bind a single ferric iron using three conserved cysteines. Finally, each of the nine conserved cysteines are individually deleted, reinserted into *A. vinelandii* using gene replacement, and the consequence of the individual cysteine mutations is assessed by their effect on the rate of diazotrophic growth.

Chapter IV provides evidence for the NifS-directed assembly of $[Fe_2S_2]$ clusters in NifU variants. The truncated form of NifU described in chapter III, termed NifU-1, is shown to assemble a reductively labile $[Fe_2S_2]^{2+}$ cluster. A mutant in full length NifU, D37A NifU, is also shown to stabilize a cluster that was assembled *in vitro*. *In vivo*

evidence for this cluster formation is also provided, using the mutant, D37A NifU-1, which purifies with a $[Fe_2S_2]$ cluster.

Chapter V provides the first evidence for the assembly of an iron-sulfur cluster in a native iron-sulfur cluster assembly protein. IscS is shown to mediate the assembly of a $[Fe_2S_2]^{2+}$ cluster upon IscU. The cluster bound form of IscU was found to be reductively and oxidatively labile, but was stable enough to allow anaerobic purification to remove exogenous iron and sulfides, affording samples which could be quantified for cluster content. The resulting samples were shown to contain one $[Fe_2S_2]^{2+}$ cluster per IscU dimer.

In Chapter VI anaerobic fast performance liquid chromatography was used to resolve different types of IscU with bound Fe-S clusters. Including the single $[Fe_2S_2]^{2+}$ cluster which is characterized in chapter IV, three different forms of Fe-S cluster bound IscU are purified and characterized. A second form of IscU, which has two $[Fe_2S_2]^{2+}$ clusters, was purified and characterized by resonance Raman, Mössbauer, and chemical analysis. A third form of IscU, containing a $[Fe_4S_4]^{2+}$ cluster which forms by the reductive coupling of the two $[Fe_2S_2]^{2+}$ clusters, is also characterized. Prior to this work, $[Fe_4S_4]^{2+}$ cluster formation by the reductive coupling of two $[Fe_2S_2]^{2+}$ clusters had only been observed in model systems (42, 43). Hence these results show that IscU provides a scaffold for the assembly of both $[Fe_2S_2]$ and $[Fe_4S_4]$ clusters and provide the first insight into the mechanism of the biosynthesis of $[Fe_4S_4]$ clusters.

Abbreviations:

iron-sulfur cluster assembly, *isc*; magnetic circular dichroism, MCD; electron paramagnetic resonance, EPR; iron-responsive protein, IRP; dithiothriotol, DTT; iron-responsive protein, IRP; anaerobic ribonucleotide reductase, ARR; nicotinamide adenine dinucleotide, NADH.

Reference List

1. DeRusso, P.A., Philpott, C.C., Iwai, K., Mostowski, H.S., Klausner, R.D., and Rouault, T.A. (1995) *J. Biol. Chem.* **270**, 15451-15454

2. Askwith, C.C., de Silva, D., and Kaplan, J. (1996) *Mol. Microbiol.* **20**, 27-34

3. Salter-Cid, L., Brunmark, A., Li, Y., Peterson, P.A., Jackson, M.R., and Yang, Y. (1999) *Proc. Natl. Acad. Sci. U.S.A.* **96**, 5434-5439

4. Aisen, P., Wessling-Resnick, M., and Leibold, E.A. (1999) *Curr. Opin. Chem. Biol.* **3**, 200-206

5. Hwang, D.M., Dempsey, A., Tan, K.T., and Liew, C.C. (1996) *J. Mol. Evol.* **43**, 536-540

6. Roll, J.T., Shah, V.K., Dean, D.R., and Roberts, G.P. (1995) *J. Biol. Chem.* **270**, 4432-4437

7. Aguilar, O.M., Taormino, J., Thony, B., Ramseier, T., Hennecke, H., and Szalay, A.A. (1990) *Mol. Gen. Genet.* **224**, 413-420

8. Johnson, M.K. (1998) *Curr. Opin. Chem. Biol.* **2**, 173-181

9. Beinert, H., Holm, R.H., and Münck, E. (1997) *Science* **277**, 653-659

10. Johnson, M.K. (1994) in *Encyclopedia of inorganic chemistry* (King, R.B., ed.) pp. 1896-1915, John Wiley & Sons, Chichester

11. Lovenberg, W. ed., (1973) *Iron-Sulfur Proteins*, Academic Press, New York

12. Mortenson, L.E., Valentine, R.C., and Carnahan, J.E. (1962) *Biochem. Biophys. Res. Commun.* **7**, 448

13. Shethna, Y.I., DerVartanian, D.V., and Beinert, H. (1968) *Biochem. Biophys. Res. Commun.* **31**, 862-868

14. Shethna, Y.I., Stombaugh, N.A., and Burris, R.H. (1968) *Biochem. Biophys. Res. Commun.* **42**, 1108-114

15. Shethna, Y.I., Wilson, P.W., and Beinert, H. (1966) *Biochim. Biophys. Acta* **113**, 225-234

16. Rieske, J.S., MacLennan, D.H., and Coleman, R. (1964) *Biochem. Biophys. Res. Commun.* **15**, 338-345

17. Buchanan, B.B., Lovenberg, W., and Rabinowitz, J.C. (1963) *Proc. Natl. Acad. Sci. U.S.A.* **49**, 345-350

18. Bartsch, R.G. (1963) in *Bacterial Photosythesis* (Gest, H., San Pietro, A., and Vernon, L.P., eds) pp. 315-326,

19. Herriott, J.R., Sieker, L.C., Jensen, L.H., and Lovenberg, W. (1970) *J. Mol. Biol.* **50** , 391-397

20. Sieker, L.C., Adman, E.T., and Jensen, L.H. (1972) *Nature* **235**, 40-46

21. Kent, T.A., Dreyer, J.-C., Kennedy, M.C., Huynh, B.H., Emptage, M.H., Beinert, H., and Münck, E. (1982) *Proc. Natl. Acad. Sci. U.S.A.* **79**, 1096-1100

22. Busby, R.W., Schelvis, J.P.M., Yu, D.S., Babcock, G.T., and Marletta, M.A. (1999) *J. Am. Chem. Soc.* **121**, 4706-4707

23. Agar, J.N., Zheng, L., Cash, V.L., Dean, D.R., and Johnson, M.K. (2000) *J. Am. Chem. Soc.* **122**, 2136-2137

24. Reichard, P. (1993) *Science* **260**, 1773-1777

25. Dailey, H.A., Finnegan, M.G., and Johnson, M.K. (1994) *Biochemistry* **33**, 403-407

26. Duin, E.C., Lafferty, M.E., Crouse, B.R., Allen, R.M., Sanyal, I., Flint, D.H., and Johnson, M.K. (1997) *Biochemistry* **36**, 11811-11820

27. Broderick, J.B., Duderstadt, R.E., Fernandez, D.C., Wojtuszewski, K., Henshaw, T.F., and Johnson, M.K. (1997) *J. Am. Chem. Soc.* **119**, 7396-7397

28. Porello, S.L., Cannon, M.J., and David, S.S. (1998) *Biochemistry* **37**, 6465-6475

29. Staples, C.R., Ameyibor, E., Fu, W., Gaudet-Salvi, L., Stritt-Etter, A.L., Schürmann, P., Knaff, D.B., and Johnson, M.K. (1996) *Biochemistry* **35**, 11425-11434

30. Johnson, M.K., Staples, C.R., Duin, E.C., Lafferty, M.E., and Duderstadt, R.E. (1998) *Pure Appl. Chem.* **70**, 939-946

31. Beinert, H., Kennedy, M.C., and Stout, C.D. (1996) *Chem. Rev.* **96**, 2335-2373

32. Flint, D.H. and Allen, R.M. (1996) *Chem. Rev.* **96**, 2315-2334

33. Reeve, J.N., Beckler, G.S., Cram, D.S., Hamilton, P.T., Brown, J.W., Krzycki, J.A., Kolodziej, A.F., Alex, L.A., Orme-Johnson, W.H., and Walsh, C.T. (1989) *Proc.Natl.Acad.Sci.U.S.A.* **86**, 3031-3035

34. Hedderich, R., Albracht, S.P.J., Linder, D., Koch, J., and Thauer, R.K. (1992) *FEBS Lett.* **298**, 65-68

35. Smith, J.L., Zaluzec, E.J., Wery, J.-P., Niu, L., Switzer, R.L., Zalkin, H., and Satow, Y. (1994) *Science* **264**, 1427-1433

36. Popescu, C.V., Bates, D.M., Beinert, H., Münck, E., and Kiley, P.J. (1998) *Proc. Natl. Acad. Sci. U.S.A.* **95**, 13431-13435

37. Khoroshilova, N., Popescu, C., Münck, E., Beinert, H., and Kiley, P.J. (1997) *Proc. Natl. Acad. Sci. U.S.A.* **94**, 6087-6092

38. Gibson, K.J., Pelletier, D.A., and Turner, I.M., Sr. (1999) *Biochem. Biophys. Res. Commun.* **254**, 632-635

39. Bui, B.T.S., Florentin, D., Fournier, F., Ploux, O., Méjean, A., and Marquet, A. (1998) *FEBS Lett.* **440**, 226-230

40. Ding, H.G., Hidalgo, E., and Demple, B. (1996) *J. Biol. Chem.* **271**, 33173-33175

41. Lou, J., Moshiri, F., Johnson, M.K., Lafferty, M.E., Sorkin, D.L., Miller, A.-F., and Maier, R.J. (1999) *Biochemistry* **38**, 5563-5571

42. Hagen, K.S., Watson, A.D., and Holm, R.H. (1983) *J. Am. Chem. Soc.* **105**, 3913

43. Hagen, K.S., Reynolds, J.G., and Holm, R.H. (1981) *J. Am. Chem. Soc.* **103**, 4054-4063

44. Münck, E., Papaefthymiou, V., Surerus, K.K., and Girerd, J.-J. (1988) in *Metal clusters in proteins* (Que, L., Jr., ed.) pp. 302-325, American Chemical Society, Washington, D. C.

45. Münck, E. and Kent, T.A. (1986) *Hyperfine Interact.* **27**, 161-172

46. Thomson, A.J., Cheesman, M.R., and George, S.J. (1993) *Meth. Enzymol.* **226**, 199-232

47. Johnson, M.K. (1988) in *Metal clusters in proteins* (Que, L., Jr., ed.) pp. 326-342, American Chemical Society, Washington, D.C.

48. Johnson, M.K. (2000) in *Physical methods in inorganic and bioinorganic chemistry: spectroscopy and magnetism* (Que, L., Jr., ed.) University Science books, Sausalito, CA

49. Lowe, D.J. and Smith, B.E. (1985) *Biochem. Soc. Trans.* **13**, 579-581

50. Drago, R.S. (1992) *Physical methods for chemists,* Saunders College Publishing and Harcourt Brace Janovich College Publishers, New York

51. Beinert, H. (1985) *Biochem. Soc. Trans.* **13**, 542-547

52. Albracht, S.P.J. (1985) *Biochem. Soc. Trans.* **13**, 582-585

53. Aasa, R. and Vänngård, T. (1975) *J. Magn. Reson.* 308-315

54. Johnson, M.K., Czernuszewicz, R.S., Spiro, T.G., Fee, J.A., and Sweeney, W.V. (1983) *J. Am. Chem. Soc.* **103**, 6671-6678

55. Fabian, H. and Anzenbacher, P. (1993) *Vib. Spectrosc.* **4**, 125-148

56. Czernuszewicz, R.S. (1993) in *Methods in molecular biology* (Jones, C., Mulloy, B., and Thomas, A.H., eds.) pp. 345-374, Humana Press, Totowa

57. Carey, P.R. (1982) in *Biochemical applications of Raman and resonance Raman spectroscopies* pp. 11-47, Academic Press, New York

58. Bangcharoenpaurpong, O. and Champion, P.M. (1986) *Biochemistry* **25**, 2374-2378

59. Kent, T.A., Dreyer, J.L., Kennedy, M.C., Huynh, B.H., Emptage, M.H., Beinert, H., and Münck, E. (1982) *Proc. Natl. Acad. Sci. U.S.A.* **79**, 1096-1100

60. Beinert, H. and Thomson, A.J. (1983) *Arch. Biochem. Biophys.* **222**, 333-361

61. Cunningham, R.P., Asahara, H., Bank, J.F., Scholes, C.P., Salerno, J.C., Surerus, K.K., Münck, E., McCracken, J., Peisach, J., and Emptage, M.H. (1989) *Biochemistry* **28**, 4450-4455

62. Duderstadt, R.E., Staples, C.R., Brereton, P.S., Adams, M.W.W., and Johnson, M.K. (1999) *Biochemistry* **38**, 10585-10593

63. Duderstadt, R.E., Brereton, P.S., Adams, M.W.W., and Johnson, M.K. (1999) *FEBS Lett.* **454**, 21-26

64. Brereton, P.S., Duderstadt, R.E., Staples, C.R., Johnson, M.K., and Adams, M.W.W. (1999) *Biochemistry* **38**, 10594-10605

65. Staples, C. R. (1997) *Structure-function relationships in iron-sulfur proteins* University of Georgia. Ph.D. Dissertation

66. Staples, C.R., Dhawan, I.K., Finnegan, M.G., Dwinell, D.A., Zhou, Z.-H., Huang, H., Verhagen, M.F.J.M., Adams, M.W.W., and Johnson, M.K. (1997) *Inorg. Chem.* **36**, 5740-5749

67. Peters, J.W., Stowell, M.H.B., Soltis, S.M., Finnegan, M.G., Johnson, M.K., and Rees, D.C. (1997) *Biochemistry* **36**, 1181-1187.

68. Nitschke, W., Joliot, P., Liebl, U., Rutherford, A.W., Hauska, G., Müller, A., and Riedel, A. (1992) *Biochim. Biophys. Acta* **1102**, 266-268

69. Gurbiel, R.J., Batie, C.J., Sivaraja, M., True, A.E., Fee, J.A., Hoffman, B.M., and Ballou, D.P. (1989) *Biochemistry* **28**, 4861-4871

70. Anemüller, S., Schmidt, C.L., Schäfer, G., Bill, E., Trautwein, A.X., and Teixeira, M. (1994) *Biochem. Biophys. Res. Commun.* **202**, 252-257

71. Averill, B.A., Herskovitz, T., Holm, R.H., and Ibers, J.A. (1973) *J. Am. Chem. Soc.* **95** , 3523-3534

72. Bobrik, M.A., Que, L., Jr., and Holm, R.H. (1974) *J. Am. Chem. Soc.* **96**, 285-287

73. Carney, M.J., Papaefthymiou, G.C., Spartalian, K., Frankel, R.B., and Holm, R.H. (1988) *J. Am. Chem. Soc.* **110**, 6084-6095

74. DePampilis, B.V., Averill, B., Herskovitz, T., Que, L., Jr., and Holm, R.H. (1974) *J. Am. Chem. Soc.* **96**, 4159-4167

75. Dukes, G.R. and Holm, R.H. (1975) *J. Am. Chem. Soc.* **97**, 528-533

76. Herskovitz, T., Averill, B.A., Holm, R.H., Ibers, J.A., Phillips, W.D., and Weiher, J.F. (1972) *Proc. Natl. Acad. Sci. U.S.A.* **69**, 2437-2441

77. Holm, R.H., Phillips, W.D., Averill, B.A., Mayerle, J.J., and Herskovitz, T. (1974) *J. Am. Chem. Soc.* **96**, 2109-2117

78. Mayerle, J.J., Frankel, R.B., Holm, R.H., Ibers, J.A., Phillips, W.D., and Weiher, J.F. (1973) *Proc. Natl. Acad. Sci. U.S.A.* **70**, 2429-2433

79. Que, L., Jr., Bobrik, M.A., Ibers, J.A., and Holm, R.H. (1974) *J. Am. Chem. Soc.* **96**, 4168-4178

80. Bonomi, F., Werth, M.T., and Kurtz, D.M. (1985) *Inorg. Chem.* **24**, 4331-4435

81. Flint, D.H., Smyk-Randall, E., Tuminello, J.F., Draczynska-Lusiak, B., and Brown, O.R. (1993) *J. Biol. Chem.* **268**, 25547-25552

82. Basilion, J.P., Kennedy, M.C., Beinert, H., Massinople, C.M., Klausner, R.D., and Rouault, T.A. (1994) *Arch. Biochem. Biophys.* **311**, 517-522

83. Lu, W.P., Schiau, I., Cunningham, J.R., and Ragsdale, S.W. (1993) *J. Biol. Chem.* **268**, 5605-5614

84. Wrigglesworth, J.M. and Baum, H. (1980) *Iron in biochemistry and medicine II*, Academic Press, London,

85. Haber, F. and Weiss, J. (1934) *Proc. Roy. Soc. London Ser. B. Biol. Sci.* **147**, 332-351

86. Lesuisse, E., Simon-Casteras, M., and Labbe, P. (1998) *Microbiology.* **144**, 3455-3462

87. Eide, D., Davis-Kaplan, S., Jordan, I., Sipe, D., and Kaplan, J. (1992) *J. Biol. Chem.* **267**, 20774-20781

88. Lesuisse, E., Raguzzi, F., and Crichton, R.R. (1987) *J. Gen. Microbiol.* **133**, 3229-3236

89. Shatwell, K.P., Dancis, A., Cross, A.R., Klausner, R.D., and Segal, A.W. (1996) *J. Biol. Chem.* **271**, 14240-14244

90. Stearman, R., Yuan, D.S., Yamaguchi-Iwai, Y., Klausner, R.D., and Dancis, A. (1996) *Science* **271**, 1552-1557

91. Askwith, C., Eide, D., Van, H.A., Bernard, P.S., Li, L., Davis-Kaplan, S., Sipe, D.M., and Kaplan, J. (1994) *Cell* **76**, 403-410

92. Vartivarian, S.E. and Cowart, R.E. (1999) *Arch. Biochem. Biophys.* **364**, 75-82

93. Neilands, J.B. (1995) *J. Biol. Chem.* **270**, 26723-26726

94. Yun, C.W., Tiedeman, J.S., Moore, R.E., and Philpott, C.C. (2000) *J. Biol. Chem.* **275**, 16354-16359

95. Dix, D.R., Bridgham, J.T., Broderius, M.A., Byersdorfer, C.A., and Eide, D.J. (1994) *J. Biol. Chem.* **269**, 26092-26099

96. Dix, D., Bridgham, J., Broderius, M., and Eide, D. (1997) *J. Biol. Chem.* **272**, 11770-11777

97. Raguzzi, F., Lesuisse, E., and Crichton, R.R. (1988) *FEBS Lett.* **231**, 253-258

98. Urbanowski, J.L. and Piper, R.C. (1999) *J. Biol. Chem.* **274**, 38061-38070

99. Lapinskas, P.J., Lin, S.J., and Culotta, V.C. (1996) *Mol. Microbiol.* **21**, 519-528

100. Fu, D., Beeler, T., and Dunn, T. (1994) *Yeast.* **10**, 515-521

101. Radisky, D.C., Snyder, W.B., Emr, S.D., and Kaplan, J. (1997) *Proc. Natl. Acad. Sci. U.S.A.* **94**, 5662-5666

102. Hamza, I., Schaefer, M., Klomp, L.W., and Gitlin, J.D. (1999) *Proc. Natl. Acad. Sci. U.S.A.* **96**, 13363-13368

103. Lin, S.J., Pufahl, R.A., Dancis, A., O'Halloran, T.V., and Culotta, V.C. (1997) *J. Biol. Chem.* **272**, 9215-9220

104. Yamaguchi-Iwai, Y., Stearman, R., Dancis, A., and Klausner, R.D. (1996) *EMBO J.* **15** , 3377-3384

105. Chen, O.S. and Kaplan, J. (2000) *J. Biol. Chem.* **275**, 7626-7632

106. Kaplan, J. (1999) *Proc. Natl. Acad. Sci. U.S.A.* **96**, 10948-10949

107. Kispal, G., Csere, P., Guiard, B., and Lill, R. (1997) *FEBS Lett.* **418**, 346-350

108. Lill, R., Diekert, K., Kaut, A., Lange, H., Pelzer, W., Prohl, C., and Kispal, G. (1999) *Biol. Chem.* **380**, 1157-1166

109. Csere, P., Lill, R., and Kispal, G. (1998) *FEBS Lett.* **441**, 266-270

110. Kispal, G., Csere, P., Prohl, C., and Lill, R. (1999) *EMBO J.* **18**, 3981-3989

111. Beynon, J., Ally, A., Cannon, M., Cannon, F., Jacobson, M., Cash, V., and Dean, D. (1987) *J. Bacteriol.* **169**, 4024-4029

112. Brigle, K.E. and Dean, D.R. (1988) *Nucleic.Acids.Res.* **16**, 5214-5217

113. Jacobson, M.R., Cash, V.L., Weiss, M.C., Laird, N.F., Newton, W.E., and Dean, D.R. (1989) *Mol. Gen. Genet.* **219**, 49-57

114. Dean, D.R., Bolin, J.T., and Zheng, L. (1993) *J. Bacteriol.* **175**, 6737-6744

115. Zheng, L., Cash, V.L., Flint, D.H., and Dean, D.R. (1998) *J. Biol. Chem.* **273**, 13264-13272

116. Zheng, L., White, R.H., Cash, V.L., Jack, R.F., and Dean, D.R. (1993) *Proc. Natl. Acad. Sci. U.S.A.* **90**, 2754-2758

117. Zheng, L., White, R.H., Cash, V.L., and Dean, D.R. (1994) *Biochemistry* **33**, 4714-4720

118. Leu, L.S. and Cook, P.F. (1994) *Biochemistry* **33**, 2667-2671

119. Wigley, D.B., Derrick, J.P., and Shaw, W.V. (1990) *FEBS Lett.* **277**, 267-271

120. Denk, D. and Bock, A.J. (1987) *J. Gen. Microbiol.* **133**, 515-520

121. Evans, D.J., Jones, R., Woodley, P.R., Wilborn, J.R., and Robson, R.L. (1991) *J. Bacteriol.* **173**, 5457-5469

122. Seaton, B.L. and Vickery, L.E. (1994) *Proc. Natl. Acad. Sci. U.S.A.* **91**, 2066-2070

123. Ta, D.T., Seaton, B.L., and Vickery, L.E. (1992) *J. Bacteriol.* **174**, 5760-5761

124. Kawula, T.H. and Lelivelt, M.J. (1994) *J. Bacteriol.* **176**, 610-619

125. Lelivelt, M.J. and Kawula, T.H. (1995) *J. Bacteriol.* **177**, 4900-4907

126. Ta, D.T. and Vickery, L.E. (1992) *J. Biol. Chem.* **267**, 11120-11125

127. Jung, Y.S., Gao-Sheridan, H.S., Christiansen, J., Dean, D.R., and Burgess, B.K. (1999) *J. Biol. Chem.* **274**, 32402-32410

128. Takahashi, Y. and Nakamura, M. (1999) *J. Biochem.* **126**, 917-926

129. Fu, W., Jack, R.F., Morgan, T.V., Dean, D.R., and Johnson, M.K. (1994) *Biochemistry* 13455-13463

130. Garg, R.P., Vargo, C.J., Cui, X., and Kurtz, D.M., Jr. (1996) *Biochemistry* **35**, 6297-6301

131. Schilke, B., Voisine, C., Beinert, H., and Craig, E. (1999) *Proc. Natl. Acad. Sci. U.S.A.* **96**, 10206-10211

132. Garvin, D., Parker, V.B., and White, H.J. (1987) *CODATA Thermodynamic Tables*, Hemisphere, New York,

133. Wagman, D.D., Evans, W.H., Parker, V.B., Schumm, R.H., Halow, I., Bailey, S.M., Churney, K.L., and Nuttall, R.L. (1982) *J. Phys. Chem. Ref. Data* **11**, suppl. 2

134. Söhnel, O. and Novotny, P. (1985) *Densities of aqueous solutions of inorganic substances*, Elsevier, Amsterdam

135. Krumgalz, B.S. (1994) *Mineral solubility in water at various temperatures*, Israel Oceanographic and Limnological Research, Hafia

136. Cowart, R.E. and Foster, B.G. (1985) *J. Infect. Dis.* **151**, 721-730

137. Rangaraj, P., Ryle, M.J., Lanzilotta, W.N., Ludden, P.W., and Shah, V.K. (1999) *J. Biol. Chem.* **274**, 19778-19784

138. Rangaraj, P., Ryle, M.J., Lanzilotta, W.N., Goodwin, P.J., Dean, D.R., Shah, V.K., and Ludden, P.W. (1999) *J. Biol. Chem.* **274**, 29413-29419

139. Goodwin, P.J., Agar, J.N., Roll, J.T., Roberts, G.P., Johnson, M.K., and Dean, D.R. (1998) *Biochemistry* **37**, 10420-10428

140. Armstrong, W.H., Spool, A., Papaefthymiou, G.C., Frankel, R.B., and Lippard, S.J. (1984) *J. Am. Chem. Soc.* **106**, 3653

141. Ward, T.R., Lutz, A., Parel, S.P., Ensling, J., Gutlich, P., Buglyo, P., and Orvig, C. (1999) *Inorg. Chem.* **38**, 5007-5017

142. Ugulava, N.B., Gibney, B.R., and Jarrett, J.T. (2000) *Biochemistry* **39**, 5206-5214

143. Nakamura, M., Saeki, K., and Takahashi, Y. (1999) *J. Biochem.* **126**, 10-18

144. Takahashi, Y. and Nakamura, M. (1999) *J. Biochem.* **126**, 917-926

145. Rouault, T.A. and Klausner, R.D. (1996) *J. Biol. Inorg. Chem.* **1**, 494-499

Figure 1-1 Prosthetic groups in the mitochondrial respiratory chain.

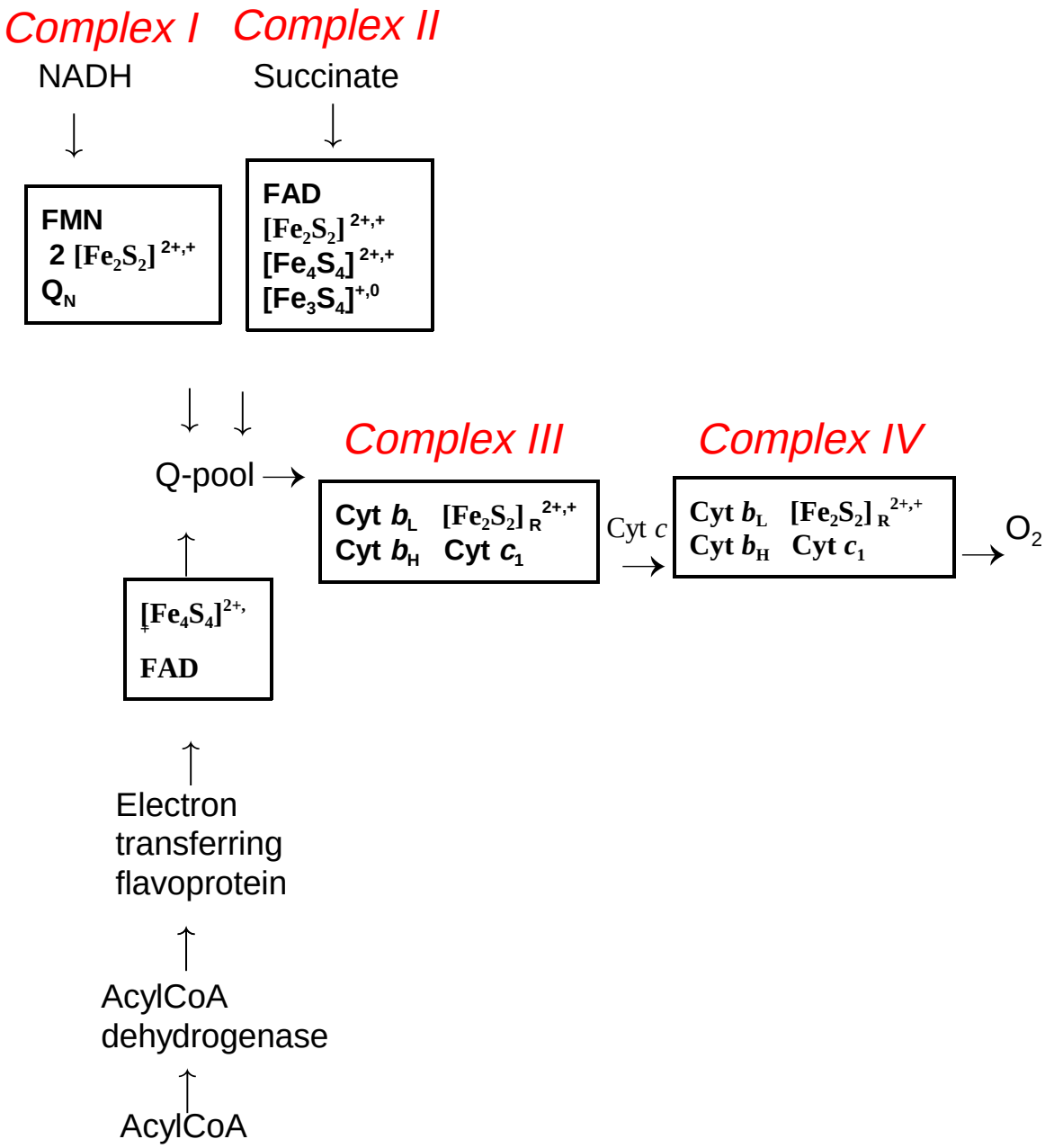
Complex I
Complex II
NADH
Succinate
FMN
2 [Fe2S2] 2+,+
QN
FAD
[Fe2S2] 2+,+
[Fe4S4] 2+,+
[Fe3S4]+,0
Q-pool
Complex III
Complex IV
Cyt bL [Fe2S2] R 2+,+
Cyt bH Cyt c1
Cyt c
Cyt bL [Fe2S2] R 2+,+
Cyt bH Cyt c1
O2
[Fe4S4]2+,
FAD
Electron transferring flavoprotein
AcylCoA dehydrogenase
AcylCoA

Figure 1-2 Oxidation states of iron and valance delocalization schemes for [Fe_2S_2], [Fe_3S_4] and [Fe_4S_4] clusters. Red indicates Fe^{3+}, blue indicates Fe^{2+}, and green indicates $Fe^{2.5+}$.

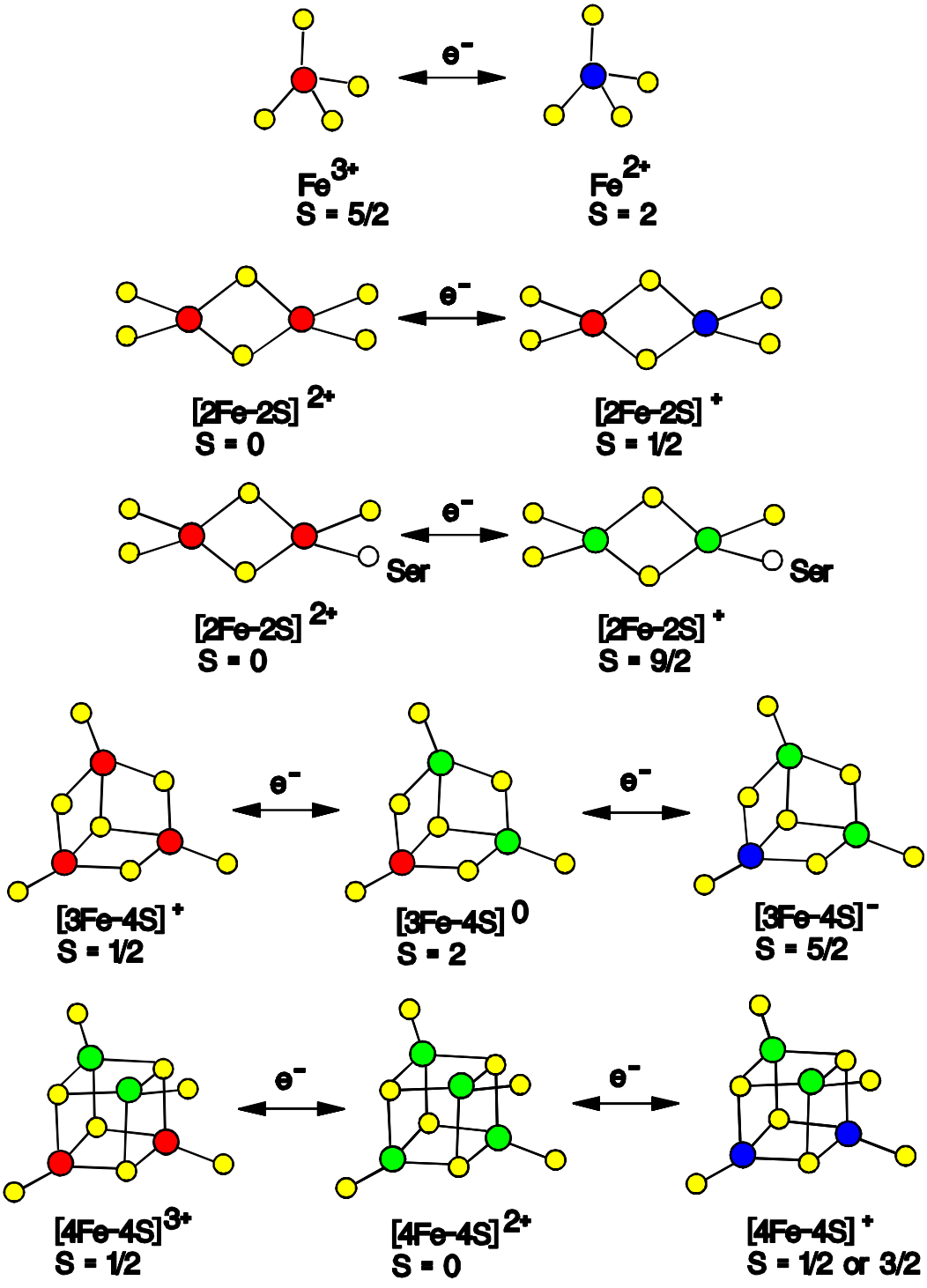
e⁻
Fe3+
S = 5/2
Fe2+
S = 2
e⁻
[2Fe-2S] 2+
S = 0
[2Fe-2S] +
S = 1/2
e⁻
Ser
Ser
[2Fe-2S] 2+
S = 0
[2Fe-2S] +
S = 9/2
e⁻
e⁻
[3Fe-4S] +
S = 1/2
[3Fe-4S] 0
S = 2
[3Fe-4S] -
S = 5/2
e⁻
e⁻
[4Fe-4S]3+
S = 1/2
[4Fe-4S] 2+
S = 0
[4Fe-4S] +
S = 1/2 or 3/2

Figure 1-3 Core oxidation states and experimentally determined spin states for crystallographically defined biological iron-sulfur clusters.

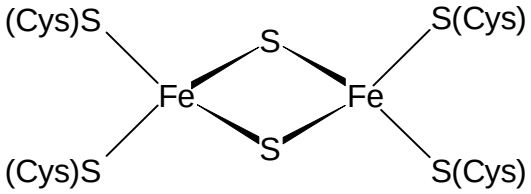

$[Fe_2S_2]^{2+}$ S = 0
$[Fe_2S_2]^{+}$ S = 1/2 or 9/2
$[Fe_2S_2]^{0}$ S = ?

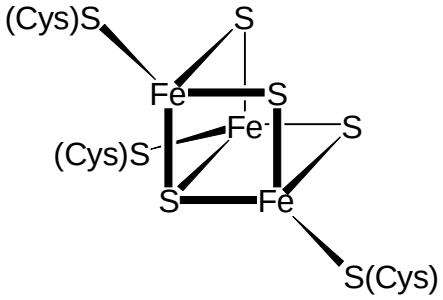

$[Fe_3S_4]^{+}$ S = 1/2
$[Fe_3S_4]^{0}$ S = 2
$[Fe_3S_4]^{-}$ S = 5/2
$[Fe_3S_4]^{2-}$ S = ?

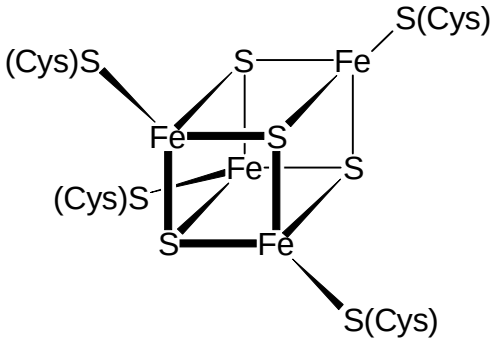

$[Fe_4S_4]^{3+}$ S = 1/2
$[Fe_4S_4]^{2+}$ S = 0
$[Fe_4S_4]^{+}$ S = 1/2 or 3/2
$[Fe_4S_4]^{0}$ S = 4

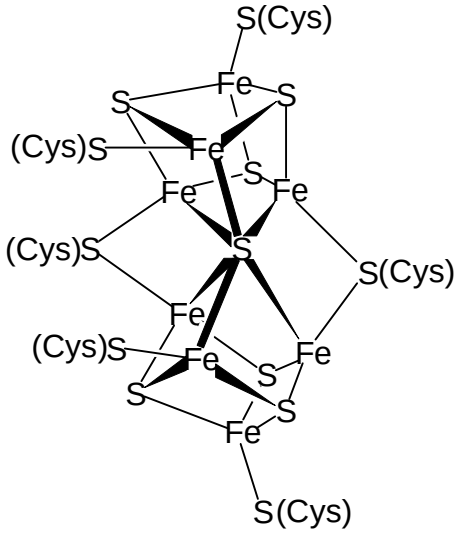

$[Fe_8S_7]^{5+}$ S = 7/2
$[Fe_8S_7]^{4+}$ S = 3 or 4
$[Fe_8S_7]^{3+}$ S = 1/2 or 5/2
$[Fe_8S_7]^{2+}$ S = 0

Figure 1-4 Characterized iron homeostasis and iron-sulfur cluster assembly gene products in the yeast, *Saccharomyces cerevisiae*. Blue colored gene products are involved in copper transport to Fet3. Yellow colors are involved in genetic regulation of iron homeostasis. Red colors are involved in iron uptake and maintenance of cellular iron levels. Pink colors are involved in iron-sulfur cluster assembly.

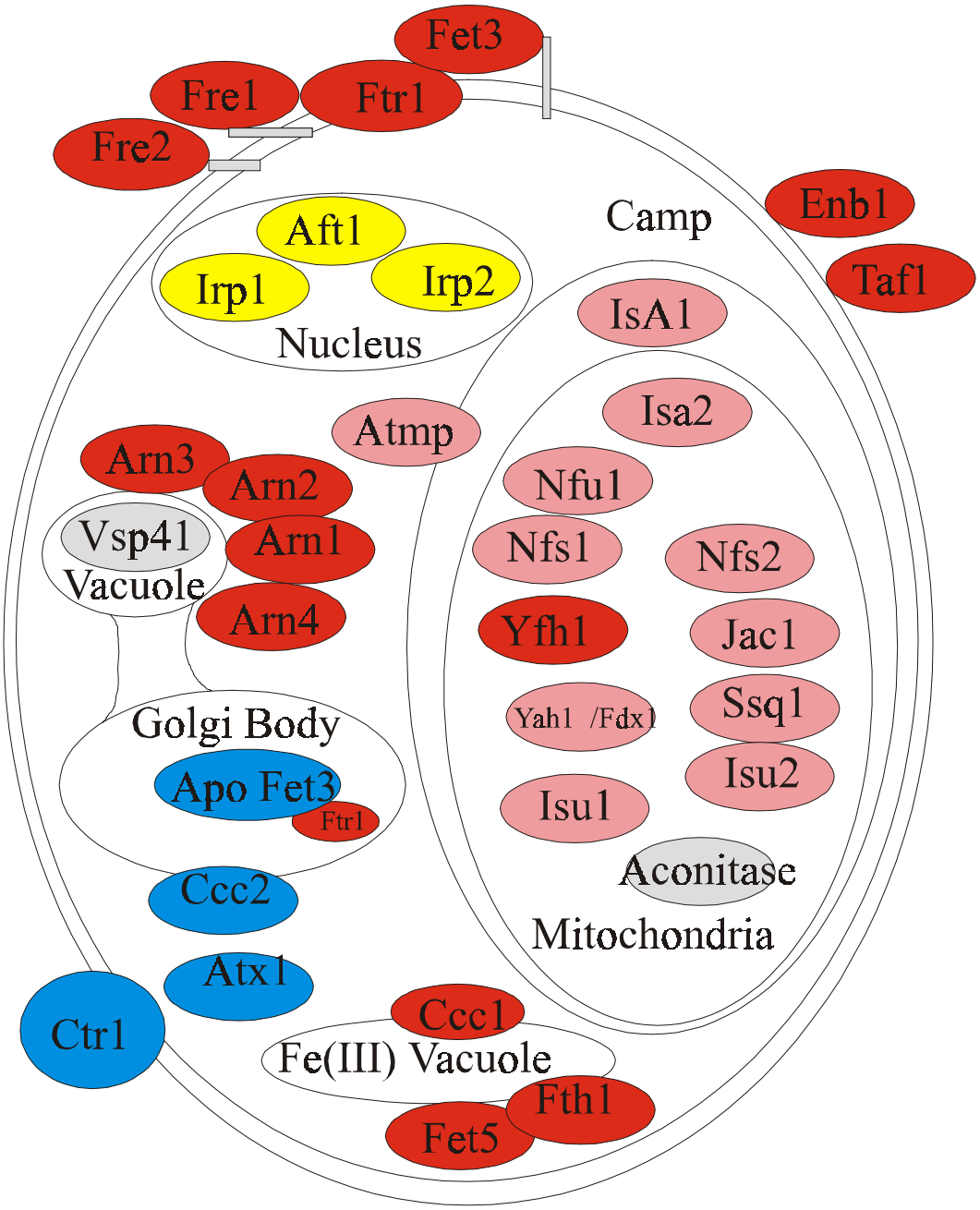
Fet3
Fre1
Ftr1
Fre2
Enb1
Camp
Taf1
Aft1
Irp1
Irp2
Nucleus
IsA1
Isa2
Atmp
Arn3
Arn2
Nfu1
Vsp41
Vacuole
Arn1
Nfs1
Nfs2
Arn4
Yfh1
Jac1
Golgi Body
Yah1 /Fdx1
Ssq1
Isu2
Apo Fet3
Ftr1
Isu1
Aconitase
Ccc2
Mitochondria
Atx1
Ctr1
Ccc1
Fe(III) Vacuole
Fth1
Fet5

Figure 1-5 Organization of iron-sulfur cluster assembly genes in *Azotobacter vinelandii* and *Escherichia coli*, and characterized iron-sulfur cluster assembly genes in the yeast *Saccharomyces cerevisiae*. The eukaryotic yeast genes are not clustered, and so their order on the figure does not represent their chromosomal organization.

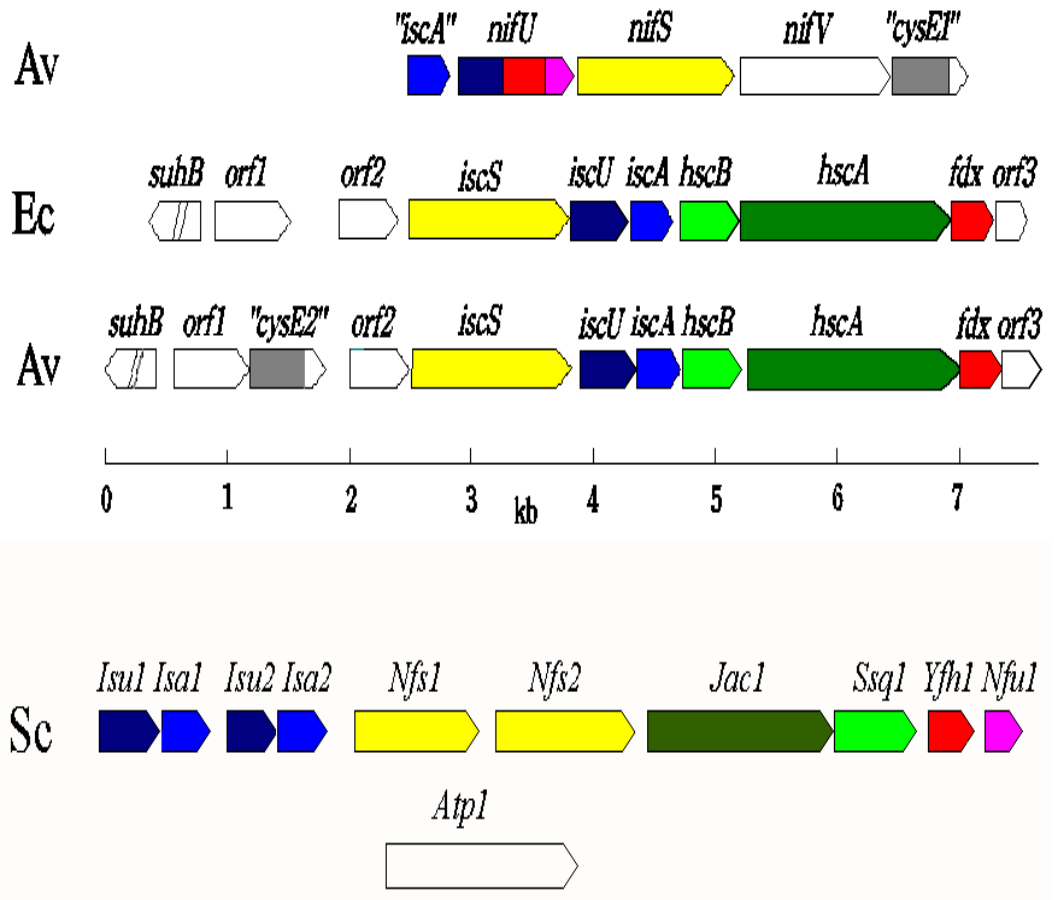
Av
"iscA"
nifU
nifS
nifV
"cysEI"
Ec
suhB
orf1
orf2
iscS
iscU
iscA
hscB
hscA
fdx
orf3
Av
suhB
orf1
"cysE2"
orf2
iscS
iscU
iscA
hscB
hscA
fdx
orf3
0
1
2
3
kb
4
5
6
7
Sc
Isu1
Isa1
Isu2
Isa2
Nfs1
Nfs2
Jac1
Ssq1
Yfh1
Nfu1
Atp1

Figure 1-6 Sequence comparison of IscA homologues.

IscA Sequence Alignments

Figure 1-7 Sequence comparison of IscU homologues.

IscU Sequence Alignments

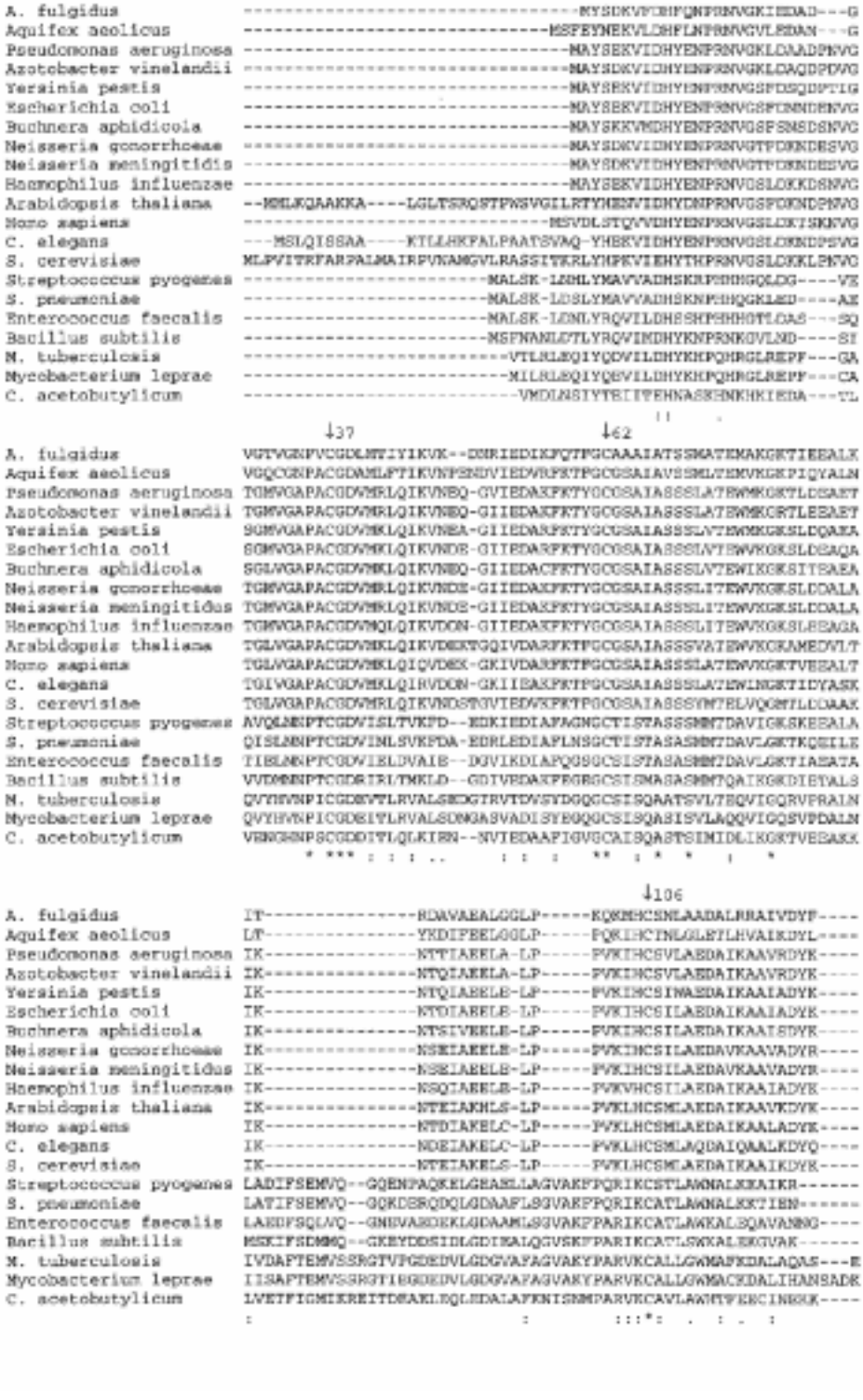

Chapter II

The *Azotobacter vinelandii* NifEN Complex Contains Two Identical [4Fe-4S] Clusters[1]

[1] Paul J. Goodwin,[‡] Jeffrey N. Agar,[§] Jon T. Roll,[¶] Gary P. Roberts,[¶] Michael K. Johnson,[§] and Dennis R. Dean[‡] (1998) *Biochemistry* **37,** 10420-10428.

[‡] *Department of Biochemistry, Virginia Tech, Blacksburg, VA 24061, and Department of Chemistry and Center for Metalloenzyme Studies,* [§]*University of Georgia, Athens, GA 30602, and* [¶]*Department of Bacteriology, the University of Wisconsin, Madison, WI 53706.*

ABSTRACT

The *nifE* and *nifN* gene products from *Azotobacter vinelandii* form an $\alpha_2\beta_2$ heterotetramer (NifEN complex) that is required for the biosynthesis of the nitrogenase FeMo-cofactor. The current model for NifEN complex organization and function is that it is structurally analogous to the nitrogenase MoFe protein and that it provides an intermediate assembly site for FeMo-cofactor biosynthesis. In the present work gene fusion and immobilized metal affinity chromatography strategies were used to elevate the *in vivo* production of NifEN complex and to facilitate its rapid and efficient purification. The NifEN complex produced and purified in this way exhibits the same FeMo-cofactor biosynthetic activity as previously described for NifEN complex purified by traditional chromatography methods. UV-visible, EPR, variable-temperature magnetic circular dichroism, and resonance Raman spectroscopies were used to show that the NifEN complex contains two identical $[4Fe\text{-}4S]^{2+,+}$. These clusters have a predominantly $S = 1/2$ ground state in the reduced form, exhibit a reduction potential of -350 mV, and are likely to be coordinated entirely by cysteinyl residues based on spectroscopic properties and sequence comparisons. A model is proposed where each NifEN complex [4Fe-4S] cluster is bridged between a NifE-NifN subunit interface at a position analogous to that occupied by the P-clusters in the nitrogenase MoFe protein. In contrast to the MoFe protein P-cluster, the NifEN complex [4Fe-4S] clusters are proposed to be asymmetrically coordinated to the NifEN complex where NifE cysteines-37, -62, and -124 and NifN cysteine-44 are the coordinating ligands. Based on a homology model of the three dimensional structure of the NifEN complex, the [4Fe-4S] cluster sites are likely to be remote from the proposed FeMo-cofactor assembly site and therefore, are unlikely to become incorporated into FeMo-cofactor during its assembly.

TEXTURAL FOOTNOTES

[1]Abbreviations: VTMCD, variable-temperature magnetic circular dichroism; RR, resonance Raman; NHE, normal hydrogen electrode

INTRODUCTION

Biological nitrogen fixation is catalyzed by nitrogenase, a metalloenzyme composed of two-component proteins called the Fe protein and MoFe protein (reviewed in 1-3). The Fe protein [also called dinitrogenase reductase (4)] is a homodimer that contains a single [4Fe-4S] cluster bridged between its identical subunits (5). The MoFe protein (also called dinitrogenase) is an $\alpha_2\beta_2$ heterotetramer that contains two pairs of novel metalloclusters called the P-cluster (Fe_8S_7) and the iron-molybdenum cofactor (FeMo-cofactor Fe_7S_9Mo:homocitrate]). Each αβ-unit of the MoFe protein is believed to comprise a single catalytic unit that contains one P-cluster and one FeMo-cofactor that are separated by approximately 17 Å. During catalysis the Fe protein delivers electrons to the MoFe protein in a process that involves association-dissociation of the component proteins, MgATP binding, and nucleotide hydrolysis (4). The nucleotide binding sites are located on the Fe protein and a minimum of two MgATP are hydrolyzed for each electron transfer event. The P-cluster is located at the αβ-interface of the MoFe protein and appears to function as an intermediate electron carrier site that accepts electrons from the Fe protein and subsequently effects their intramolecular delivery to FeMo-cofactor (6-8) the site of substrate binding and reduction (9-11).

Because FeMo-cofactor provides the site of substrate binding and reduction, its structure and assembly has attracted considerable attention. X-ray crystallographic analyses have shown that FeMo-cofactor consists of a metal sulfur core (Fe_7S_9Mo) and one molecule of (R)-homocitrate (12). The metal-sulfur core is constructed from Fe_3S_3Mo and Fe_4S_3 fragments that are connected by three inorganic sulfide bridges located between pairs of Fe atoms from opposing fragments. Homocitrate is coordinated to the Mo atom through its 2-hydroxyl and 2-carboxyl groups.

Biochemical and genetic studies using both *Azotobacter vinelandii* and *Klebsiella pneumoniae* have revealed that at least six *nif*-specific gene products, including NifB, NifE, NifN, NifV, NifQ, and NifH, are directly involved in the biosynthesis of

FeMo-cofactor (13). NifB catalyzes the formation of an FeMo-cofactor precursor called B-cofactor which is composed of an iron-sulfur core that does not include Mo or homocitrate (14). NifE and NifN form an $\alpha_2\beta_2$ heterotetramer (15) that is able to bind B-cofactor (16, 17), and in doing so provide an intermediate site for FeMo-cofactor biosynthesis. NifQ appears to have a role in the activation of Mo for FeMo-cofactor assembly (18), and NifV is a homocitrate synthase that provides the organic constituent of FeMo-cofactor (19, 20). The role of NifH (Fe protein) in FeMo-cofactor assembly is not yet understood but its role does not appear to involve either electron transfer or MgATP hydrolysis (21- 23). The Fe protein and the product of another gene [NifY in the case of *K. pneumoniae* (24, 25) and a protein called gamma in the case of *A. vinelandii* (26, 27)] also appear to have some role in the incorporation of FeMo-cofactor into the apo-MoFe protein. Other *nif*-specific gene products that might also participate in FeMo-cofactor biosynthesis include NifS [mobilization of S for Fe-S core formation (28)], NifU (mobilization of Fe for Fe-S core formation (29)) and NifWZ [possible roles in the incorporation of homocitrate during FeMo-cofactor formation (21)].

Most of what is known about the assembly of FeMo-cofactor has involved the application of *in vitro* reconstitution (9) and *in vitro* biosynthetic assays (30) developed by Shah and coworkers. For example, *in vitro* reconstitution assays were used to show that FeMo-cofactor is separately synthesized and then inserted into the apo-MoFe protein rather than being assembled stepwise into the apo-MoFe protein (31). This observation, primary sequence comparisons (32, 33), and the two-dimensional electrophoretic properties of NifE and NifN (34) ultimately led to the hypothesis that the NifEN complex provides a molecular scaffold for at least a portion of FeMo-cofactor biosynthesis (32). In related experiments it was found that NifB- and NifE- or NifN-deficient extracts could be mixed to achieve FeMo-cofactor formation, providing that Mo and MgATP were also added to the reaction mixture (30). Experiments of this sort provided an assay that permitted the isolation of small amounts of the NifEN complex (15), which was shown to

be an $\alpha_2\beta_2$ heterotetramer that contains Fe-S cluster(s). One problem encountered in the isolation and characterization of FeMo-cofactor biosynthetic enzymes is that they are only present in very low intracellular amounts. To date, this feature has precluded the purification of the NifEN complex in the quantities necessary for detailed biophysical characterization of its associated Fe-S cluster(s). In the present work a gene fusion approach for overproduction of the NifEN complex in *A. vinelandii* and the application of immobilized metal affinity chromatography for NifEN complex purification are described. These procedures have permitted purification of active NifEN complex in sufficient quantities for biophysical characterization.

EXPERIMENTAL PROCEDURES

DNA biochemistry and strain constructions. Transformation of *A. vinelandii* was performed as previously described by Page & von Tigerstrom (35). Strain DJ1061 (Figure 1) was constructed in several steps. In the first step, polymerase-chain-reaction (PCR)-directed DNA amplification and mutagenesis was used to obtain an approximately 0.9 Kb *Msc*I-*Sal*I fragment of *A. vinelandii* genomic DNA (32) that was incorporated into *Sma*I-*Sal*I-digested pUC119 vector DNA. This plasmid was designated pDB902 and it contains the *A. vinelandii nifE* promoter, as well as upstream and downstream sequences extending approximately 450 base-pairs in each direction. Plasmid pDB902 was also constructed so that a unique *Nde*I restriction enzyme site overlaps the *nifE* translation initiation site. Plasmid pDB904 was constructed by digesting pDB902 with *Nde*I and incorporating a kanamycin-resistance cartridge derived from pUC4-KAPA (36) at the *Nde*I site of pDB902. Plasmid pDB906 was constructed by digesting pDB902 with *Nde*I and then ligating a synthetic DNA cartridge into this site. The sense strand of the synthetic cartridge has the sequence: 5'T<u>ATG</u>CATCACCACCATCACCACCA3'. The triplet that corresponds to the *nifE* translation initiation codon is underlined in the synthetic DNA cartridge shown above. This construction places seven in-frame histidine codons between the initiating methionine-codon and the second codon of the cloned

portion of *nifE* carried on pDB906. Restriction enzyme mapping and DNA sequence analyses were used to confirm all plasmid constructions. Wild-type *A. vinelandii* cells were transformed using pDB904 DNA as the donor and then selecting for kanamycin resistance and scoring for ampicillin sensitivity. One transformant that resulted from double-reciprocal crossover events, and which is Nif-minus, kanamycin-resistant, and ampicillin-sensitive, was designated DJ1057. Strain DJ1061 was constructed by transformation of DJ1057, using pDB906 DNA as the donor, resulting in a Nif-plus, kanamycin-sensitive phenotype. Strain DJ1061 is genotypically identical to the wild-type except that there are seven histidine codons immediately following the initiating methionine codon at the N-terminus of *nifE*. It should be noted that none of the plasmids used for strain constructions described in the present work are capable of autonomous replication in *A. vinelandii*.

Strain DJ1041 (Figure 1) was also constructed in several steps. In the first step a DNA cartridge, extending from the *nifH* translation initiation site to approximately 500 base-pairs upstream, was generated by PCR amplification. This cartridge was constructed so that an *Nde*I restriction enzyme site was located at the *nifH* translation initiation site, and a *Bgl*II site was located approximately 500 base-pairs upstream of the *nifH* translation initiation site. This cartridge was digested by *Nde*I and *Bgl*II and ligated into *Nde*I-*Bgl*II-digested pT_7-7 plasmid vector DNA (37) to form plasmid pDB591. In the second step a *nifE* -gene cartridge was generated by PCR amplification so that an *Nde*I site was located at the *nifE*-initiation codon and a *Bam*HI site was located shortly downstream of the *nifE*-coding sequence. This cartridge was ligated into *Nde*I-*Bam*HI-digested pT_7-7 vector DNA to form pDB558. In the next step pDB558 was digested with *Nde*I and *Bam*HI and the resulting *nifE*-cartridge purified and ligated into *Nde*I-*Bam*HI-digested pDB591 to form pDB597. Construction of pDB597 results in a fusion of the *nifH*-transcriptional and -translational elements to the coding portion of the *nifE* gene. In the final step of plasmid constructions pDB597 was digested with *Nde*I and

ligated with the same synthetic DNA cartridge described above to form plasmid pDB867. This construction places seven in-frame histidine codons between the initiating methionine-codon and the second codon of the *nifE* -coding sequence. The fusion of the *nifH* promoter sequence with the *nifE*-coding sequence carried by pDB867 was then transferred to the *A. vinelandii* chromosome to yield strain DJ1041. This construction was accomplished by transformation using congression (coincident transfer of unlinked genetic markers) where the rifampicin-resistance marker contained in pDB303 (38) was used as the selected marker. The phenotype of DJ1041 is Nif-minus and rifampicin-resistant.

Cell growth, purification of the NifEN complex, and assays. A. vinelandii cells were grown at 30°C in a 150 liter custom-built fermenter (W. B. Moore, Inc. Easton , PA) in modified Burk medium (39) containing 10 mM Na_2MoO_4 and 10 mM urea. Cultures were sparged with pressurized air (80 l/min at 5 psi) and agitated at 125 rpm. When the cell density reached 180 Klett units (red filter) they were derepressed for *nif*-gene expression by concentration and resuspension in Burk medium with no added nitrogen source (40). Harvested cells were stored at -80°C until used. Crude extracts were prepared by the osmotic shock method (41) in degassed buffer containing 25 mM Tris-HCl (pH 7.9) and 1 mM sodium dithionite. Prior to NifEN complex purification, the extracts were made 500 mM in NaCl by the addition of degassed, granular NaCl. All biochemical manipulations were performed under an Argon atmosphere using a Schlenk apparatus. Approximately 120 grams of cells (wet weight) were processed for each purification yielding approximately 10 g of total protein in the crude extract. The NifEN complex was purified using immobilized-metal-affinity-chromatography (IMAC) and DEAE-sepharose anion-exchange chromatography (Amersham-Pharmacia, Piscataway, NJ). Cell extracts were loaded on an IMAC Zn(II)-charged column (30 ml of resin in a 1.5 cm x 15 cm column) using a peristaltic pump. After loading the extract, the column was washed with three column volumes of the above buffer containing 20 mM

imidazole-HCl. The protein that remained bound to the column was then eluted using the above buffer containing 250 mM imidazole-HCl. The eluted protein was collected and diluted 7 x in a degassed buffer (25 mM Tris-HCl, pH 7.9) containing 1 mM sodium dithionite. The diluted protein was then loaded onto a DEAE-sepharose column (30 ml of resin in a 1.5 cm x 15 cm column) and eluted using a linear NaCl gradient (100 mM to 300 mM NaCl over 5 column volumes). The NifEN fraction, which eluted at approximately 250 mM NaCl, was collected and concentrated using an Amicon concentrator (Beverly, MA) fitted with a YM100 filter. Concentrated protein was pelleted and stored in liquid nitrogen until used. Protein purity was monitored by SDS-PAGE electrophoresis as previously described (40). Protein was quantitated by the BCA method using bovine serum albumin as the standard (42).

NifEN activity was determined by slight modifications of previously described procedures (14, 17). Each degassed 9-ml reaction vial included 0 to 60 mg of isolated NifEN, 100 ml of 25 mM Tris-HCl (pH 7.4, 1.0 mM sodium dithionite), 20 ml of 5 mM homocitrate, 10 ml of 1.0 mM Na_2MoO_4, 200 ml of an ATP-regenerating system, and 200 ml of DJ1007 (Δ*nifE*) crude extract. The reaction vial also included an excess of B-cofactor, which is necessary for FeMo-cofactor biosynthesis (20 ml of an isolated B-cofactor preparation provided by V. K. Shah was used [14]). Vials were incubated at 30 °C for 30 min to allow FeMo-cofactor biosynthesis and insertion into apo-MoFe protein present in the DJ1007 crude extract. An additional 800 ml of the ATP-regenerating system was then added, the vials brought to 1 atm, and a 30 min acetylene reduction assay was performed under a 10% acetylene atm at 30 °C. Ethylene formation was monitored using a Hewlett Packard 5890A gas chromatograph equipped with an FID detector. The amount of apo-MoFe protein present in the DJ1007 extract was estimated by the reconstitution system using isolated FeMo-cofactor as previously described (9). FeMo-cofactor used in the present work was a gift from V. K. Shah.

Preparation of Antisera Against NifN. For the preparation of antibodies against NifN for use in western analyses, NifN was produced at a high level in *E. coli* and purified. For this purpose a PCR-generated *nifN* gene cartridge was cloned into the *Nde*I-*Bam*HI sites of the cloning vector pT_7-7 to form pDB560. This construct places expression of *nifN* under the T_7 control elements. Plasmid pDB560 was then transformed into the *E. coli* host strain BL21(DE3). NifN was then produced at a high level and purified by using essentially the same procedures previously described for the high level of expression and purification of NifU (29). Purified NifN was then sent to Cocalico Biologicals Inc., Reamstown, PA, for commercial production of Rabbit anti-NifN antisera. Chemicals for western analysis were obtained from ICN Biomedicals (Costa Mesa, CA) and the procedures recommended by the supplier were followed.

Spectroscopic Characterization of NifEN. The sample concentrations given in the figure captions are based on the quantitation of the purified protein solution by the BCA method (42). Spectroscopic results and spin quantitations are per αβ-heterodimer. UV-visible absorption spectra were recorded under anaerobic conditions in septum-sealed 1-mm cuvettes using a Shimadzu 3101PC scanning spectrophotometer. Variable-temperature magnetic circular dichroism (VTMCD) spectra were recorded on samples containing 55% (v/v) glycerol in 1-mm cuvettes using an Oxford Instruments Spectromag 4000 (0-7 T) split coil superconducting magnet (1.5-300 K) mated to a Jasco J-715C spectropolarimeter. Experimental protocols used for VTMCD studies were performed as previously described (43,44). X-band (~9.6 GHz) EPR spectra were recorded on a Bruker ESP-300E EPR spectrometer equipped with a dual mode ER-4116 cavity and an Oxford Instruments ESR-9 flow cryostat. Frequencies were measured with a Systron-Donner 6054B frequency counter, while the magnetic field was calibrated with a Bruker ER035M gaussmeter. Spin quantitations were carried out under non saturating conditions with 1mM Cu(II)EDTA as the standard, using the procedures outlined by Aasa and Vänngård (45).

Resonance Raman (RR) spectra were recorded using an Instruments SA Ramanor U1000 spectrometer fitted with a cooled RCA 31034 photomultiplier tube with 90° scattering geometry. Spectra were recorded digitally using photon-counting electronics, and signal-to-noise was improved by signal averaging of multiple scans. Band positions were calibrated using the excitation frequency and CCl_4 and are accurate to $\pm 1 cm^{-1}$. Laser excitation lines were from a Coherent Innova 100 10-W argon ion laser, with plasma lines removed using a Pellin Broca Prism premonochromater. Raman samples were placed in a specially designed sample cell (46) at the end of an Air Products Displex Model CSA-202E closed-cycle refrigerator and remained at 28 K and under an atmosphere of argon throughout scanning. The low sample temperature facilitates improved spectral resolution and prevents laser-induced sample degradation. Scattering was collected from the surface of a frozen 12 µL droplet.

EPR redox titration was performed at ambient temperature (25-27°C) within a glovebox under anaerobic conditions, using 20 mM Tris-HCl buffer (pH 7.8) and 300 mM NaCl. The concentration of the NifEN complex was 140 mM. Each mediator dye was added to a concentration of 50 mM in order to cover the range of -500 through -100 mV (vs NHE). The mediator dyes used were methyl viologen, benzyl viologen, neutral red, safranin O, anthraquinone-2-sulfonate, phenosafranin, and anthraquinone-1-5-disulfonate. Samples were first reduced by addition of excess sodium dithionite followed by oxidative titration with potassium ferricyanide. Potentials were measured with a platinum working electrode and a saturated Ag/AgCl reference electrode. After equilibration at the desired potential, a 250 mL aliquot was transferred to a calibrated EPR tube and frozen immediately in liquid nitrogen. Redox potentials are reported relative to the NHE.

RESULTS

Expression and Purification of the NifEN complex. Figure 1 shows a schematic of the relevant genomic *nif*-region for the wild type (DJ) and the two strains (DJ1061 & DJ1041) that were constructed by gene-directed mutagenesis and gene-replacement

techniques. Strain DJ1041 was designed for elevated production of the *nifEN* gene products and facile purification of the NifEN complex by using IMAC. The first of these goals was achieved by deleting the intervening region between the relatively strong *nifH* promoter and the *nifEN* structural genes, thereby placing the expression of *nifEN* under the direction of the *nifH* transcriptional and translational control elements. The second goal was made possible by placing seven histidine codons between the methionine initiation codon and the second codon of the *nifE*-coding sequence.

Strain DJ1061 was constructed to: (a) determine whether or not insertion of the polyhistidine coding sequence at the N-terminus of *nifE* alters the *in vivo* activity of the NifEN complex and, (b) permit the comparison of the relative amounts of the NifEN complex that accumulate when *nifEN* expression is driven by either the *nifE*- or the *nifH*-control elements. Both the wild type and DJ1061 grow at the same rate (doubling-time of 2.2 - 2.4 hours) when cultured under diazotrophic growth conditions. Thus, because strains deleted for *nifE* are unable to grow diazotrophically (33), this result indicates that placement of the poly-histidine tail at the N-terminal region of NifE does not impair the NifEN complex to an extent that can be detected *in vivo*.

Figure 2A and 2B show SDS-PAGE profiles for fractions obtained during the purification of the NifEN complex from DJ1061 and DJ1041, respectively. The simple four-step purification procedure involves passing a crude extract prepared from *nif*-derepressed cells over a Zn(II) charged IMAC column, washing the column with a 20 mM imidazole-HCl buffer, eluting the bound protein with 250 mM imidazole-HCl buffer, and purifying by anion-exchange column chromatography. The relative amounts of NifEN complex purified from DJ1061 and DJ1041 shown in Figure 2, which represent different purifications performed on different days, cannot be quantitatively compared. Nevertheless, examination of the individual panels in Figure 2, which compare individual fractions at different stages of purification, clearly indicate that the amount of NifEN complex that can be purified from DJ1041 is much higher than from DJ1061. About 70

mg of pure NifEN complex can be routinely obtained from 10 gm of DJ1041 crude extract protein whereas only about 7 mg of NifEN complex can be obtained from the same amount of DJ1061 crude extract protein. Also, the estimated amount of NifEN complex obtained from DJ1061 crude extracts is probably an overestimation because there is a significant amount of contaminating proteins in the purified sample from DJ1061, as can be seen by close inspection of lane 5 in Figure 2A. Identification of the protein bands indicated as NifEN in Figure 2 was confirmed in two different ways. First, bands at a similar location were not recognized when crude extract from the wild-type strain was processed in the same way. This result is consistent with the fact that NifE from the parental wild-type strain does not have a polyhistidine tail. Second, the bands corresponding to NifN of the NifEN complex in Figure 2 were identified by western analysis (data not shown) using rabbit antibodies raised against purified NifN protein that was heterologously expressed in *E. coli*. Although the amount of NifEN complex accumulated by DJ1041 is much greater than that accumulated by DJ1061, the yield is still lower than might be expected for proteins whose synthesis is directed by the *nifH*-control elements. For example, in related studies we have also placed a polyhistidine tag near the N-terminus of *nifD*, which encodes the a-subunit of the MoFe protein, and whose synthesis is naturally directed by the *nifH*-promoter. By using the same IMAC approach described here for NifEN purification, 350 mg of polyhistidine tagged MoFe protein, having full catalytic activity ($\approx$ 2,000 nmoles H_2 evolved • min^{-1} • mg^{-1} protein), can be routinely isolated from 10 g of nitrogenase-derepressed crude extract (Christiansen, Goodwin, Zheng & Dean, unpublished). Although it is not known why NifEN from DJ1041 accumulates to levels lower than might be expected, it was found that the amount of NifEN that can be detected in crude extracts by western analysis drops dramatically after about three hours of nitrogenase derepression (data not shown). This result indicates that the NifEN complex might have a relatively short *in vivo* half-life. Roll *et al.* (17) have

also reported that the yield of NifEN complex obtained by using other purification methods is dependent upon the genetic background from which the complex is isolated.

IMAC-Purified NifEN Complex Activity. Previous work has shown that the NifEN complex isolated from a *nifB*-deficient *A. vinelandii* strain can be added to a *nifEN*-deficient crude extract to achieve activation of the apo-MoFe protein, providing other factors necessary for FeMo-cofactor biosynthesis (MgATP, Mo, and homocitrate) are also included (15, 17). Furthermore, FeMo-cofactor biosynthetic activity is maximized in this system when an excess of B-cofactor, product of NifB activity, is also added to the reaction mixture. In the present work it was important to establish that the NifEN complex isolated by the IMAC method has the same composition and at least a similar ability to effect *in vitro* activation of apo-MoFe protein as previously reported for NifEN complex isolated by other methods. These features were demonstrated in the following ways. The ability of IMAC-purified NifEN complex to activate apo-MoFe protein in extracts prepared from a *nifE*-deletion mutant was shown to be almost identical to that described for NifEN complex that was purified using the original purification scheme reported by Paustian *et al*. (Figure 3B; see Figure 5 in ref. 15). The maximum amount of activation of apo-MoFe protein effected by IMAC-purified NifEN complex (Figure 3B) also corresponds to the maximum amount of reconstitution that can be achieved by addition of isolated FeMo-cofactor to the same extract (Figure 3A). It was also found that, like the NifEN complex previously characterized (15), IMAC-purified NifEN complex is an $\alpha_2\beta_2$ heterotetramer, is oxygen labile, contains Fe, and exhibits a characteristic UV-visible spectrum in its oxidized and reduced states (Figure 4).

Biophysical Characterization of the NifEN Complex Fe-S Clusters:

UV-Visible Absorption. Figure 4 shows the UV-visible absorption of oxidized and reduced NifEN. The oxidized spectrum with its pronounced shoulder at 410 nm is characteristic of proteins containing $[4Fe\text{-}4S]^{2+}$ clusters (47). Upon reduction with dithionite, the peak at 410 nm diminishes and a broad featureless spectrum indicative of a

$[4Fe\text{-}4S]^{+}$ cluster appears. The molar extinction coefficients for oxidized (ε_{410}=13,500 $M^{-1}cm^{-1}$) and reduced (ε_{390}= 9,500 $M^{-1}cm^{-1}$) NifEN (expressed per $\alpha\beta$) indicate two $[4Fe\text{-}4S]^{2+,+}$ clusters per NifEN $\alpha_2\beta_2$-heterotetramer. These results are also in good agreement with iron analyses of NifEN, which indicate 9.5 ± 0.5 iron atoms per $\alpha_2\beta_2$ heterotetramer.

EPR and EPR-monitored Redox Titration. X-band EPR spectra of dithionite-reduced NifEN were recorded at temperatures in the range 4.2-100 K with microwave powers between 0.001 and 100 mW. A less extensive series of experiments were conducted on NifEN samples containing 55% (v/v) glycerol (i.e. the same samples used for VTMCD studies), and the EPR properties were found to be unperturbed by the presence of glycerol. A representative EPR spectra of dithionite-reduced NifEN is shown in Figure 5. The protein exhibits a fast relaxing rhombic resonance, g = 2.098, 1.927, 1.850, that is only clearly discernible at temperatures below 30 K. This resonance accounts for 2.3 ± 0.3 spins/$\alpha_2\beta_2$-heterotetramer and except for a minor adventitious Fe^{3+} ion signal centered at g = 4.3, there was no evidence for any $S > 1/2$ resonances in the low field region. Taken together, the spin quantitation, g-values and the relaxation properties indicate two S = 1/2 $[4Fe\text{-}4S]^{+}$ clusters per $\alpha_2\beta_2$. In order to assess the midpoint potential of the $[4Fe\text{-}4S]^{2+,+}$ couple, a dye-mediated EPR-monitored redox titration of purified NifEN was carried out at pH 7.8. Figure 6 shows a plot of the intensity of the S = 1/2 resonance as a function of the potential. A one-electron Nernst plot overlays the individual data points to a good approximation, indicating a midpoint potential of -350 ± 20 mV.

VTMCD. Temperature-dependant MCD bands are observed throughout the 300-800 nm region in the VTMCD spectra of reduced NIFEN (Figure 7). The pattern of these bands is characteristic of a $[4Fe\text{-}4S]^{+}$ cluster (47-50), with the derivative feature centered around 410 nm arising at least in part from a very minor heme contaminant. While the absence of a pronounced negative feature centered around 650 nm is generally

indicative of a $S = 3/2$ $[4Fe\text{-}4S]^{+}$ cluster (48, 49), MCD magnetization data collected at 536 nm (Figure 9) indicate that the cluster ground state is predominantly $S = 1/2$, in accord with the EPR results. The magnetization data collected at three fixed temperatures (1.8 K, 4.2 K and 10.0 K) are fit to first approximation by theoretical data constructed using the EPR-determined *g*-values, $g_{\parallel} = 2.098$ and $g_{\perp} = 1.888$. The intensities of the low-temperature MCD spectra of paramagnetic Fe-S clusters, compared under equivalent conditions after normalizing for concentration and path length, and correcting for sample depolarization (43, 44), provide an approximate estimation of cluster concentration. Synthetic and biological $S = 1/2$ $[4Fe\text{-}4S]^{+}$ clusters have Δ values for the positive band at 520 nm in the range of 60-90 $M^{-1}\,cm^{-1}$ at 4.5 T and 2 K (47, 48). The 2 K MCD spectrum of NifEN, which has $\Delta = 76\ M^{-1}\,cm^{-1}$ when quantified per αβ-heterodimer, complements the UV-visible molar extinction coefficients and the EPR spin quantitation in suggesting that there is one $[4Fe\text{-}4S]^{+}$ cluster per NifEN αβ-heterodimer.

Resonance Raman. Resonance Raman spectra in the Fe-S stretching region, 200-450 cm^{-1} provide a means for identifying both Fe-S type in diamagnetic redox states (52, 53) and assessing the cluster ligation (54, 55). The RR spectrum of thionine-oxidized NifEN complex obtained with 457.9-nm laser excitation is shown in Figure 9. The vibrational frequencies and relative intensities of the Fe-S stretching modes are characteristic of those established for $[4Fe\text{-}4S]^{2+}$ clusters (56, 57) and can be assigned by direct analogy under idealized tetrahedral symmetry for the $Fe_4S_4{}^{b}S_4{}^{t}$ unit (b = bridging and t = terminal), i.e. $\nu(T_2)$ $Fe\text{-}S^{b}$, 251 cm^{-1}; $\nu(T_1)$ $Fe\text{-}S^{b}$, 265 cm^{-1}; $\nu(E)$ $Fe\text{-}S^{b}$, 280 cm^{-1}; $\nu(A_1)$ $Fe\text{-}S^{b}$, 340 cm^{-1}; $\nu(T_2)$ $Fe\text{-}S^{t}$, 356 cm^{-1}, $\nu(T_2)$ $Fe\text{-}S^{b}$, 383 cm^{-1}, $\nu(A_1)$ $Fe\text{-}S^{t}$, 390 cm^{-1}. For example, resonance Raman spectra having similar relative band intensities and frequencies are observed for the $[4Fe\text{-}4S]^{2+}$ cluster contained in the nitrogenase Fe protein (56) and in synthetic analog complexes having benzyl thiolate ligands (57). The frequency of the most intense band, which corresponds to the totally symmetric breathing mode of the Fe_4S_4 cubane, has been found to a be a useful indicator of noncysteinyl coordination at

a specific Fe (49). This band occurs at 340 cm^{-1} in NifEN, just outside the range established for $[4Fe\text{-}4S]^{2+}$ clusters with complete cysteinyl ligation [333-339 cm^{-1} (49)] and within the range established for clusters with oxygenic ligation at a specific Fe site [339-342 cm^{-1} (54, 58)]. Although, this raises the possibility of an oxygenic cluster ligand, the slightly higher $\nu(A_1)$ Fe-S^b frequency could equally well be the result of a hitherto uninvestigated arrangement of coordinating cysteine residues. For example, sequence comparisons with the FeMo protein suggest cluster ligation by three cysteines from the NifE subunit and one from the NifN subunit, see below. This type of subunit bridging arrangement would be unique among Fe-S proteins and hence could account for a slightly higher frequency for the totally symmetric breathing mode.

DISCUSSION

It was previously shown (32, 33) that the products of the FeMo-cofactor biosynthetic genes, *nifE* and *nifN*, bear sequence identity when respectively compared to the α- and β-subunits of the MoFe protein. In other words, NifE has a primary sequence similar to NifD (MoFe protein α-subunit), and NifN has a primary sequence similar to NifK (MoFe protein β-subunit). Such primary sequence comparisons, the relative migration patterns of NifD, NifK, NifE and NifN on two-dimensional electrophoretic gels (34), the *in vivo* mutual stability requirements for NifE and NifN (34), and the observation that FeMo-cofactor biosynthesis is completed prior to its insertion into apo-MoFe protein (31), led to the hypothesis that NifE and NifN form a complex (34) that is structurally homologous to the MoFe protein and which provides a scaffold for one or more steps in FeMo-cofactor biosynthesis (33). This hypothesis was supported by Paustian *et al.* (26) who purified a heterotetrameric form of NifEN from *A. vinelandii*, and reported evidence that the as-isolated NifEN complex contains an Fe-S cluster. In the case of the MoFe protein there are two different types of metalloclusters, the P-cluster and the FeMo-cofactor (1-3). Thus, by analogy to the MoFe protein, it is reasonable to expect that the NifEN complex could also have two types of metalloclusters. One such site

within the NifEN complex could be analogous to the MoFe protein P-cluster site, while the other provides an FeMo-cofactor intermediate assembly site. In this model the NifEN complex is expected to cycle between a "charged" form that contains an FeMo-cofactor intermediate and a "discharged" form that has released the FeMo-cofactor intermediate during maturation of the apo-MoFe protein (59). Strong evidence supporting this possibility was reported by Roll *et al*. (17), who found that the native electrophoretic mobility of the NifEN complex is different in crude extracts prepared from different genetic backgrounds. For example, the native electrophoretic mobility of the NifEN complex present in a NifB-deficient crude extract is different than the native electrophoretic mobility of NifEN complex present in a MoFe protein-deficient crude extract. Importantly, the addition of B-cofactor to a NifB-deficient crude extract alters the native electrophoretic mobility of the NifEN complex so that it now has the same native electrophoretic mobility as NifEN complex present in a MoFe protein-deficient crude extract. Because the originally purified NifEN complex was obtained from a NifB-deficient background and therefore can not contain B-cofactor, the question arises about the nature and function of the Fe-S cluster contained in the as-isolated NifEN complex. It should be noted that, although it appears that B-cofactor is attached to the NifEN complex in the early stages of its purification from a MoFe protein-deficient background, NifEN complexes isolated from either a NifB-deficient or MoFe protein-deficient background appear to be identical (17). In other words, B-cofactor is lost from the NifEN complex during its purification from a MoFe protein-deficient background.

In order to purify enough NifEN complex for rigorous biophysical analyses, gene fusion and affinity purification methods were respectively used to elevate the *in vivo* level of NifEN complex and to facilitate its rapid and efficient purification. The NifEN complex produced and purified in this way is apparently unaltered in either its *in vivo* or *in vitro* activities. In the present study a combination of UV-visible, EPR, VTMCD, and RR

spectroscopies have been used to show that the Fe contained in the as-isolated NifEN complex is organized into two identical [4Fe-4S]$^{2+,+}$ clusters. These clusters are ligated to the protein complex for the most part or entirely by cysteine residues, have predominantly S = 1/2 ground states in the reduced form, and exhibit a midpoint potential of -350 mV. What then is the function of the [4Fe-4S] clusters contained within the as-isolated NifEN complex? Among the obvious possibilities are: (i) they play a structural role in formation or stabilization of the heterotetrameric complex, (ii) they have a redox function that is necessary for FeMo-cofactor formation, (iii) they are FeMo-cofactor precursors, or (iv) some combination of these possibilities.

Muchmore *et al.* (21) have previously developed a homology model for the three-dimensional structure of the NifEN complex that is based on the crystallographically solved MoFe protein structure (1). This model places four cysteine residues (three from NifE - residues-37, -62 and -124; and one from NifN - residue-44) in the appropriate geometry to form a [4Fe-4S] cluster that is located at the NifE-NifN interface at a position analogous to the MoFe protein P-cluster site (Figure10). We favor this model because the four proposed [4Fe-4S] cysteine ligands, and the proposed FeMo-cofactor assembly site cysteine [residue-250 (32, 33)], are the only conserved cysteines among all known NifE and NifN primary sequences (60). This model indicates that the NifEN complex [4Fe-4S] clusters are most likely to play structural and/or redox roles rather than becoming incorporated into FeMo-cofactor during its assembly, because it places the proposed [4Fe-4S] cluster sites at positions that are remote from the proposed FeMo-cofactor assembly sites (21). Site-directed mutagenesis and gene-replacement experiments similar to those used to alter the functional properties of the P-cluster (61) should be useful in clarifying the functional role of the [4Fe-4S] clusters contained within the NifEN complex. This approach, and the availability of relatively large amounts of purified NifEN complex, should also help extend the experimental strategy described Roll *et al.* (17) to clarify the nature of the interaction of B-cofactor with the NifEN complex and to determine if the

B-cofactor Fe-S core is rearranged or further processed upon its binding to the NifEN complex.

Acknowledgements We thank Vinod Shah for supplying samples of B-cofactor and FeMo-cofactor and for providing invaluable advice. We thank Chris Staples and Shannon Garton for help with the spectroscopic measurements.

References

1. Howard, J. B., and Rees, D. C. (1994) *Annu. Rev. Biochem*. **63**, 235-264.

2. Peters, J. W., Fisher, K., and Dean, D. R. (1995) *Ann. Rev. Microbiol*. **49**, 335-366.

3. Burgess, B. K., and Lowe, D. J. (1996) *Chem. Rev*. **96**, 2983-3011.

4. Hageman, R. V., and Burris, R. H. (1978) *Proc. Natl. Acad. Sci. U.S.A.* **75**, 2699-2702.

5. Hausinger, R. P., and Howard, J. B. (1983) *J. Biol. Chem*. **258**, 13486-13492.

6. Lowe, D. J., Fisher, K., and Thorneley, R. N. F., (1993) *Biochem. J*. **292**, 93-98.

7. Peters, J. W., Fisher, K., Newton, W. E., and Dean, D. R. (1995) *J. Biol. Chem.* **270**, 27007-27013.

8. Lanzilotta, W. N., and Seefeldt, L. C. (1996) *Biochemistry* **35**, 16770-16776.

9. Shah, V. K., and Brill, W. J. (1977) *Proc. Natl. Acad. Sci. U.S.A*. **74**, 3249-3253.

10. Hawkes, T. R., McLean, P. A., and Smith, B. E. (1984) *Biochem. J*. **217**, 317-321.

11. Scott, D. J., May, H. D., Newton, W. E., Brigle, K. E., and Dean, D. R. (1990) *Nature* **343**, 188-190.

12. Kim, J., and Rees, D. C. (1992) *Science* **257**, 1677-1682.

13. Ludden, P. W., Shah, V. K., Roberts, G. P., Ruttiman-Johnson, C., Rangaraj, P., Foulger, T., Allen, R. M., Homer, M., Roll, J., Zhang, X., and Chatterjee, R. (1998) in *Biological Nitrogen Fixation for the 21st Century* (Elmerich, C., Kondorosi, A., and Newton, W. E., Eds.) pp 33-38, Kluwer Academic Publishers, Dordrecht, The Netherlands.

14. Shah, V. K., Allen, J. R., Spangler, N. J., and Ludden, P. W. (1994) *J. Biol. Chem*. **269**, 1154-1158.

15. Paustian, T. D., Shah, V. K., and Roberts, G. P. (1989) *Proc. Natl. Acad. Sci. U.S.A.* **86**, 6082-6086.

16. Allen, R. M., Chatterjee, R., Ludden, P. W., and Shah, V. K. (1995) *J. Biol. Chem*. **270**, 26890-26896.

17. Roll, J. T., Shah, V. K., Dean, D. R., and Roberts, G. P. (1995) *J. Biol. Chem*. **270**, 4432-4437.

18. Imperial, J., Ugalde, R. A., Shah, V. K., and Brill, W. J. (1984) *J. Bacteriol*. **158**, 187-194.

19. Hoover, T. R., Imperial, J., Ludden, P. W., and Shah, V. K. (1989) *Biochemistry* **28**, 2768-2771.

20. Zheng, L., White, R. H., and Dean, D. R. (1997) *J. Bacteriol*. **179**, 5963-5966.

21. Muchmore, S. W., Jack, R. F., and Dean, D. R. (1996) in *Mechanisms of Metallocenter Assembly* (Hausinger, R. P., Eichhorn, G. L., and Marzilli, L. G., Eds.) pp111-132, VCH Publishers Inc., New York.

22. Gavini, N., and Burgess, B. K. (1992) *J. Biol. Chem*. **267**, 21179-21186.

23. Rangaraj, P., Shah, V. K., and Ludden, P. W. (1997) *Proc. Natl. Acad. Sci. U.S.A.* **94**, 11250-11255.

24. White, T. C., Harris, G. S., and Orme-Johnson, W. H. (1992) *J. Biol. Chem*. **267**, 24007-24016.

25. Homer, M. J., Paustian, T. D., Shah, V. K., and Roberts, G. P. (1993) *J. Bacteriol*. **175**, 4907-4910.

26. Paustian, T. D., Shah, V. K., and Roberts, G. P. (1990) *Biochemistry* **29**, 3515-3522.

27. Homer, M. J., Dean, D. R., and Roberts, G. P. (1995) *J. Biol. Chem*. **270**, 24745-24752.

28. Zheng, L., White, R. H., Cash, V. L., Jack, R. F., and Dean, D. R. (1993) *Proc. Natl. Acad. Sci. U.S.A.* **90**, 2754-2758.

29. Fu, W., Jack, R. F., Morgan, T. V., Dean, D. R., and Johnson, M. K. (1994) *Biochemistry* **33**, 13455-13463.

30. Shah, V. K., Imperial, J., Ugalde, R. A., Ludden, P. W., and Brill, W. J. (1986) *Proc. Natl. Acad. Sci. U.S.A.* **83**, 1636-1640.

31. Ugalde, R. A., Imperial, J., Shah, V. K., and Brill, W. J. (1984) *J. Bacteriol*. **159**, 888-893.

32. Dean, D. R., and Brigle, K. E. (1985) *Proc. Natl. Acad. Sci. U.S.A.* **82**, 5720-5723.

33. Brigle, K. E., Weiss, M. C., Newton, W. E., and Dean, D. R. (1987) *J. Bacteriol*. **169**, 1547-1553.

34. Roberts, G. P., and Brill, W. J. (1980) *J. Bacteriol*. **144**, 210-216.

35. Page, W. J., and von Tigerstrom, M. (1979) *J. Bacteriol*. **139**,1058-1061.

36. Vieira, J., and Messing, J. (1982) *Gene* **19**, 259-268.

37. Tabor, S., and Richardson, C. C. (1985) *Proc. Natl. Acad. Sci. U.S.A.* **82**, 1074-1078.

38. Robinson, A. C., Burgess, B. K., and Dean, D. R. (1986) *J. Bacteriol.* **166**, 180-186.

39. Stranberg, G. W., and Wilson, P. W. (1968) *Can. J. Microbiol*. **14**, 25-31.

40. Scott, D. J., Dean, D. R., and Newton, W. E. (1992) *J. Biol. Chem.* **267**, 20020-20010.

41. Shah, V. K., Davis, L. C., and Brill, W. J. (1972) *Biochim. Biophys. Acta.* **256**, 498-511.

42. Smith, P. K., Krohn, R. I., Hermanson, G. T., Mallia, A. K., Gartner, F. H., Provenzano, M. D., Fujimoto, E. K., Goeke, N. M., Olson, B. J., and Klenk, D. C. (1985) *Anal. Biochem.* **150**, 76-85.

43. Johnson, M. K. (1988) in *Metal Clusters in Proteins* (Que, L., Ed.) ACS Symposium Series, Vol. 372, pp. 326-342, Washington D.C.

44. Thomson, A. J., Cheeseman, M. R., and George, S. J. (1993) *Meth. Enzymol.* **226**, 199-232.

45. Aasa, R., and Vänngård, T. (1975) *J. Magn. Reson.* **19**, 308-315.

46. Drozdzewski, P. M., and Johnson, M. K. (1988) *Appl. Spectros.* 42, 1575-1577.

47. Johnson, M. K., Robinson, A. E., and Thomson, A.J. (1982) in *Iron-Sulfur Proteins* (Spiro, T.G., Ed.) pp 367-406, Wiley-Interscience, New York.

48. Onate, Y. A, Finnegan, M. G., Hales, B. J., and Johnson, M. K. (1993) *Biochim. Biophys. Acta.* **1164**, 113-123.

49. Conover, R. C., Kowal, A. T., Fu, W. Park, J. B. Aono, S., Adams, M. W. W., and Johnson, M. K. (1990) *J. Biol. Chem.* **265**, 8533-8541.

50. Conover, R. C., Park, J. B., Adams, M. W. W., and Johnson, M. K. (1991) *J. Am. Chem. Soc.* **113**, 2799-2800.

51. Thomson, A. J., and Johnson, M. K. (1980) *Biochem. J.* **191**, 411-420.

52. Spiro T. G., Hare, J., Yachandra, V., Gewirth, A., Johnson, M. K., and Remsen, E. (1982) in *Iron-Sulfur Proteins* (Spiro, T. G., Ed.) pp 407-423, Wiley-Interscience, New York.

53. Spiro, T. G., Czernuszewicz, R. S., and Han, S. (1988) in *Resonance Raman Spectra of Heme and Metalloproteins* (Spiro, T. B., Ed.) pp 523-554, John Wiley & Sons, New York.

54. Conover, R. C., Kowal, A. T., Fu, W., Park, J. B., Aono, S., Adams, M. W. W., and Johnson M. K. (1990) *J. Biol. Chem.* **265**, 8533-8541.

55. Duin, E. C., Lafferty, M. E., Crouse, B. R., Allen, R. M., Sanyal, I., Flint, D. H., and Johnson, M. K. (1997) *Biochemistry* **36**, 11811-11820.

56. Czernuszewicz, R. S., Macor, K. A., Johnson, M. K., Gewirth, A., and Spiro, T. G. (1987) *J. Am. Chem. Soc*. **109**, 7178-7187.

57. Fu, W., Morgan, T. V., Mortenson, L.E., and Johnson, M. K. (1991) *FEBS Lett*. **284**, 165-168.

58. Kilpatrick, L. K., Kennedy, M. C., Beinert, H., Czernuszewicz, R. S., Qiu, D., and Spiro, T. G. (1994) *J. Am. Chem. Soc.* **116**, 4053-4061.

59. Dean, D. R., Bolin, J. T., and Zheng, L. (1993) *J. Bacteriol.* **175**, 6737-6744.

60. Dean, D. R., and Jacobson, M. R. (1992) in *Biological Nitrogen Fixation* (Stacey, G., Burris, R. H. and Evans, H. J. Eds.) pp.763-834 Chapman and Hall, New York.

61. Dean, D. R., Setterquist, R. A., Brigle, K. E., Scott, D. J., Laird, N. F., and Newton, W. E. (1990) *Molec. Microbiol.* **4**, 1505-1512.

62. Peters, J. W., Stowell, M. H. B., Soltis, M. S, Finnegan, M. G., Johnson, M. K. and Rees, D. C. (1997) *Biochemistry* **36**, 1181-1187.

Figure 2-1 Organization of *nif*-specific genes relevant to the present work. Horizontal arrows indicate the direction of transcription. The approximate position of the *nifH* promoter is indicated by a filled box, and filled circles indicate the approximate positions of promoters for other transcription units. The cross-hatched bar indicates the region deleted from the chromosome in construction of DJ1041. The filled portion at the begininng of the *nifE* gene for DJ1061 and DJ1041 indicates the position of the respective polyhistidine tags.

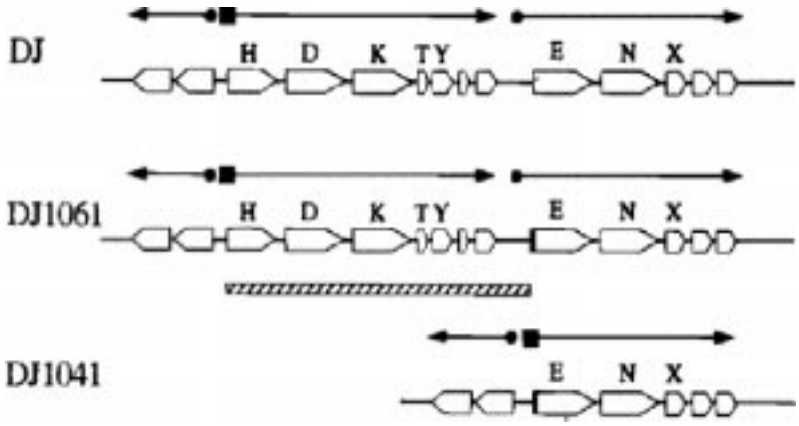
DJ
H
D
K
TY
E
N
X
DJ1061
H
D
K
TY
E
N
X
DJ1041
E
N
X

Figure 2-2 IMAC purification of the NifEN complex from DJ1061 (panel A) and DJ1041 (panel B). The proteins were separated by 12% SDS-PAGE and stained with coomasie brilliant blue. Lane 1, M_r standards (phosphorylase *b*, bovine serum albumin, carbonic anhydrase and, soybean trypsin inhibitor); Lane 2, crude extract; Lane 3, column flow through; Lane 4, 20 mM imidazole-HCl wash fraction; Lane 5, purified NifEN complex. Leftward arrows indicate the position of NifE (upper band) and NifN (lower band). The rightward arrow in panel B indicates the position of the MoFe protein α- and β-subunits. Corresponding MoFe protein subunit bands are not seen in panel B because *nifDK* are deleted in strain DJ1061.

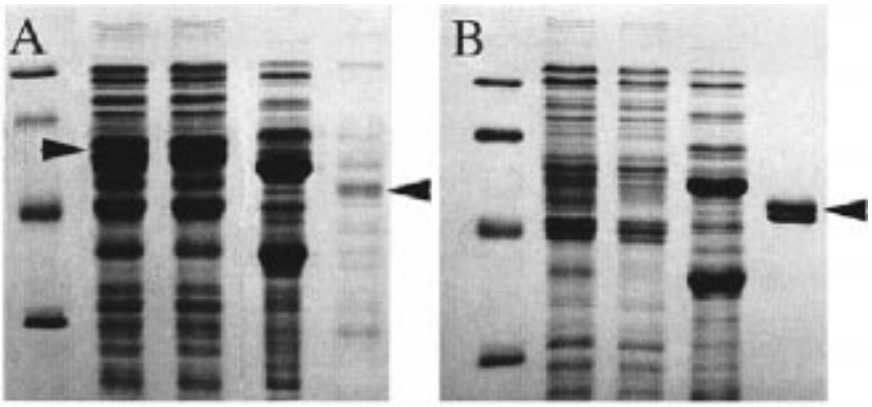
A
B

Figure 2-3 Reconstitution of apo-MoFe protein using either isolated FeMo-cofactor (panel A) or the FeMo-cofactor biosynthesis system (panel B). Activity is expressed as nanomoles of ethylene produced per min. Assay conditions are described in Experimental Procedures. For the biosynthetic assay shown in panel B all known components required for FeMo-cofactor biosynthesis are present in excess except for the NifEN complex. The same crude extract (9.0 mg for each assay) was used for all reconstitution assays shown in panel A and panel B. Data points represent the average of two independent assays.

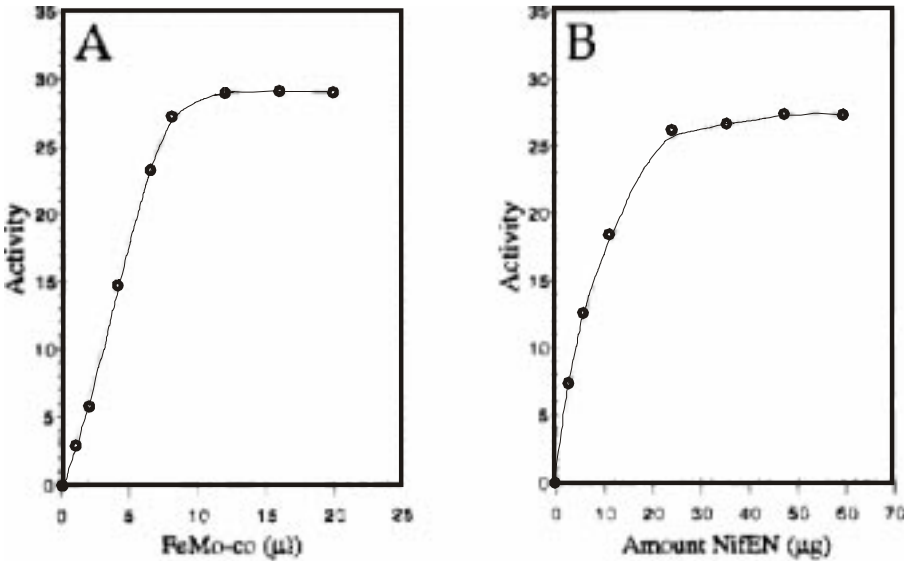
A
Activity
FeMo-co (µl)
B
Activity
Amount NifEN (µg)

Figure 2-4 UV-visible absorption for oxidized and reduced NifEN. Excess sodium dithionite was removed from reduced NifEN (lower spectrum) by anaerobic buffer exchange. NifEN was oxidized with thionine (upper spectrum) and the excess was removed by anaerobic buffer exchange.

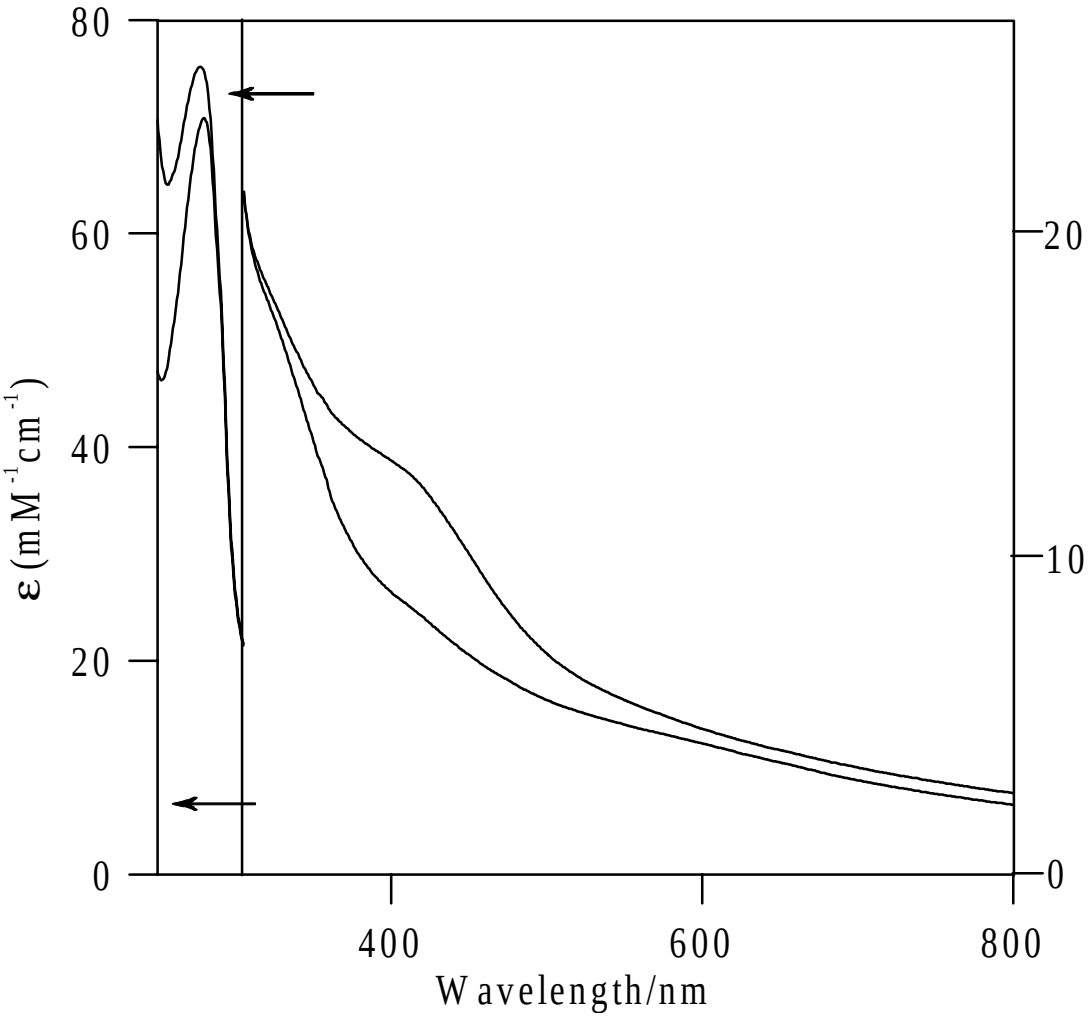
80
60
40
20
0
20
10
0
400
600
800
Wavelength/nm
ε (mM-1cm-1)

Figure 2-5 X-band EPR spectrum of dithionite-reduced NifEN. The sample (0.4 mM) was in 20 mM Tris-HCl buffer, pH 7.8, with 1 mM sodium dithionite. Conditions of measurement: microwave frequency, 9.6 GHz; modulation amplitude, 0.64 mT: microwave power, 20 mW; temperature 10 K.

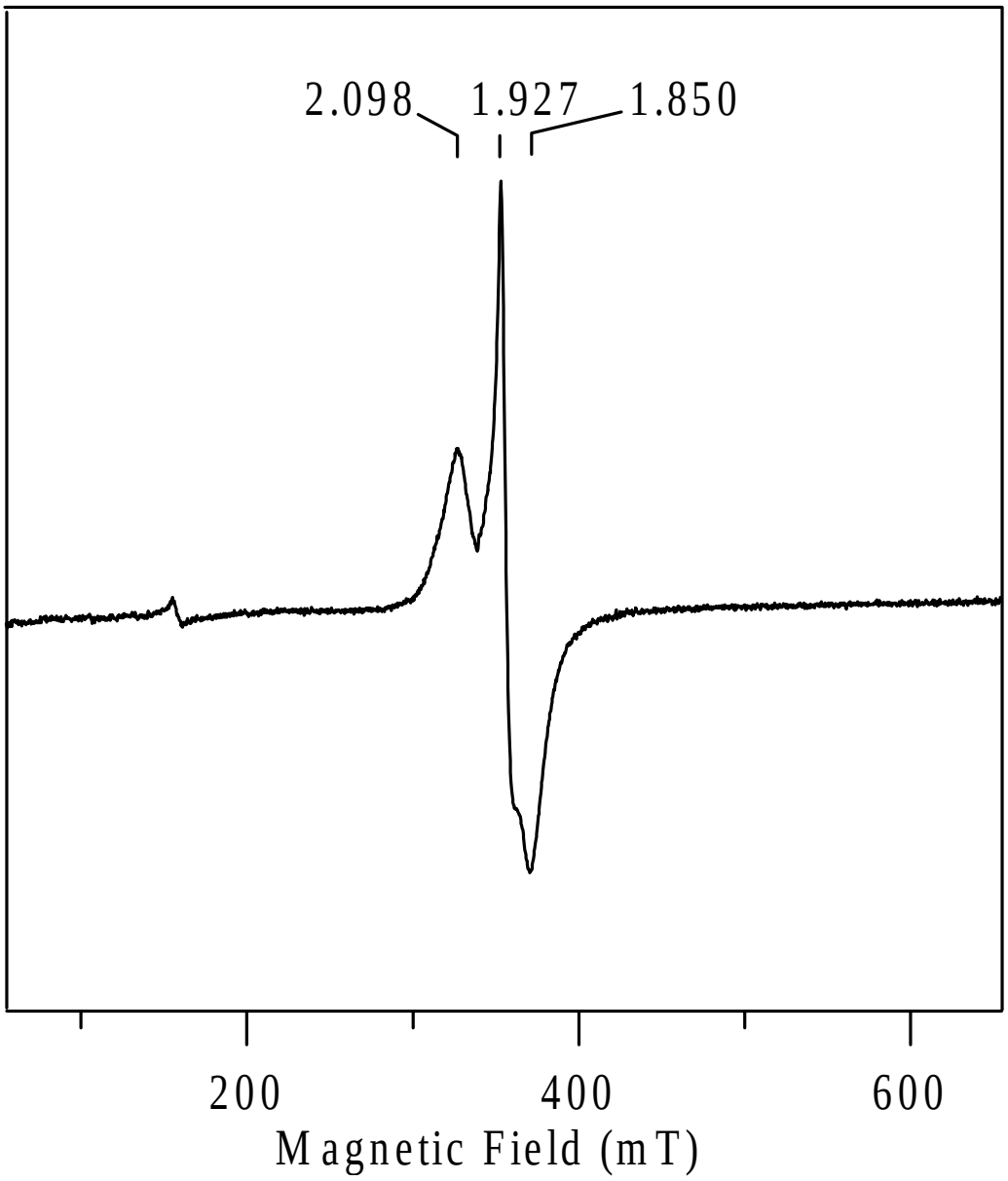
2.098
1.927
1.850
200
400
600
Magnetic Field (mT)

Figure 2-6 EPR signal intensity (arbitrary units) for NifEN (0.15 mM) as a function of poised potential. Dye-mediated redox titrations were carried out as described in the Experimental section. Data points correspond to the peak-to-trough intensity (g = 1.927 - 1.850) at 10 K. Solid lined represents a one-electron Nernst equation with a midpoint potential (*vs* NHE) of -350 mV. EPR conditions: temperature 10 K; microwave power, 20 mW; modulation amplitude, 1.02 mT; microwave frequency, 9.60 GHz.

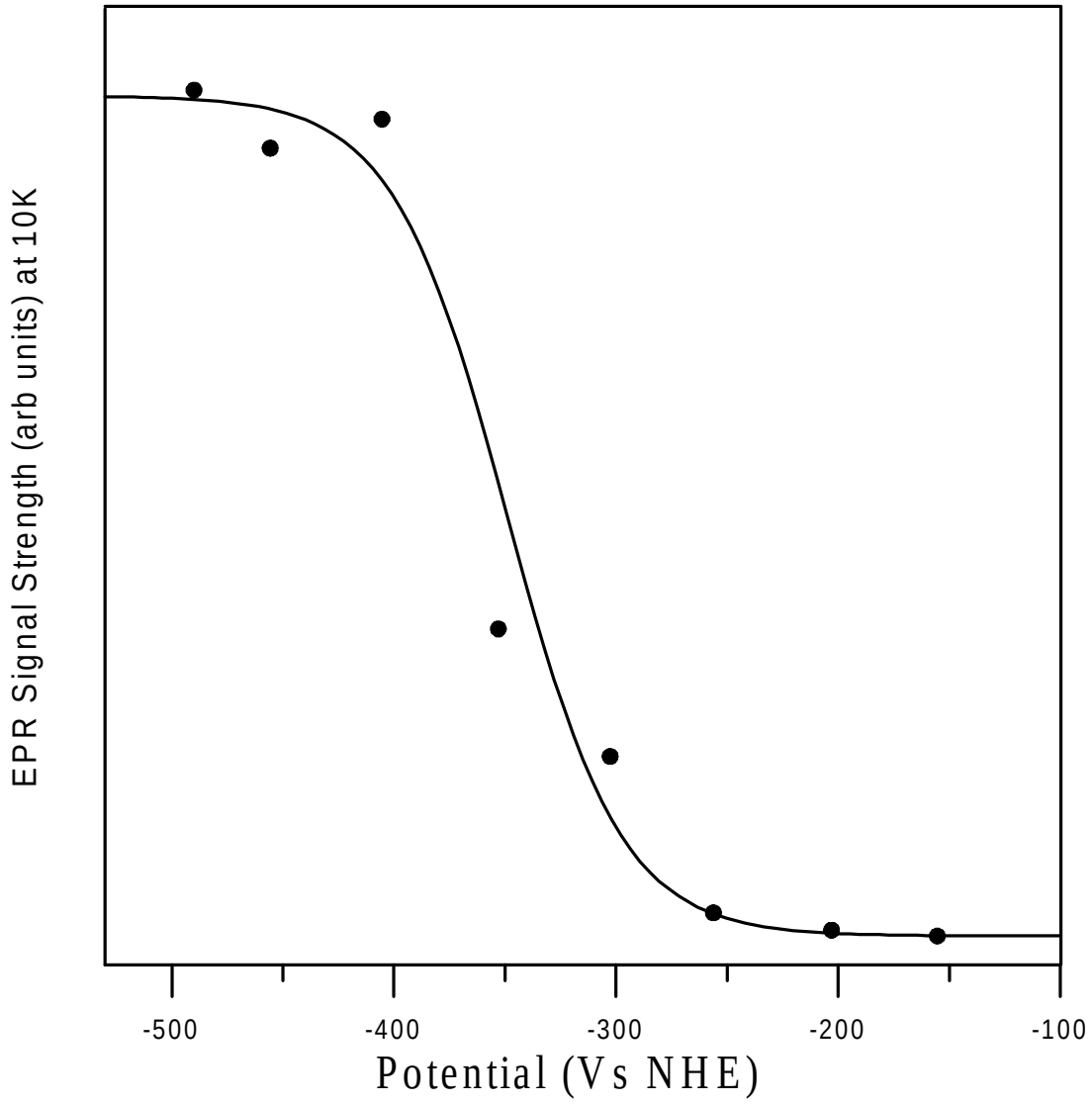
EPR Signal Strength (arb units) at 10K
-500
-400
-300
-200
-100
Potential (Vs NHE)

Figure2- 7 VTMCD spectra of dithionite-reduced NifEN. The sample (0.1 mM) was in 20 mM Tris-HCl buffer, pH 7.8, with 1 mM sodium dithionite and 55% (v/v) glycerol. The MCD spectra were recorded in a 1-mm cuvette with a magnetic field of 6.0 T, at 1.8, 4.2, and 10.0 K. All bands increase in intensity with decreasing temperature.

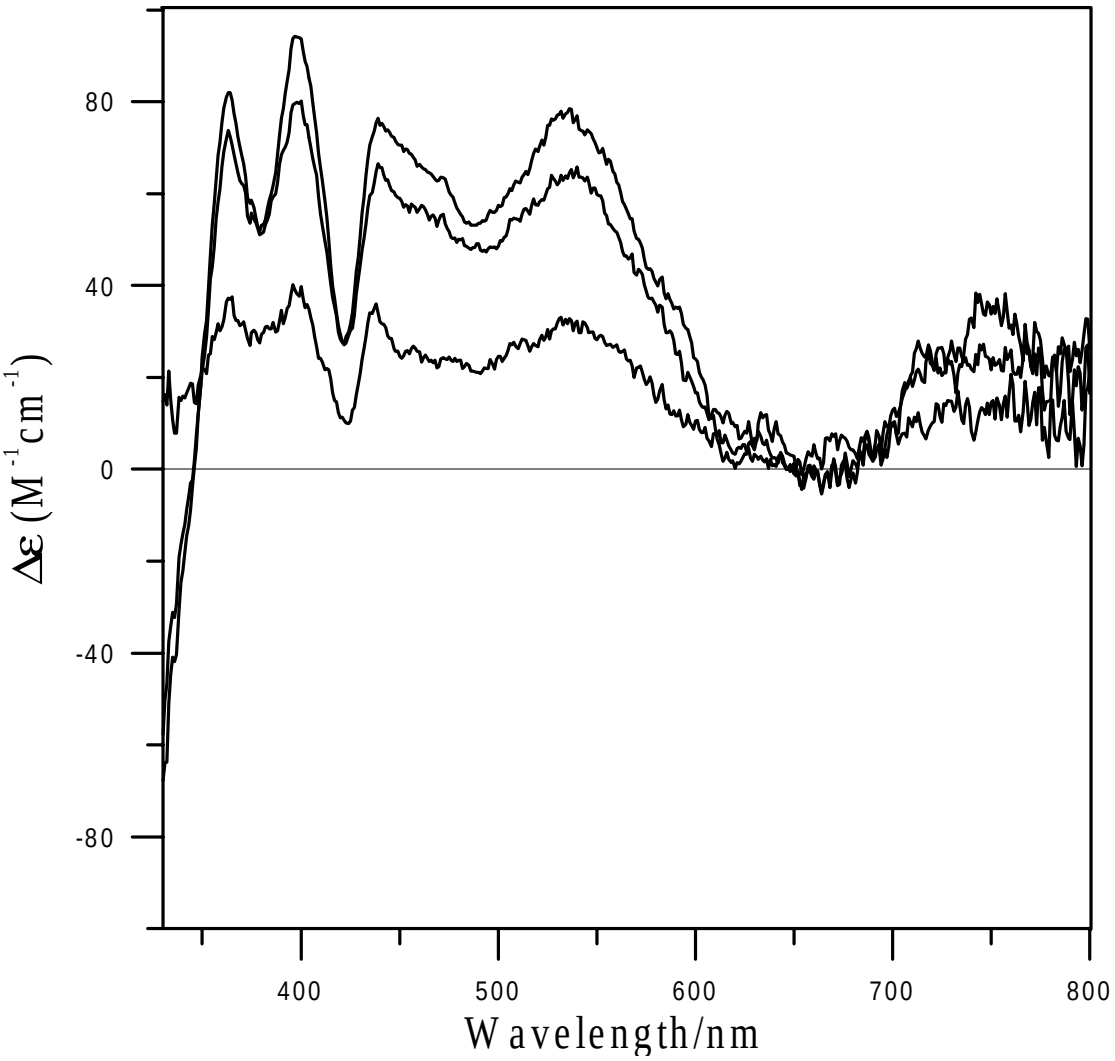
80
40
0
-40
-80
Δε (M-1cm-1)
400
500
600
700
800
Wavelength/nm

Figure 2-8 MCD magnetization data for dithionite-reduced NifEN. The sample is described in Figure 8. NifEN magnetization collected at 536 nm using magnetic fields between 0 and 6 T, fixed temperatures: 10.0 K (◆), 4.2 K, (□) 1.8 K (○). Solid line is theoretical magnetization data for a $S = 1/2$ ground state using EPR-determined g-values $g_{\parallel} = 2.098$ and $g_{\perp} = 1.888$ and with $m_{z/xy} = 1.1$.

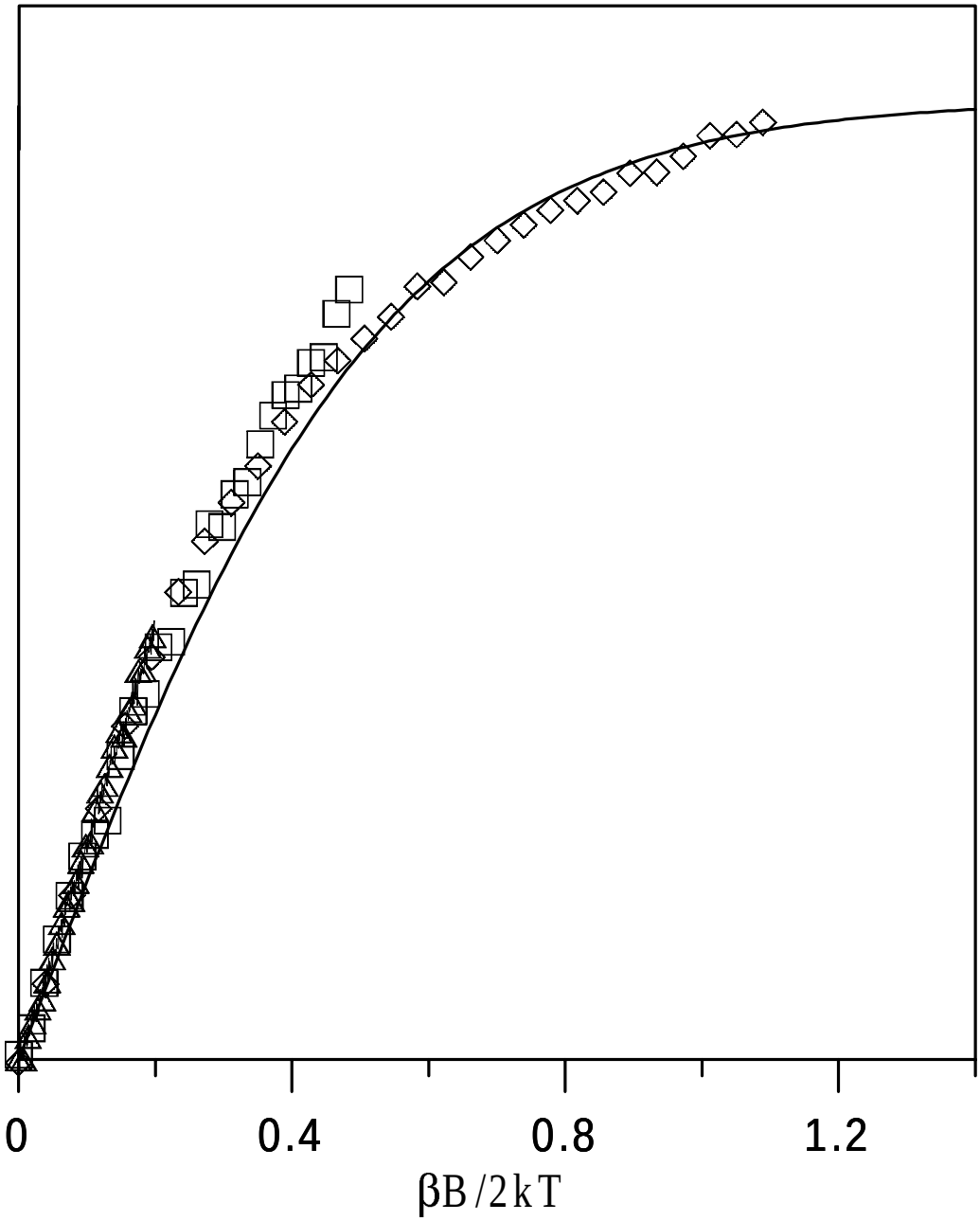
0
0.4
0.8
1.2
βB/2kT

Figure 2-9 Low-temperature resonance Raman spectra of thoinin-oxidized NifEN. Protein concentration was ~3 mM, and the buffering medium was 20 mM Tris HCl, pH 7.8. The spectrum was obtained at 28 K using 457.9-nm argon laser excitation and is the sum of 103 scans. Each scan involved advancing the spectrometer in 0.5 cm^{-1} increments, and photon counting for 1s/point with 6 cm^{-1} spectral resolution. A linear ramp was subtracted to correct for background fluorescence and lattice modes of ice are indicated by an asterisk.

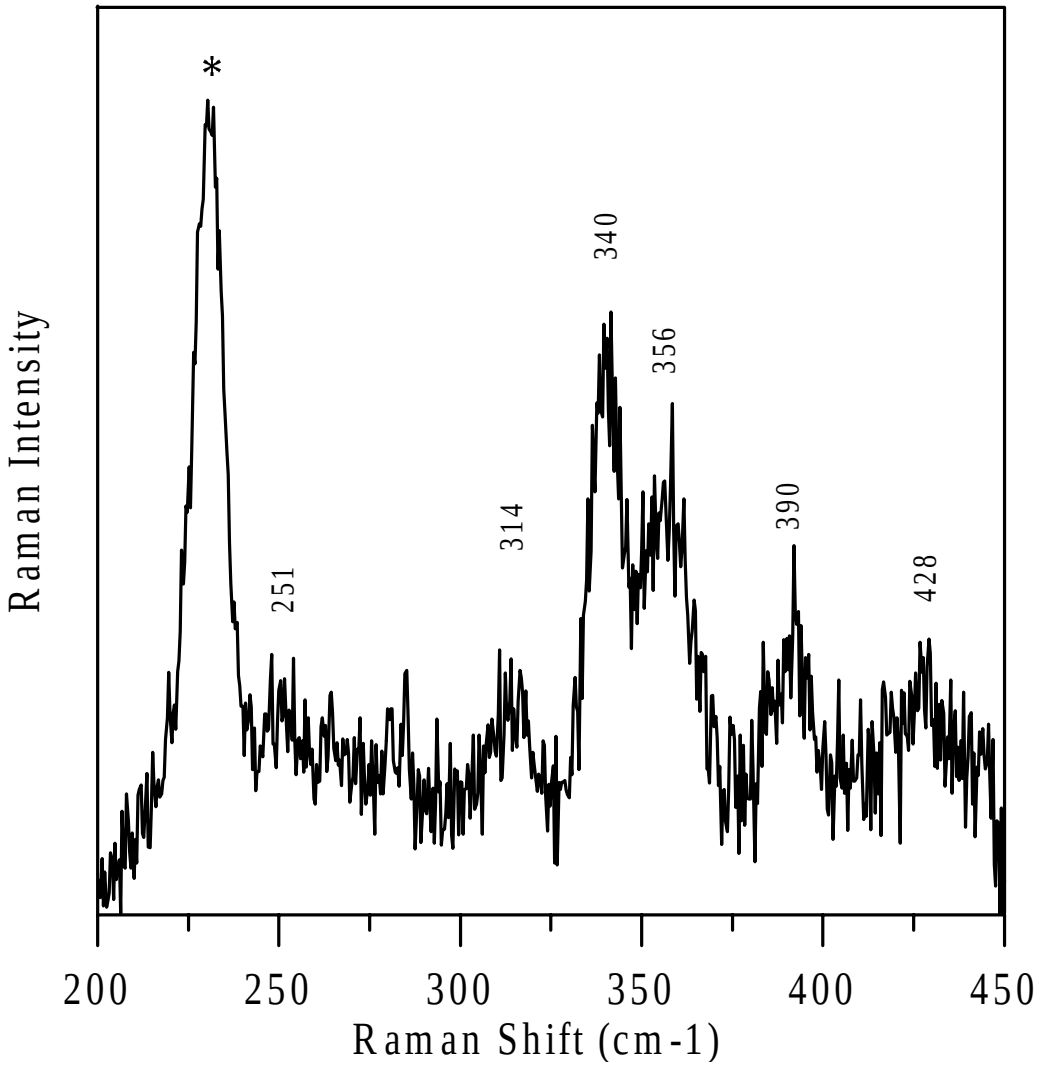
*
251
314
340
356
390
428
Raman Intensity
200
250
300
350
400
450
Raman Shift (cm-1)

Figure 2-10 Comparison of the structural model for the P-cluster (62) in its as-isolated P^N state (A) and the proposed structure and organization of the NifEN complex [4Fe-4S] cluster (B). In the scheme for the NifEN complex residues from the NifE subunit are indicated as (a) and the residue from the NifN subunit is indicated as (b). Primary sequence comparisons (21, 33) indicate that MoFe protein residues α-62, α-88, α-154, and β-70 are located at equivalent positions to residues α-37, α-62, α-124, and β-44, respectively, in the primary sequence of the NifEN complex.

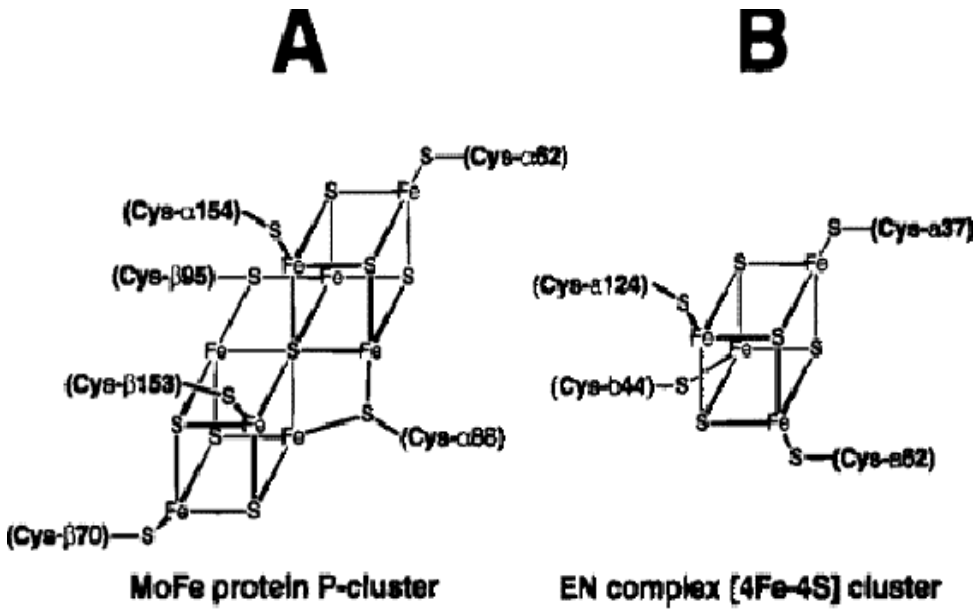
A
B
S—(Cys-α62)
(Cys-α154)
(Cys-β95)
(Cys-β153)
(Cys-α88)
(Cys-β70)—S
S—(Cys-α37)
(Cys-α124)
(Cys-b44)—S
S—(Cys-α82)
MoFe protein P-cluster
EN complex [4Fe-4S] cluster

Chapter III

Modular Organization and Identification of a Mononuclear Iron-Binding Site Within the NifU Protein[2]

[2] Jeffrey. N. Agar,[§] Pramvadee Yuvaniyama,[‡] Richard F. Jack,[‡] Valerie L. Cash,[‡] Archer D. Smith[§], Dennis R. Dean[‡], Michael K. Johnson[§], (2000) *J. Biol. Inorg. Chem.* **5**, 167-177 [‡] Department of Biochemistry, Virginia Polytechnic Institute and State University, Blacksburg, Virginia 24061. [§] Department of Chemistry and Center for Metalloenzyme Studies, University of Georgia, Athens, Georgia 30602

Abstract: The NifS and NifU nitrogen fixation-specific gene products are required for the full activation of both the Fe-protein and MoFe-protein of nitrogenase from *Azotobacter vinelandii*. Because the two nitrogenase component proteins both require the assembly of [Fe-S]-containing clusters for their activation, it has been suggested that NifS and NifU could have complementary functions in the mobilization of sulfur and iron necessary for nitrogenase-specific [Fe-S] cluster assembly. The NifS protein has been shown to have cysteine desulfurase activity and can be used to supply sulfide for the *in vitro* catalytic formation of [Fe-S] clusters. The NifU protein was previously purified and shown to be a homodimer with a [2Fe-2S] cluster in each subunit. In the present work, primary sequence comparisons, amino acid substitution experiments, and optical and resonance Raman spectroscopic characterization of recombinantly produced NifU and NifU fragments, are used to show that NifU has a modular structure. One module is contained in approximately the N-terminal third of NifU and is shown to provide a labile rubredoxin-like ferric-binding site. Cysteine residues Cys^{35}, Cys^{62} and Cys^{106} are necessary for binding iron in the rubredoxin-like mode and visible extinction coefficients indicate that up to one ferric ion can be bound per NifU monomer. The second module is contained in approximately the C-terminal half of NifU and provides the [2Fe-2S] cluster-binding site. Cysteine residues Cys^{137}, Cys^{139}, Cys^{172}, and Cys^{175} provide ligands to the [2Fe-2S] cluster. The cysteines involved in ligating the mononuclear Fe in the rubredoxin-like site and those that provide the [2Fe-2S] cluster ligands are all required for the full physiological function of NifU. The only two other cysteines contained within NifU, Cys^{272} and Cys^{275}, are not necessary for iron binding at either site nor are they required for the full physiological function of NifU. The results provide the basis for a model where iron bound in labile rubredoxin-like sites within NifU is used for [Fe-S] cluster formation. The [2Fe-2S] clusters contained within NifU are proposed to have a redox function involving the release of Fe from bacterioferritin and/or the release of Fe or an [Fe-S] cluster precursor from the rubredoxin-like binding site.

Textural Footnotes:

Abbreviations- PLP pyridoxal phosphate · SHE standard hydrogen electrode · VTMCD variable-temperature magnetic circular dichroism · RR resonance Raman · DTT: dithiothreitol

Introduction

The *A. vinelandii nifU* and *nifS* gene products (NifU and NifS) are proposed to have specific roles in the formation or repair of the [Fe-S] cores of metalloclusters contained within the catalytic components of nitrogenase (*1*). NifS is a pyridoxal phosphate (PLP)-dependent L-cysteine desulfurase (*2, 3*) that is able to catalyze the *in vitro* reconstitution of an apo-form of the nitrogenase Fe protein whose [4Fe-4S] cluster has been removed by chelation (*4*). The active species in this reaction is an enzyme-bound persulfide that is formed through the nucleophilic attack by an active site cysteine on the PLP-substrate cysteine adduct (*3*).

Although a specific function for NifU in nitrogenase [Fe-S] cluster formation is not known, the available evidence points to a role either as the iron source necessary for [Fe-S] cluster formation or as an intermediate site for [Fe-S] cluster assembly (*1*). For NifU to serve either of these functions it must have the ability to transiently bind iron that is destined for [Fe-S] cluster formation. Previous work has shown that isolated NifU is a homodimer that contains two identical [2Fe-2S] clusters (*5*). It seems unlikely, however, that these [2Fe-2S] clusters represent the source of iron necessary for nitrogenase [Fe-S] cluster formation, since they are tightly bound within the NifU protein and cannot be removed even with strong chelating reagents (*5*). Thus, we have speculated that the redox-active $[2Fe\text{-}2S]^{2+,+}$ clusters contained within NifU (E_m = -254 mV *vs* SHE), have a redox role involved in the binding or release of or an [Fe-S] cluster intermediate at a second site within NifU (*5*). The NifU protein contains nine cysteine residues, Cys^{35}, Cys^{62}, Cys^{106}, Cys^{137}, Cys^{139}, Cys^{172}, Cys^{175}, Cys^{272} and Cys^{275} (*5, 6*). Based on primary sequence comparisons to other [2Fe-2S]-containing proteins, NifU residues Cys^{137}, Cys^{139}, Cys^{172} and Cys^{175} are the most likely cluster-coordinating residues (*5*). Thus, any or all of the remaining cysteine residues could be involved in binding iron at a second site or participate in the assembly of an [Fe-S] cluster intermediate.

Comparison of NifU primary sequences to other proteins contained within the data base has led to speculation that NifU is a modular protein that is organized into distinct structural domains (*7, 8*). One of these modules includes the central portion of NifU which encompasses the proposed [2Fe-2S] cluster ligands. Another module corresponds to the N-terminal third of NifU and it contains residues Cys^{35}, Cys^{62}, Cys^{106} (Figure 1). Counterparts to each of the cysteine residues contained within the proposed N-terminal module of NifU are also strictly conserved in a family of small proteins designated IscU (*9*). In the cases of *Escherichia coli*, *Azotobacter vinelandii*, and a variety of other prokaryotic organisms, the *iscU* gene is cotranscribed with another gene designated *iscS* (*9*). The IscS protein shares considerable primary sequence identity when compared to NifS and it exhibits the same L-cysteine desulfurase activity as NifS (*9, 10*). Homologs to *iscU* and *iscS* are also widely conserved in nature. For example, a search of the protein database reveals that homologs to these genes are encoded within the yeast, mouse, arabidopsis and human genomes. Indeed, Hwang *et al*. (*8*) have suggested that the N-terminal domain of NifU represents one of the most highly conserved protein sequence motifs in nature. The wide conservation of *iscS* and *iscU* genes in nature, and their apparent co-transcription in many prokaryotic organisms, suggests that IscU and IscS have housekeeping roles involved in the general mobilization of Fe and S for [Fe-S] cluster formation (*9*). This hypothesis is further supported by recent studies of *Saccharomyces cerevisiae* which demonstrated the crucial role of two *iscU* genes in mitochondrial iron metabolism (*11)* and of a NifS-like protein in mitochondrial and cytosolic [Fe-S] cluster formation (*12*). Hence, the cysteine residues conserved between NifU and the IscU family of proteins (Figure 1) are excellent candidates for the proposed second iron-binding site within NifU.

In the present work, the functional significance of each of the nine cysteine residues encoded within the *A. vinelandii nifU* gene was assessed by site-directed mutagenesis and gene-replacement techniques. Purification and spectroscopic

characterization of NifU proteins altered in this way were also used to identify the [2Fe-2S] cluster-coordinating cysteine residues. The existence of a labile rubredoxin-like ferric-binding site in wild type and $Asp^{37}Ala$ NifU is demonstrated by the combination of optical absorption and resonance Raman (RR) spectroscopies. Finally the modular nature of the NifU polypeptide and the ligands to both metal sites are addressed by spectroscopic and redox studies of the purified N-terminal and C-terminal fragments of NifU. These fragments are shown to contain the labile monomeric Fe-binding site and the indigenous [2Fe-2S] cluster, respectively, each with properties very similar to those established in holo NifU.

Materials and Methods

DNA biochemistry, plasmids, and strain constructions.

Site-directed mutagenesis and gene-replacement procedures were performed as previously described (*13*). Isolated pDB800 DNA was used for mutagenesis. This plasmid was constructed by ligating an approximately 1.0 kb *Xba*I DNA fragment isolated from pDB525 (*5*) into the pUC119 cloning vector. Plasmid pDB800 contains the entire *nifU*-coding sequence. Point mutations generated within pDB800 were transferred to the *A. vinelandii* chromosome using congression as previously described (*13*). Preparation of competent *A. vinelandii* cells for transformation was performed as previously described by Page and von Tigerstrom (*14*). The following plasmids were used for the high level, heterologous, expression of *nifU* and *nifU* fragments in the *E. coli* host strain BL21(DE3) (*15*): pDB525, pDB937, pDB938, pDB822, pDB965, pDB966, pDB967, and pDB1027. The construction of pDB525 was previously described (*5*). It contains the entire *A. vinelandii nifU* gene cloned into the pT_7-7 vector so that the expression of *nifU* is regulated by the T_7 transcription and translation control elements. Plasmid pDB822 and pDB1027 are the same as pDB525 except that the *nifU* Cys137 codon was substituted by an Ala codon (pDB822) or the *nifU* Asp37 codon was substituted by Ala (pDB1027). Plasmid pDB937 was generated by polymerase-chain-reaction (PCR) amplification of the

first 393 base-pairs of the *nifU*-coding sequence and the subsequent cloning this DNA fragment into the pT_7-7 cloning vector in the appropriate orientation. In this construction the *nifU* Glu^{131} codon was substituted by a termination codon. The NifU polypeptide fragment produced using this construct is referred to as NifU-1 (Figure 1). Plasmid pDB938 was similarly generated by PCR amplification of a 564 base-pair fragment that extends from codon 126 within the *nifU*-coding sequence to several base-pairs past the natural *nifU* termination codon. In this construction the *nifU* Ile^{126} codon was substituted by a translation-initiating Met codon. The NifU polypeptide fragment produced in this way is referred to as NifU-2 (Figure 1). Oligonucleotides used for PCR-amplification of the gene cartridges encoding NifU-1 and NifU-2 had the following sequences: 5'ATGCATATGTGGGATTATTCGGA3' and 5'TGTCGGATCCCTCTTAGTGGTCGTCC3' for NifU-1; and 5'CATGCATATGGAGGACGACCACGAAGAG3' and 5'CATGCATAGGAGGACGACCACGAAGAG3' for NifU-2. Details of the PCR-based strategy for construction of pDB937 and pD938 were the same as previously described in detail for pDB525 (*5*). Plasmids pDB965, pDB966, and pDB967 are identical to pDB937 except for the following substitutions in the *nifU-1* coding sequence: codon Cys^{35} substituted by an Ala codon (pDB965), codon Cys^{62} substituted by an Ala codon (pDB966), and codon Cys^{106} substituted by an Ala codon (pDB967).

Protein biochemistry

NifU and altered forms of NifU from *A. vinelandii* that were generated by site-directed mutagenesis were expressed in *E. coli* and purified as previously described (*5*). NifU-1 and altered forms of NifU-1 were heterologously produced in 500 mL batch cultures of *E. coli* strain BL21(DE3) as described by Fu *et al*. (*5*). Protein was typically purified from 30 to 45 grams of wet-weight cells and all manipulations were performed under an Ar atmosphere. Crude extracts were prepared by resuspension of cell pellets in a 25 mM Tris-HCl, pH 7.4 buffer, rupturing cells by sonication and centrifugation as

previously described (*5*). Crude extract was fractionated by the addition of solid streptomycin sulfate to 1%, w/v at ambient temperature and centrifugation at 20,000 rpm for 20 min in a Beckman Type 35 rotor. NifU-1 was then precipitated from the streptomycin sulfate-treated crude extract by bringing it to 60% saturation with solid ammonium sulfate. Precipitated NifU-1 was collected by centrifugation as above and resuspended in buffer at a volume equal to the original supernatant volume. The sample was then loaded on a 2.5 x 20 cm Q Sepharose column (Pharmacia, Piscataway, NJ) using a peristaltic pump and eluted using a linear 1.5 L (0.1-to-1.0 M) NaCl gradient. NifU-1 elutes between 0.42 and 0.50 M NaCl. Concentrated sample was then passed over a 2.5 x 20 cm Sephacryl-300 column and eluted using a flow rate of 2.0 mL/min. Purified NifU-1 samples were greater than 95% pure based on denaturing polyacrylamide gel electrophoresis (Figure 2). Protein concentrations were determined by the biuret reaction or the BCA method (*16, 17*). Buffer, preparation of crude extracts, streptomycin sulfate treatment and ammonium sulfate fractionation used for NifU-2 purification were the same as for NifU-1 purification except that 2.0 mM dithiothreitol (DTT) was added to all buffers and NifU-2 was precipitated at 45% ammonium sulfate saturation. The NifU-2 sample obtained after ammonium sulfate fractionation was further purified as described above using a Q sepharose column chromatography except that a 0.6 L (0.1-to-0.6 M) linear NaCl gradient was used. NifU-2 elutes between 0.3 and 0.4 M NaCl. The eluted NifU-2 fraction was concentrated and brought to 0.4 M ammonium sulfate by the addition of an equal volume of buffer (25 mM Tris-HCl pH 7.4) containing 0.8 M ammonium sulfate. The diluted NifU-2 sample was applied to a Pharmacia 1.5 x 15 cm Phenyl Sepharose column and eluted using a 150 mL linearly decreasing (0.4 to 0.0 M) ammonium sulfate gradient. Purified NifU-2 was greater than 95% pure based on polyacrylamide gel electrophoresis (Figure 2). The nitrogenase Fe protein and MoFe protein were assayed in crude extracts of nitrogenase-derepressed cells by using the same conditions for the acetylene reduction assay as previously described by Jacobson *et al*.

(*18*). Units for nitrogenase component protein activities are expressed as nanomoles acetylene reduced per minute per mg of crude extract protein. *A. vinelandii* cells were cultured in Burk medium (*19*) and grown at 30°C with or without the addition of ammonium acetate (30 mM final concentration) as a fixed nitrogen source.

Spectroscopic and electrochemical characterization of NifU, NifU-1 and NifU-2.

The sample concentrations given in the figure captions and used to quantify the intensity of absorption, EPR and variable-temperature magnetic circular dichroism (VTMCD) spectra, are based on protein determinations and are expressed per NifU, NifU-1 or NifU-2 monomer. UV-visible absorption spectra were recorded under anaerobic conditions in septum-sealed 1 mm and 1 cm cuvettes, using a Shimadzu 3101PC scanning spectrophotometer fitted with a TCC-260 temperature controller. VTMCD spectra were recorded using samples containing 55% (v/v) glycerol in 1 mm cuvettes using an Oxford Instruments Spectromag 4000 (0-7 T) split-coil superconducting magnet (1.5-300 K) mated to a Jasco J-715 spectropolarimeter. The experimental protocols used for accurate sample temperature and magnetic field measurement, anaerobic sample handling, and assessment of residual strain in frozen samples have been described in detail elsewhere (*20, 21*). X-band (~ 9.6 GHz) EPR spectra were recorded using a Bruker ESP-300E EPR spectrometer equipped with a dual-mode ER-4116 cavity and an Oxford Instruments ESR-9 flow cryostat. Frequencies were measured with either a Systron-Donner 6054B frequency counter or Hewlett Packard 5350B microwave frequency counter, and the magnetic field was calibrated with a Bruker ER035M gaussmeter. Spin quantitations were carried out under non-saturating conditions with 1mM Cu(II)EDTA as the standard, as described by Aasa and Vänngård (*22*). Spectral simulations were carried out using the QPOW program developed by Prof. R. L. Belford and coworkers.

Resonance Raman spectra were recorded using an Instruments SA Ramanor U1000 spectrometer fitted with a cooled RCA 31034 photomultiplier tube with 900

scattering geometry. Spectra were recorded digitally using photon-counting electronics, and signal/noise was improved by signal averaging multiple scans. Band positions were calibrated using the excitation frequency and CCl_4 and are accurate to ±1 cm^{-1}. Laser excitation lines were generated by Coherent Innova 100 10-W argon ion, and Coherent Innova 200 krypton ion lasers. Plasma lines were removed using a Pellin Broca Prism premonochromator. For RR studies, a 12-μL droplet of concentrated protein (1-4 mM) was placed in a specially designed sample cell (*23*) attached to the cold finger of an Air Products Displex model CSA-202E closed-cycle refrigerator. The sample temperature was maintained at 18 K during scanning in order to minimizes laser-induced sample degradation. Bands due to the frozen buffer solutions have been subtracted from all the spectra shown in this work after normalization of lattice modes of ice centered at 229 cm^{-1}.

Iron-binding studies of NifU-1, NifU and Asp^{37}Ala NifU at 2 °C were carried out under strict anaerobic conditions after gel filtration to remove DTT, using a Shimadzu TCC-260 temperature controller and monitoring the absorption changes over a period of 90 mins following the addition of a 1.2 or 2.4-fold excess of freshly prepared ferric citrate. The samples of NifU and Asp^{37}Ala NifU used in iron binding studies were purified in the presence of 1 mM DTT and NifU-1 samples were pre-treated with 1 mM DTT prior to use. RR samples of Fe-bound NifU-1, NifU and Asp^{37}Ala NifU were prepared by anaerobic incubation of DTT-free, highly concentrated samples (~ 4 mM) with 5 equivalent/monomer of ferric citrate for 1 hour at 2 °C

Midpoint potentials of $[2Fe\text{-}2S]^{2+,+}$ clusters in NifU and NifU-2 were measured by cyclic voltammetry at a glassy carbon electrode using neomycin (2 mM) as a promoter. The electrochemistry cell used was identical to that described by Hagen (*24*), with glassy carbon, Pt and Ag/AgCl as the working, counter and reference electrodes, respectively. The working electrode was prepared by polishing it with an Al_2O_3 slurry (0.3 μm) and

then with diamond spray (1 μm). The scan rate was 10 mV/sec over the potential range -200 to -900 mV (versus the Ag/AgCl electrode).

Results

Identification of cysteine residues required for full NifU function

Each of the nine cysteine codons contained within *nifU* were individually substituted by alanine codons and, in some cases, by a variety of other codons. Mutations resulting in such amino acid substitutions were transferred to the *A. vinelandii* chromosome using a gene-replacement procedure (*13*). Mutant strains constructed in this way were isogenic to the wild-type control strain except for the particular mutation. Because there is no direct enzymatic assay for the effect of amino acid substitutions within NifU, their effect on the maturation of the nitrogenase catalytic components can only be evaluated by indirect physiological effects upon diazotrophic growth rates and by their effect on nitrogenase component protein activities. Typical results for the effects of amino acid substitutions within NifU on diazotrophic growth rates are summarized in Table 1. Figure 3 compares the diazotrophic growth rates for the wild-type strain, a mutant strain that produces an altered NifU protein having Cys^{106} substituted by alanine, and a strain deleted for *nifU*. The results show that substitution at the Cys^{106} position results in a lowered diazotrophic growth capability for the mutant strain, but that the effect is not as severe as for a strain having *nifU* deleted (*18*). Analogous results were obtained for all strains having substitutions for any of the cysteine residues except those substituted at the Cys^{272} or Cys^{275} positions. These latter strains exhibited normal diazotrophic growth that could not be distinguished from the wild-type. The low diazotrophic growth rates for the other mutant strains are also reflected in lower activities for both the nitrogenase Fe protein and MoFe protein in nitrogenase-derepressed crude extracts. For example, the wild-type strain exhibits an Fe protein specific activity of 42 units and MoFe protein specific activity of 52 units, whereas, the strain having Cys^{106} substituted by alanine has an Fe protein specific activity of 12 units and MoFe protein a specific activity of 22 units (see

Materials and Methods for activity units). Thus, as in the case of the *nifU* deletion strain (*18*), substitution for any NifU cysteine residue except Cys^{272} or Cys^{275} results in a mutant strain having substantially lower specific activities for both the Fe protein and MoFe protein.

Cysteine residues 137, 139, 172 and 175 provide [2Fe-2S] cluster ligands and are contained within a modular domain.

In order to determine which of the 9 cysteine residues provide the [2Fe-2S] cluster ligands, altered NifU was purified from each of nine *E. coli* strains which individually produce an altered NifU protein having one of the cysteines substituted by alanine. On the basis of the UV-visible spectra of the oxidized proteins and the EPR spectra of the reduced proteins, variant NifU proteins with Cys^{35}, Cys^{62}, Cys^{106}, Cys^{272}, or Cys^{275} individually replaced by Ala, still contained a [2Fe-2S] cluster with properties indistinguishable from that of wild-type. In contrast, variant NifU proteins with Cys^{137}, Cys^{139}, Cys^{172} or Cys^{175} individually replaced by Ala, did not contain a [2Fe-2S] cluster. To further confirm that residues Cys^{137}, Cys^{139}, Cys^{172} and Cys^{175} are [2Fe-2S] cluster ligands, and that they are contained within a modular domain, a gene cartridge was produced and cloned, which directs the synthesis of a NifU fragment that includes residues 126 to the C-terminus of NifU (designated NifU-2, see Figure 1). NifU-2 that was heterologously produced in *E. coli* was isolated (Figure 2) and found to contain a $[2Fe\text{-}2S]^{2+,+}$ cluster. Gel exclusion chromatography showed that isolated NifU-2 is a homodimer (data not shown). The midpoint potentials for the $[2Fe\text{-}2S]^{2+,+}$ clusters in NifU and NifU-2 were determined by cyclic voltammetry at a glassy carbon electrode using neomycin as a promoter. Within experimental error, the midpoint potentials were the same for NifU and NifU-2, $E_m = -250 \pm 10$ mV (*vs* SHE), and this value is in excellent agreement with that determined by dye-mediated optical redox titrations for NifU, $E_m = -254 \pm 20$ mV (*5*).

The ground and excited properties of the [2Fe-2S] cluster in oxidized and reduced forms of NifU-2 were investigated using the combination of UV/visible absorption, EPR, VTMCD and RR spectroscopies. The UV/visible absorption characteristics of as-purified and dithionite-reduced NifU-2 (Figure 4) are quantitatively indistinguishable from those of the NifU holoprotein (*5*). As previously discussed (*5*), the spectra and extinction coefficients are indicative of one $[2Fe\text{-}2S]^{2+,+}$ cluster per NifU-2 monomer. RR spectra of diamagnetic $[2Fe\text{-}2S]^{2+}$ clusters in the Fe-S stretching region provide a more rigorous assessment of the structural integrity of the cluster in NifU-2 fragment compared to the holoprotein. The spectra are particularly sensitive to the Fe-S-C-C dihedral angles and hydrogen-bonding interactions of coordinating cysteine residues (*25-27*). Consequently, different subclasses of 2Fe-containing ferredoxins, each with complete cysteinyl ligation, but differing in terms of the primary sequence arrangements of coordinating cysteines, are readily distinguishable by RR spectroscopy (*26, 27*). As shown in Figure 5, the RR spectrum of the $[2Fe\text{-}2S]^{2+}$ center in NifU-2 is broader than that obtained for the holoprotein under identical conditions, indicating greater inhomogeneity in the cluster environment, but the relative intensities and the frequencies of individual bands are in good agreement. On the basis of the assignments advanced for the all-cysteine-ligated $[2Fe\text{-}2S]^{2+}$ center in NifU under effective D_{2h} symmetry (*5*), the most significant frequency difference lies in predominantly bridging $B_{3u}{}^{b}$ mode which shifts from 356 cm^{-1} in NifU to 364 cm^{-1} in NifU-2. Since the frequency separation in the predominantly bridging and terminal B_{3u} modes is known to be dependent on the cysteinyl dihedral angles (*25*), and the $B_{3u}{}^{t}$ modes are assigned to the bands at 288 cm^{-1} and 289 cm^{-1} in NifU and NifU-2, respectively (*5*), this difference is tentatively attributed to minor changes in the dihedral angles of one or more of the coordinating cysteine residues.

The ground and excited properties of paramagnetic $[2Fe\text{-}2S]^{+}$ cluster in reduced NifU-2 have been investigated using EPR (Figure 6) and VTMCD (Figure 7) spectroscopies, and the results are compared to those previously obtained and analyzed

for NifU (*5*). Reduced NifU-2 exhibits an S =1/2 EPR signal, g = 2.022, 1.928, and 1.890 (based on spectral simulation), that is observed without significant broadening up to 50 K and accounts for 0.9 spin/monomer. These g-values and relaxation properties are characteristic of a $[2Fe\text{-}2S]^{+}$ cluster and indicate that the ground-state properties are essentially identical to those of the completely cysteinyl-ligated $[2Fe\text{-}2S]^{+}$ cluster in the holoprotein, g = 2.019, 1.927, 1.892 (based on spectral simulation). The VTMCD spectrum of paramagnetic $[2Fe\text{-}2S]^{+}$ clusters provides a more sensitive monitor of the excited state properties than the absorption spectrum (*5*). Hence, the near identical VTMCD spectra of reduced NifU-2 and NifU (Figure 7) attest to the same excited state structure for the $[2Fe\text{-}2S]^{+}$ clusters. Thus, both NifU and NifU-2 contain one $[2Fe\text{-}2S]^{+}$ cluster per monomer and neither the ground nor the excited state properties are significantly perturbed when the $[2Fe\text{-}2S]^{+}$ clusters from the NifU and NifU-2 proteins are compared.

Identification of a monomeric Fe-binding site in NifU.

Evidence for ferric ion binding to NifU and the $Asp^{37}Ala$ variant of NifU was provided by optical absorption and RR studies of samples treated with ferric citrate. DTT was removed by anaerobic gel filtration just prior to iron binding studies in order to avoid complications due to the formation of iron-DTT complexes. The $Asp^{37}Ala$ variant of NifU was originally constructed to address the possibility that Asp^{37} is involved with iron-ligation. Although the results presented below show that this is not the case, the ferric-bound form of this variant was more stable and yielded analogous, but higher quality spectroscopic data.

The visible absorption of NifU gradually increased at all wavelengths over a period of 40 mins on anaerobic incubation with a 1.2-fold excess of ferric citrate at 2°C (upper panel of Figure 8A). The absorption changes were monitored for up to 90 mins, but the data after 40 mins are complicated by the progressive increase of a scattering baseline attributed to protein aggregation. Analogous changes in the absorption spectrum were

observed in parallel experiments with Asp^{37}Ala NifU (upper panel of Figure 8B). For this variant, the spectral changes were complete after 55 mins, and no further changes were apparent after an additional 1 hour at 2 °C or after adding an additional 1.2-fold excess of ferric citrate. The additional absorption was gradually lost over a period of 1 hr on warming ferric citrate-treated samples of wild-type and Asp^{37}Ala NifU to room temperature, indicating that it originates from a kinetically labile chromophore.

The absorption spectrum of the additional chromophore generated in wild type and Asp^{37}Ala NifU on incubation with ferric citrate was assessed by difference spectra (middle panels of Figs. 8A and 8B). The resulting spectra are quantitatively very similar and are characteristic of a rubredoxin-type ferric center, i.e. a tetrahedral ferric center with predominant or exclusive thiolate ligation. On the basis of the detailed electronic assignments available for rubredoxin-type FeS_4 centers (*28-31*), the bands centered at 360 nm and 490 nm are assigned to multiple overlapping (Cys)Sp$\sigma \rightarrow$ Fe(III) charge transfer transitions. In rubredoxins, the Fe is coordinated by two pairs of cysteines in C-X-X-C arrangements, and each of these bands is split into two resolvable components largely a result of predominantly axial distortion of the idealized tetrahedral geometry. However, the absence of resolvable splittings in these bands for the rubredoxin-type ferric center in NifU does not in itself enable assessment of the extent of cysteinyl ligation. For example, both desulforedoxin [absorption bands centered at 370 nm and 507 nm (*32*)] and the Cys^{9}Asp variant of *Clostridium pasteurianum* rubredoxin [absorption bands centered at 365 nm and 515 nm (*33*)] exhibit unresolved absorption bands very similar to those of rubredoxin-type ferric center in wild-type and Asp^{37}Ala NifU. In desulforedoxin, the Fe center is coordinated by four cysteines in -C-X-X-C- and -C-C- arrangements (*34*), whereas in the rubredoxin variant, the Fe is coordinated by three cysteines and presumably an aspartate in -C-X-X-D- and -C-X-X-C- arrangements (*33*). The extinction coefficient for the rubredoxin-type ferric center in wild type and Asp^{37}Ala NifU (ε_{490} = 4200 $M^{-1}cm^{-1}$) is comparable to those reported for desulforedoxin [ε_{507} = 7000 $M^{-1}cm^{-1}$ (*32*)]

and the Cys^{9}Asp variant of *C. pasteurianum* rubredoxin [ε_{515} = 5200 $M^{-1}cm^{-1}$ (*33*)]. Since the RR data presented below indicate that the rubredoxin-type ferric center in NifU is ligated by three cysteine residues, Cys^{9}Asp variant of *C. pasteurianum* rubredoxin is more appropriate for quantitative comparison. Hence we conclude that NifU can bind up to one ferric ion per monomer. The lability of the bound ferric ion at room temperature prevented meaningful assessment of the stoichiometry via quantitative iron analysis.

NifU residues Cys^{137}, Cys^{139}, Cys^{172}, and Cys^{175} were identified as providing the [2Fe-2S] cluster ligands, and residues Cys^{272} and Cys^{275} were not found to be necessary for the full physiological function of NifU. It therefore seemed logical to expect that residues Cys^{35}, Cys^{62} and Cys^{106} would participate in binding of ferric ion in the rubredoxin-type site. This possibility is supported by the strict conservation of residues corresponding to Cys^{35}, Cys^{62} and Cys^{106} within a class of proteins designated IscU which are proposed to have housekeeping functions related to [Fe-S] cluster formation (*9*), see Figure 1. The IscU proteins are much smaller than NifU and exhibit a high degree of primary sequence identity when compared to the N-terminal region of NifU (*9*). The primary sequence comparisons between NifU and IscU (Figure 1) provided the rationale for the design of a *nifU* gene fragment cartridge which includes Cys^{35}, Cys^{62} and Cys^{106} and therefore encompasses the region encoding the proposed second Fe-binding domain within NifU. This *nifU* fragment encodes NifU residues 1 through 131 and the corresponding protein, designated NifU-1 (Figure 1), was heterologously produced in *E. coli* and isolated (Figure 2). Gel exclusion chromatography showed that isolated NifU-1 is a homodimer (data not shown).

In order to test the hypothesis that the rubredoxin-type ferric binding site resides in the NifU-1 domain, iron binding experiments analogous to those described above for wild type and Asp^{37}Ala NifU were conducted with the NifU-1 fragment. Anaerobic incubation of NifU-1 with a 1.2-fold excess of ferric citrate at 2°C resulted in the gradual appearance of the same rubredoxin-type chromophore that was apparent by difference spectroscopy in

ferric citrate treated wild type and $Asp^{37}Ala$ NifU (middle and lower panels of Figure 8A and 8B, respectively). The absorption was maximal after 20 min and no additional increase in the absorption intensity was apparent for samples treated in the same way with a 2.4-fold excess of ferric citrate. Although the maximal extinction coefficient (ε_{490} = 850 $M^{-1}cm^{-1}$) indicates sub-stoichiometric (~20%) ferric ion binding to the NifU-1 fragment, as compared to full length NifU under these conditions, the close similarity in the absorption spectra demonstrates that this domain contains the rubredoxin-type ferric binding site.

Strong support for an analogous rubredoxin-type center in ferric-bound forms of NifU-1, NifU and $Asp^{37}Ala$ NifU comes from low-temperature RR studies (Figure 9A and 9B). The samples of ferric-bound proteins used in RR experiments were prepared using the same protocol developed for the optical absorption studies by incubating concentrated samples of precooled protein (~ 2 mM) with a 5-fold excess of ferric citrate and incubating for 1 hour at 2 °C under strict anaerobic conditions. As for the absorption studies, the RR spectra of the monomeric ferric centers in wild type and $Asp^{37}Ala$ NifU were obtained by subtracting the spectra associated with the indigenous $[2Fe\text{-}2S]^{2+}$ centers (spectra c in Figs. 9A and 9B). The intensities of the dominant 288-cm^{-1} band of the $[2Fe\text{-}2S]^{2+}$ centers were equalized prior to subtraction. The resulting RR spectra for the monomeric ferric sites in NifU-1 and $Asp^{37}Ala$ NifU are in excellent agreement (Figure 9B), demonstrating that Asp^{37} is not an Fe ligand and that the coordination environment at this site is not perturbed by the C-terminal truncation. In both cases the spectra comprise two broad bands of comparable intensity centered at 314 and 368 cm^{-1}. Although the same bands are apparent in the difference spectrum corresponding to the mononuclear ferric center in wild-type NifU, the spectrum is broader with additional features centered at 325 and 356 cm^{-1} (cf .spectra c and d in Figure 9A). On the basis of the absorption results discussed above, this heterogeneity is likely to be a consequence of protein aggregation.

The RR bands at 314 and 368 cm^{-1} associated with the mononuclear ferric site in NifU proteins are readily identified as the symmetric and asymmetric Fe-S stretches of approximately tetrahedral rubredoxin-like center units by analogy with the spectra and assignments made for wild-type and mutant rubredoxins (*33, 35-37*) and wild-type desulforedoxin (*38*). Distorted tetrahedral FeS_4 units in rubredoxins and desulforedoxins have intense symmetric Fe-S stretching bands in the range 312-320 cm^{-1} and weaker, partially-resolved asymmetric Fe-S stretching bands in the range 335-382 cm^{-1}. The splitting in the asymmetric Fe-S stretching modes is most pronounced for the more axially distorted site in desulforedoxin which has well resolved bands at 343 and 381 cm^{-1} (*38*). Although the Fe-S stretching frequencies of rubredoxin-type site in NifU proteins are in accord with a distorted tetrahedral FeS_4 site, the relative intensities of the symmetric and asymmetric stretching modes and the absence of a resolvable splitting in the asymmetric stretching mode are not. Replacing one of the coordinating cysteines with an oxygenic ligand (serinate or aspartate) in mutant rubredoxins has been found to result in major and diverse changes in the RR spectra in the Fe-S stretching region (*33, 36, 37*). However, there are examples of mutant rubredoxins with one oxygenic ligand, such as the $Cys^{39}Ser$ variant of *C. pasteurianum* rubredoxin that have RR spectra comprising two bands of comparable intensity centered at 324 cm^{-1} and 377 cm^{-1} (*37*). The ~10-cm^{-1} downshifts for labile mononuclear ferric site in NifU-1 and $Asp^{37}Ala$ NifU are readily rationalized in terms of slightly weaker Fe-S bonds. Hence the overall weakness and relative intensity of the symmetric and asymmetric Fe-S modes of the mononuclear ferric site in NifU are best interpreted in terms of a tetrahedral FeS_3X site with Cys^{35}, Cys^{62} and Cys^{106} providing the thiolate ligands and X being an unknown O or N ligand..

Attempts to characterize the ground and excited state properties of the monomeric Fe site in NifU-1, NifU and $Asp^{37}Ala$ NifU using EPR and VTMCD spectroscopy were only partially successful. EPR studies of the ferric-bound forms of NifU-1, NifU and $Asp^{37}Ala$ NifU at 4 K and 10 K revealed weak absorption-shaped features centered at g =

9.6 and an intense derivative-shaped feature at $g = 4.3$. Such a resonance is indicative a rhombic $S = 5/2$ species ($E/D \sim 0.33$). However, these are also the EPR properties of ferric citrate and adventitiously bound ferric ion, as well as those of tetrahedral ferric centers with complete cysteinyl ligation or three cysteines and one oxygenic ligand (serine or aspartate) (*33, 36, 37*). Consequently EPR is of little utility for discriminating between different types of high-spin ferric species in NifU proteins. Addition of 50% (v/v) glycerol to ferric-bound NifU-1, NifU and Asp^{37}Ala NifU at room temperature or 2 °C resulted in complete and immediate loss of absorption features associated with monomeric ferric center. Hence the addition of the glycerol enhances the lability of the bound ferric ion, thereby preventing the investigation of the electronic excited state properties via VTMCD studies. The mononuclear Fe site also appears to be reductively labile, as evidenced by the complete absence of charge transitions characteristic of Fe(II)-rubredoxin type centers in the 300-350 nm region (*33, 39*) in both the 2°C absorption and VTMCD spectra of dithionite-reduced samples of ferric-bound NifU-1 (data not show).

Residues Cys^{35}, Cys^{62} and Cys^{106} are necessary for Fe binding to NifU-1.

The results presented above indicate that residues Cys^{35}, Cys^{62} and Cys^{106} within NifU are involved in the transient binding of Fe that is destined for nitrogenase [Fe-S] cluster core formation. If this is correct, substitution of alanine for any of these three cysteine residues would be expected to eliminate the second Fe-binding site within NifU. This possibility was tested by producing three different NifU-1 forms that each have one of the respective cysteine residues substituted by alanine. Each of these altered NifU-1 proteins was purified and compared to intact NifU-1 in terms of their ability to bind Fe based on optically monitored ferric citrate titrations. None of the altered NifU-1 proteins exhibited the characteristic absorption bands associated with the rubredoxin-type ferric center on anaerobic incubation of DTT-treated samples with up to a 5-fold of ferric citrate at 2 °C (data not shown). Coupled with the spectroscopic results presented above, the mutagenesis result strongly suggests that all three of the N-terminal domain cysteines in

NifU, i.e.Cys^{35}, Cys^{62} and Cys^{106}, are involved with ligating iron bound at the rubredoxin-type site.

Discussion

Spectroscopic and functional characterization of site-directed variants of NifU in which each the nine cysteine residues have been targeted individually, and of heterologously expressed N-terminal and C-terminal fragments of NifU containing the first three and last six cysteine residues, respectively, have shown that NifU is a modular protein with at least two distinct domains. The C-terminal half, NifU-2, contains a [2Fe-2S]$^{2+,+}$ cluster coordinated by residues Cys^{137}, Cys^{139}, Cys^{172}, and Cys^{175}, as evidenced by the observation that the cluster is not assembled in variants in which any one of these cysteines residues is substituted by alanine. The important role of the NifU [2Fe-2S]$^{2+,+}$ cluster in nitrogenase [Fe-S] cluster assembly is demonstrated by the low diazotrophic growth rates and specific activities of the nitrogenase Fe-protein and MoFe-proteins in strains grown with variant NifU proteins that are deficient in this cluster. Substitutions for either of the cysteines closest to the C-terminus, Cys^{272} or Cys^{275}, did not alter the spectroscopic properties of the indigenous [2Fe-2S]$^{2+,+}$ cluster, and produced no effect on diazotrophic growth or the ability of the NifU/NifS system to assemble [Fe-S] clusters in the nitrogenase Fe-protein and MoFe-protein. However, a gene encoding a protein with sequence identity to the C-terminal region of NifU and containing only the two C-terminal cysteine residues, has recently been identified in *S. cerevisiae* and shown to be involved with mitochondrial iron metabolism (*11*). Hence the C-terminal region of NifU containing Cys^{272} and Cys^{275} is likely to correspond to a third domain, but the function of the two conserved cysteines residues has yet to be determined.

The ability of NifU-2 to assemble a [2Fe-2S]$^{2+,+}$ cluster with spectroscopic and redox properties almost identical to that of the holoprotein, coupled with the evidence that NifU-1 and NifU are capable of binding ferric ion at a similar rubredoxin-like site, is consistent with NifU having a modular nature in which the C-terminal (NifU-2) domain

can function separately from the N-terminal (NifU-1) domain, as previously suggested by Hwang *et al*. (*8*). Moreover, there are examples of NifU-2-like proteins, such as the bacterioferritin-associated ferredoxin from *E. coli* (*40, 41*), which have the same arrangement of cluster-ligating cysteines as NifU, but lack the three N-terminal and two C-terminal cysteines (Figure 1). Bacterioferritin-associated ferredoxin contains a $[2Fe\text{-}2S]^{2+,+}$ cluster with UV-visible absorption, RR, VTMCD, EPR, and redox properties very similar to those of the equivalent cluster in NifU and NifU-2 (*40, 41*). It has been suggested, although not yet proven, that bacterioferritin-associated ferredoxin plays a crucial redox role in mediating the release or uptake of Fe from bacterioferritin (*41*). In light of the nearly identical properties of NifU-2 and bacterioferritin-associated ferredoxin, their respective functions are likely to be similar. Hence a possible role for the indigenous [2Fe-2S] cluster in NifU lies in redox chemistry related to the acquisition of Fe for [Fe-S] cluster formation. Alternatively, the [2Fe-2S] cluster in NifU may play a redox role in the release of bound ferric ion from the NifU-1 domain and/or the formation/release of an [Fe-S] cluster intermediate from the NifU-1 domain. Defining more precisely the role of the [2Fe-2S] cluster in NifU is a major goal of our ongoing research into [Fe-S] cluster assembly.

By working at low temperatures and utilizing a variant form of NifU ($Asp^{37}Ala$) that is less susceptible to aggregation in the absence of DTT, both NifU-1 and NifU have been shown to be capable to binding a mononuclear ferric ion in an analogous rubredoxin-like environment, using the combination of optical absorption and RR spectroscopies. The lability of the Fe bound at this site inhibits accurate assessment of the binding stoichiometry. Nevertheless, the RR spectra are best interpreted in terms of an approximately tetrahedral site involving three rather than four cysteinate ligands, and the maximal visible extinction coefficient are comparable to those observed for rubredoxin variants with three cysteine and one oxygenic ligand. Hence we conclude that up to one ferric ion can be bound per monomer in a site with three cysteine ligands. The nature of

the fourth ligand is undetermined at present and water or a protein based oxygenic or nitrogenous ligands are all viable candidates. Compelling evidence that all three of the cysteines in the NifU-1 domain are involved with Fe binding and the role of NifU in [Fe-S] cluster assembly is provided by amino acid substitution results. Individual Cys-to-Ala substitutions involving each of the three N-terminal cysteines in NifU, Cys^{35}, Cys^{62}, and Cys^{106}, show that all three are essential for optimal diazotrophic growth rates, producing nitrogenase component proteins with optimal activities, and binding ferric ion in a labile rubredoxin-type site in the NifU-1 domain. Moreover, the NifU-1 domain is very similar in size and shows a high degree of primary sequence identity when compared to the IscU proteins that are widespread in prokaryotic and eukaryotic organisms (*8*) and implicated in the general mobilization of iron for [Fe-S] cluster formation (*9, 11*).

The ability of NifU to bind ferric ion provided the first direct evidence in support of the hypothesis that NifU is involved with the mobilization of Fe for [Fe-S] cluster assembly. However, many questions still remain concerning the function of NifU. Of paramount importance is the question of whether NifU provides an Fe or [Fe-S] cluster delivery system. Binding Fe to NifU may be the precusor to assembly of a transient [Fe-S] cluster in the presence of NifS which is then transferred intact to an apoprotein. Indeed we have recently been successful in obtaining optical absorption and RR evidence for the assembly of a labile $[2Fe\text{-}2S]^{2+}$ in wild-type and $Asp^{37}Ala$ NifU-1 and in $Asp^{37}Ala$ NifU in the presence of ferric ion, L-cysteine and catalytic amounts of NifS (*42*). Hence the notion of NifU as a scaffold for assembly of a [2Fe-2S] unit that can be inserted intact into an apoprotein is a viable hypothesis. The possibility that it is capable of performing either Fe or [Fe-S] delivery roles as the need dictates, must also be considered. For both processes the question of the mechanism of release of the transiently bound Fe or [Fe-S] cluster fragment has yet to be addressed. Reductive release mediated by the indigenous $[2Fe\text{-}2S]^{2+,+}$ cluster is an attractive hypothesis in light of the absence of spectroscopic evidence for a cysteinyl-ligated Fe(II) site in reduced NifU-1.

In summary, site-directed mutagenesis and gene replacement techniques have been used to determine that NifU cysteine residues Cys^{35}, Cys^{62}, Cys^{106}, Cys^{137}, Cys^{139}, Cys^{172}, and Cys^{175} are all necessary for full physiological function. Residues Cys^{137}, Cys^{139}, Cys^{172}, and Cys^{175} have been identified as the [2Fe-2S] cluster ligands and residues Cys^{35}, Cys^{62}, Cys^{106} have been shown to be necessary for binding Fe at a second site within NifU. These results, and the lability of Fe binding at the second site, are consistent with a model where Fe destined for [Fe-S] cluster formation is transiently bound at this site.

Acknowledgment

This work was supported by grants from the National Science Foundation (MCB9630127 to DRD), the National Institutes of Health (GM51962 to M.K.J.) and by a National Science Foundation Research Training Group Award to the Center for Metalloenzyme Studies (BIR-9413236). We thank Dr. Marc Verhagen for helpful discussion and for assistance with redox measurements, and Brian Crouse for carrying out some of the initial spectroscopic characterizations of NifU variants.

References

1. Dean DR, Bolin JT, Zheng L (1993) *J Bacteriol* **175**: 6737-6744
2. Zheng L, White RH, Cash VL, Jack RF, Dean DR (1993) *Proc Natl Acad Sci U.S.A.* **90**: 2754-2758
3. Zheng L, White RH, Cash VL, Dean DR (1994) *Biochemistry* **33**: 4714-4720
4. Zheng L, Dean DR (1994) *J Biol Chem* **269**: 18723-18726
5. Fu W, Jack RF, Morgan TV, Dean DR, Johnson MK (1994) *Biochemistry* **33**: 13455-13463
6. Beynon J, Ally A, Cannon M, Cannon F, Jacobson MR, Cash VL, Dean DR (1987) *J Bacteriol* **169**: 4024-4029
7. Ouzounis C, Bork P, Sander C (1994) *Trends Biochem Sci* **19**: 199-200
8. Hwang DM, Dempsey A, Tan KT, Liew CC (1996) *J Mol Evol* **43**: 536-540
9. Zheng L, Cash VL, Flint DH, Dean DR (1998) *J Biol Chem* **273**: 13264-13272
10. Flint DH (1996) *J Biol Chem* **271**: 16068-16074
11. Schilke B, Voisine C, Beinert H, Craig E (1999) *Proc Natl Acad Sci USA* **96**: 10206-10211
12. Kispal G, Csere P, Prohl C, Lill R (1999) *EMBO J* **18**: 3981-3989
13. Brigle KE, Setterquist RA, Dean DR, Cantwell JS, Weiss MC, Newton WE (1987) *Proc Natl Acad Sci USA* **84**: 7066-7069
14. Page WJ, von Tigerstrom M (1979) *J Bacteriol* **139**: 1058-1061
15. Tabor S, Richardson CC (1985) *Proc Natl Acad Sci USA* **82**: 1074-1078
16. Gornall AG, Bardawill CJ, David MM (1949) *J Biol Chem* **177**: 751-766
17. Smith PK, Krohn RL, Hermanson GT, Mallia AK, Gartner FH, Provenzano MD, Fujimoto EK, Goeke NM, Olson BJ, Klenk DC (1985) *Methods Enzymol* **226**:199-232

18. Jacobson MR, Cash VL, Weiss MC, Laird NF, Newton WE, Dean DR (1989) *Mol Gen Genet* **219**: 49-57

19. Strandberg GW, Wislon PW (1968) *Can J Microbiol* **14**: 25-31

20. Johnson MK (1988) In: Que L (ed) Metal clusters in proteins, ACS Symposium Series Vol.372, American Chemical Society, Washington, DC, pp 326-342

21. Thomson AJ, Cheesman MR, George SJ (1993) *Methods Enzymol* **226**:199-232

22. Aasa R, Vanngard T (1975) *J Magn Reson* **19**:308-315

23. Drozdzewski PM, Johnson MK (1988) *Appl Spectrosc* **42**:1575-1577

24. Hagen WR (1989) *Eur J Biochem* **182**: 523-530

25. Han S, Czernuszewicz RS, Spiro TG (1989) *J Am Chem Soc* **111**: 3496-3504

26. Han S, Czernuszewicz RS, Kimura T, Adams MWW, Spiro TG (1989) *J Am Chem Soc* **111**: 3505-3511

27. Fu W, Drozdzewski PM, Davies MD, Sligar SG, Johnson MK (1992) *J Biol Chem* **267**: 15502-15510

28. Eaton WA, Lovenberg W (1973) In: Lovenberg W (ed) Iron-sulfur proteins, Academic Press, New York, pp 131- 162

29. Bennett DE, Johnson MK (1987) *Biochim Biophys Acta* **911**: 71-80

30. Gebhard MS, Deaton JC, Koch SA, Millar M, Solomon EI (1990) *J Am Chem Soc* **112**: 2217-2231

31. Oganesyan VS, George SJ, Cheesman MR, Thomson AJ (1999) *J Chem Phys* **110**: 762-777

32. Moura I, Bruschi M, LeGall J, Moura JJG, Xavier AV (1977) *Biochem Biophys Res Commun* **75**: 1037-1044

33. Staples CR (1997) PhD dissertation, University of Georgia, Athens, Georgia

34. Archer M, Huber R, Tavares P, Moura I, Moura JJG, Carrondo MA, Sieker LC, LeGall J, Romão MJ (1995) *J. Mol. Biol.* **251**: 690-702

35. Czernuszewicz RS, LeGall J, Moura I, Spiro TG (1986) *Inorg Chem* **25**: 696-700

36. Meyer J, Gaillard J, Lutz M (1995) *Biochem Biophys Res Commun* **212**: 827-833

37. Xiao Z, Lavery MJ, Ayhan M, Scrofani SDB, Wilce MCJ, Guss JM, Tregloan PA, George GN, Wedd AG (1998) *J Am Chem Soc* **120**: 4135-4150

38. Tavares P, Ravi N, Moura JJG, LeGall J, Huang Y-H, Crouse BR, Johnson MK, Huynh BH, Moura I (1994) *J Biol Chem* **269**: 10504-10510

39. Werth MT, Johnson MK (1989) *Biochemistry* **28**: 3982-3988

40. Garg RP, Vargo CJ, Cui X, Kurtz DM, Jr (1996) *Biochemistry* **35**: 6297-6301

41. Quail MA, Jordon P, Grogan JM, Butt JN, Lutz M, Thomson AJ, Guest JR (1996) *Biochem Biophys Res Commun* **227**: 635-642

42. Yuvaniyama P, Agar JN, Cash VL, Johnson MK, Dean DR (1999) *Proc Natl Acad Sci U.S.A.* **97**: 599-604

Table 3-4. Effects of substituting NifU cysteine residues

Residue Substituted[a]	Diazotrophic Growth[b]	*S* =1/2 EPR Signal[c]
Cys-35	Slow	Yes
Cys-62	Slow	Yes
Cys-106	Slow	Yes
Cys-137	Slow	No
Cys-139	Slow	No
Cys-172	Slow	No
Cys-175	Slow	No
Cys-272	Normal	Yes
Cys-275	Normal	Yes

[a]All residues were substituted by alanine and, in some cases, by a variety of other amino acids. All phenotypes were the same for any substitution at a particular position. [b]Typical diazotrophic growth rates are shown in Figure 3. [c]Indicates the presence or absence of the characteristic EPR spectrum of the isolated NifU protein. This spectrum is shown in Figure 6.

Figure3-1. Comparison of the primary sequence of NifU from *A. vinelandii* (Av-NifU) to the sequence of IscU from *A. vinelandii* (Av-IscU) and the primary sequence of the bacterioferritin-associated ferredoxin from *E. coli* (Ec-Fdx). Conserved sequences are blue. The nine cysteines contained within NifU are indicated by a dagger above the sequence. A schematic representation of NifU and the nine cysteines contained within NifU is shown below the sequence comparisons. The segments of NifU corresponding to NifU-1 and NifU-2 are also shown.

```
Av-NifU      MWDYSEKVKEHFYNPKNAGAVEGANA---IG
Av-IscU       MAYSDKVIDHYENPRNVGKLDAQDPDVGTG

                   †35
Av-NifU      DVGSLSCGDALRLTLKVDPETDVILDAGFQT
Av-IscU      MVGAPACGDVMRLQIKVN-EQGIIEDAKFKT

               †62
Av-NifU     FGCGSAIASSSALTEMVKGLTLDEALKISNQDIA
Av-IscU     YGCGSAIASSSLATEWMKGRTLEEAETIKNTQIA

                        †106
Av-NifU     DYLDGLPPEKMHCSVMGREALQAAVANYRGETIEDD
Av-IscU     EELA-LPPVKIHCSVLAEDAIKAAVARDYKHKKGLV
```

NifU-1

```
                  137† †139
Av-NifU     HEEGALICKCFAVDEVMVRDTIRANKLSTVEDVTNYTKAG
Ec-Bfd          MYVCLCNGISDKKIRQAVRQFSPHSFQQLKKFIPVG

               172†  †175
Av-NifU      GGCSACHEAIERVLTEELAARGEVFVAAPIKAKKKV
Ec-Bfd       NQCGKCVRAAREVMEDELMQLPEFKESA
```

NifU-2

```
Av-NifU     KVLAPEPAPAPVAEAPAAAPKLSNLQRIRRIETVLAAIRPTLQR
            DKGDV
                           272†  †275
Av-NifU     ELIDVDGKNVYVKLTGACTGCQMASMTLGGIQQRLIEELGEFVK
            VIPVS
```

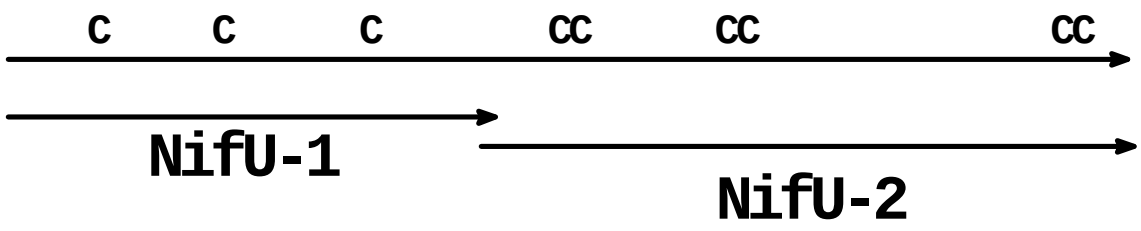

Figure 3-2. Polyacrylamide gel electrophoretic analysis of purified NifU, NifU-1, and NifU-2. Lanes: A, molecular weight standards that include phosphorylase *b*, bovine serum albumin, ovalbumin, trypsin inhibitor, and lysozyme; B, purified NifU; C, purified NifU-1; D, purified NifU-2.

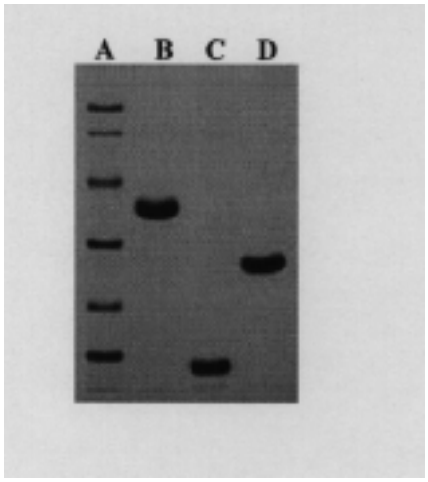
A
B
C
D

Figure 3-3. Growth of wild-type and mutant strains of *A. vinelandii* using N_2 as the sole nitrogen source. Growth was monitored using a Summerson-Klett meter, equipped with a # 66 filter; Wild-type (●), strain DJ961 (■), strain DJ105 (▲). Strain DJ961 has the *nifU* cysteine 106 residue substituted by alanine and strain DJ105 is deleted for *nifU*.

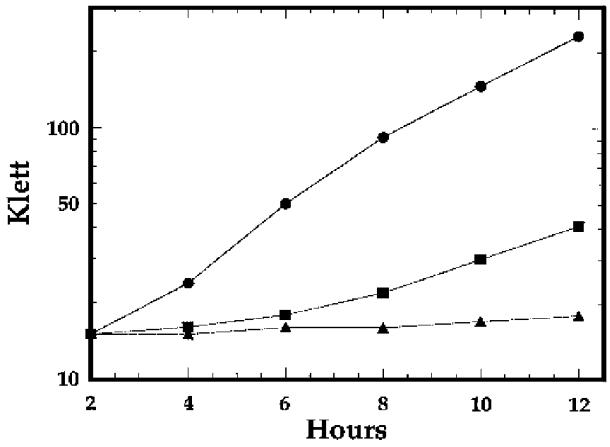
Klett
100
50
10
2
4
6
8
10
12
Hours

Figure3-4. Room temperature UV-visible absorption spectra of NifU-2. The upper spectrum is NifU-2 as isolated, and the lower spectrum is NifU-2 with a 10-fold stoichiometric excess of sodium dithionite. Protein concentration was 0.21 mM, and the buffering medium was 25 mM Tris/HCl buffer, pH 7.4. The dominant absorption centered at 314 nm in the reduced spectrum results from dithionite.

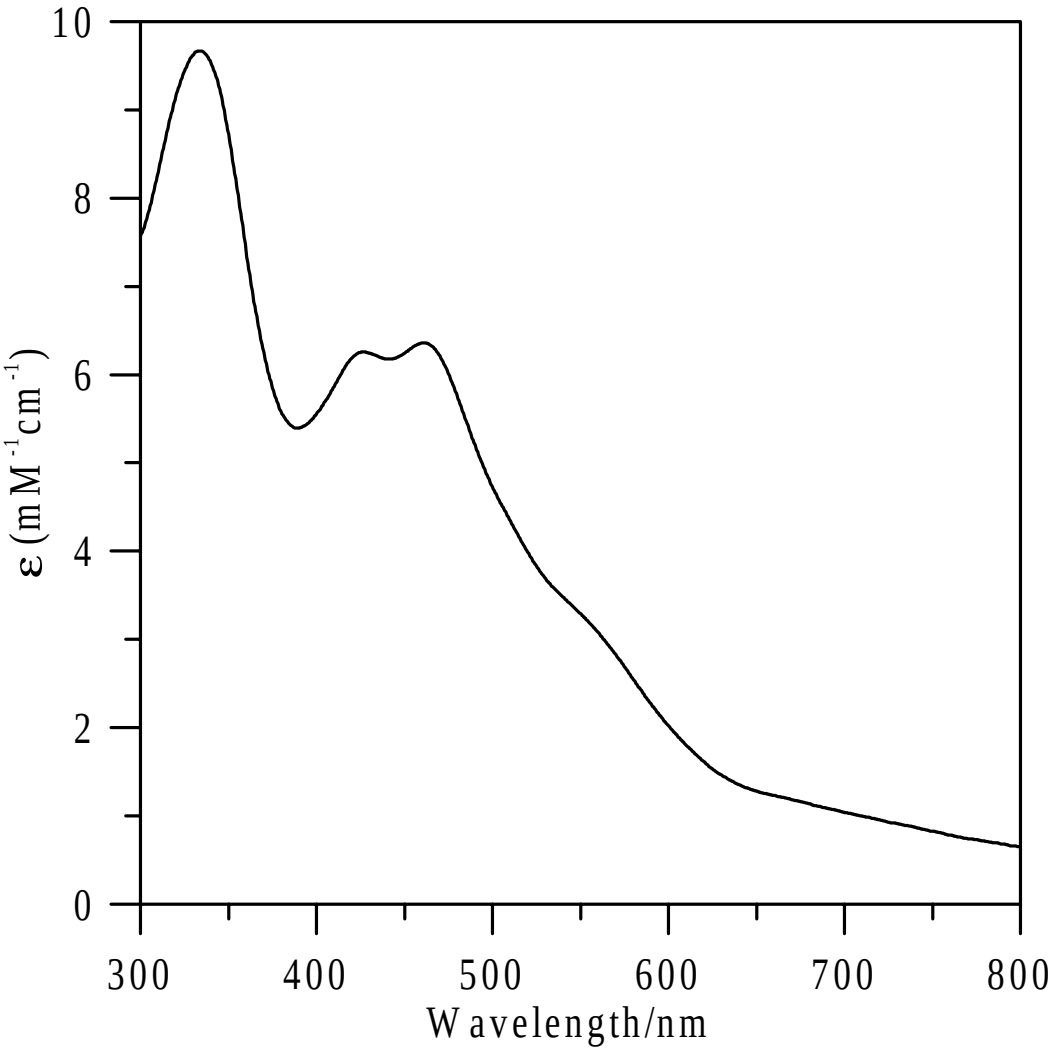
10
8
6
4
2
0
ε (mM-1cm-1)
300
400
500
600
700
800
Wavelength/nm

Figure 3-5. Comparison of the low-temperature resonance Raman spectra of NifU and NifU-2 as prepared. Protein concentrations were ~ 1mM, and the buffering medium was 25 mM Tris/HCl, pH 7.4. The spectra were obtained at 18 K using 457.9 nm argon laser excitation and each is the sum of 40 scans. Each scan involved advancing the spectrometer in 0.5 cm^{-1} increments and photon counting for 1 s/point with 6 cm^{-1} resolution.

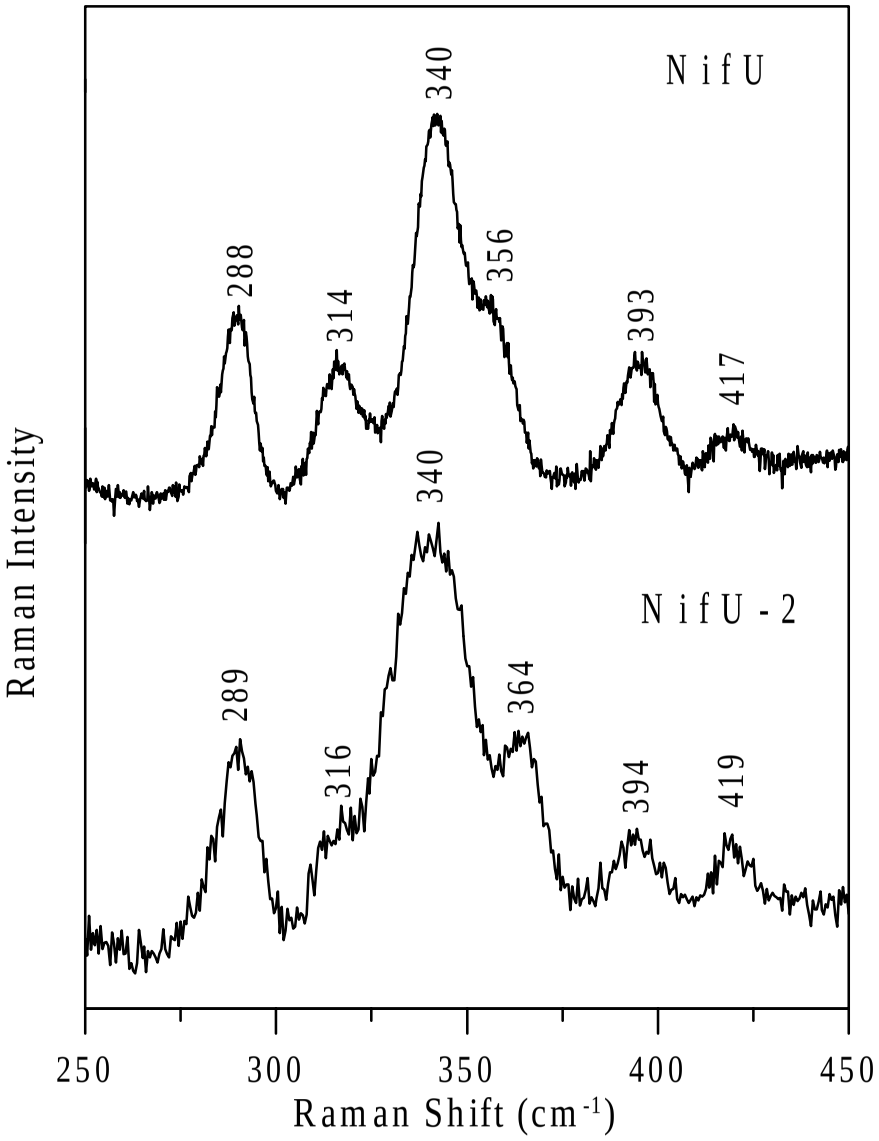
NifU
340
288
314
356
393
417
NifU-2
340
289
316
364
394
419
Raman Intensity
250
300
350
400
450
Raman Shift (cm-1)

Figure 3-6. Comparison of the X-band EPR spectra of dithionite-reduced NifU and NifU-2. Conditions of measurement: microwave frequency, 9.60 GHz; modulation amplitude, 6.43 G; microwave power, 0.51 mW; temperature, 20 K. Protein concentrations were 0.3 mM, and the buffering medium was 25 mM Tris/HCl, pH 7.4. Simulated spectra are offset directly under each of the experimental spectra. The spectra were simulated with the following parameters: NifU, $g_{1,2,3}$ = 2.019, 1.927, 1.892 and linewidths $l_{1,2,3}$ = 1.12, 1.10, 3.34 mT; NifU-2, $g_{1,2,3}$ = 2.022, 1.928, 1.890 and linewidths $l_{1,2,3}$ = 0.90, 0.93, 3.00 mT.

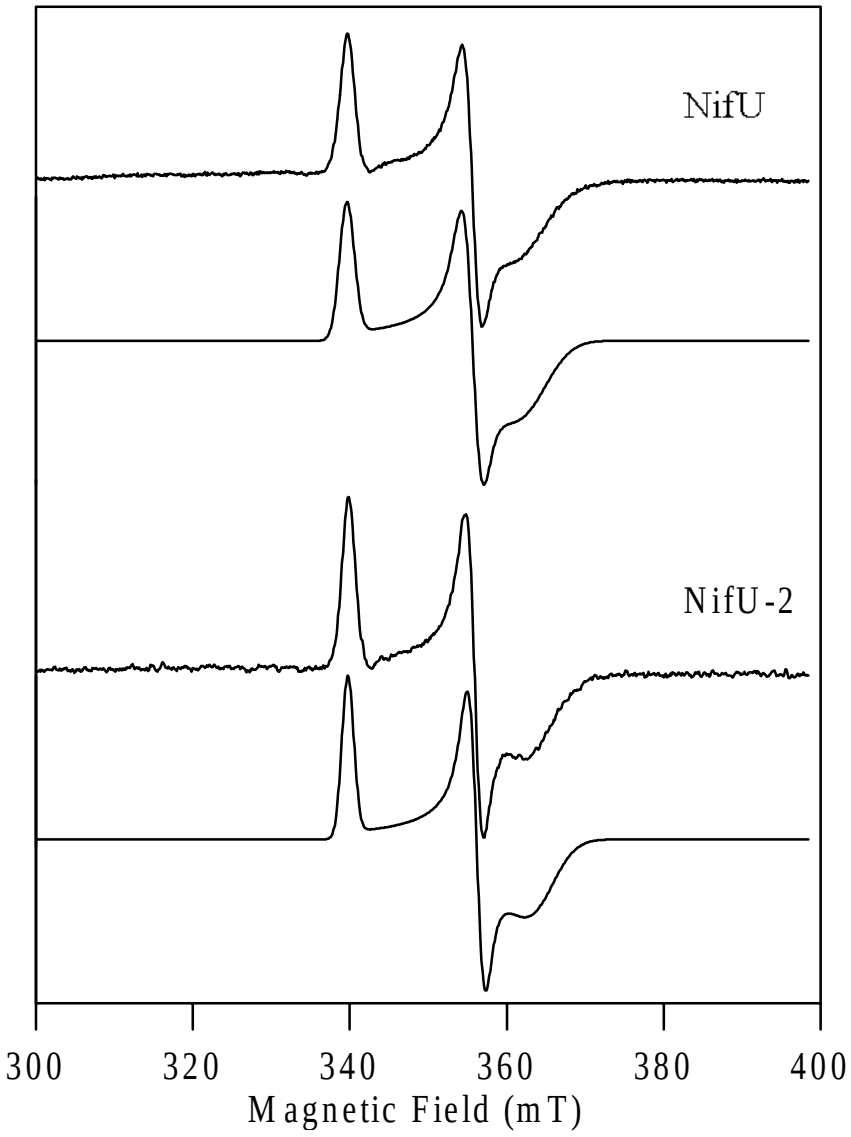
NifU
NifU-2
300
320
340
360
380
400
Magnetic Field (mT)

Figure 3-7. Comparison of the VTMCD spectra of dithionite-reduced NifU and NifU-2. Protein concentrations were 0.11 mM, and the buffering medium was 25 mM Tris/HCl, pH 7.4, with 55% (v/v) ethylene glycol. MCD spectra were recorded in 1-mm cuvettes with a magnetic field of 6.0 T, at 1.70, 4.22, and 10.0 K. All bands increase in intensity with decreasing temperature.

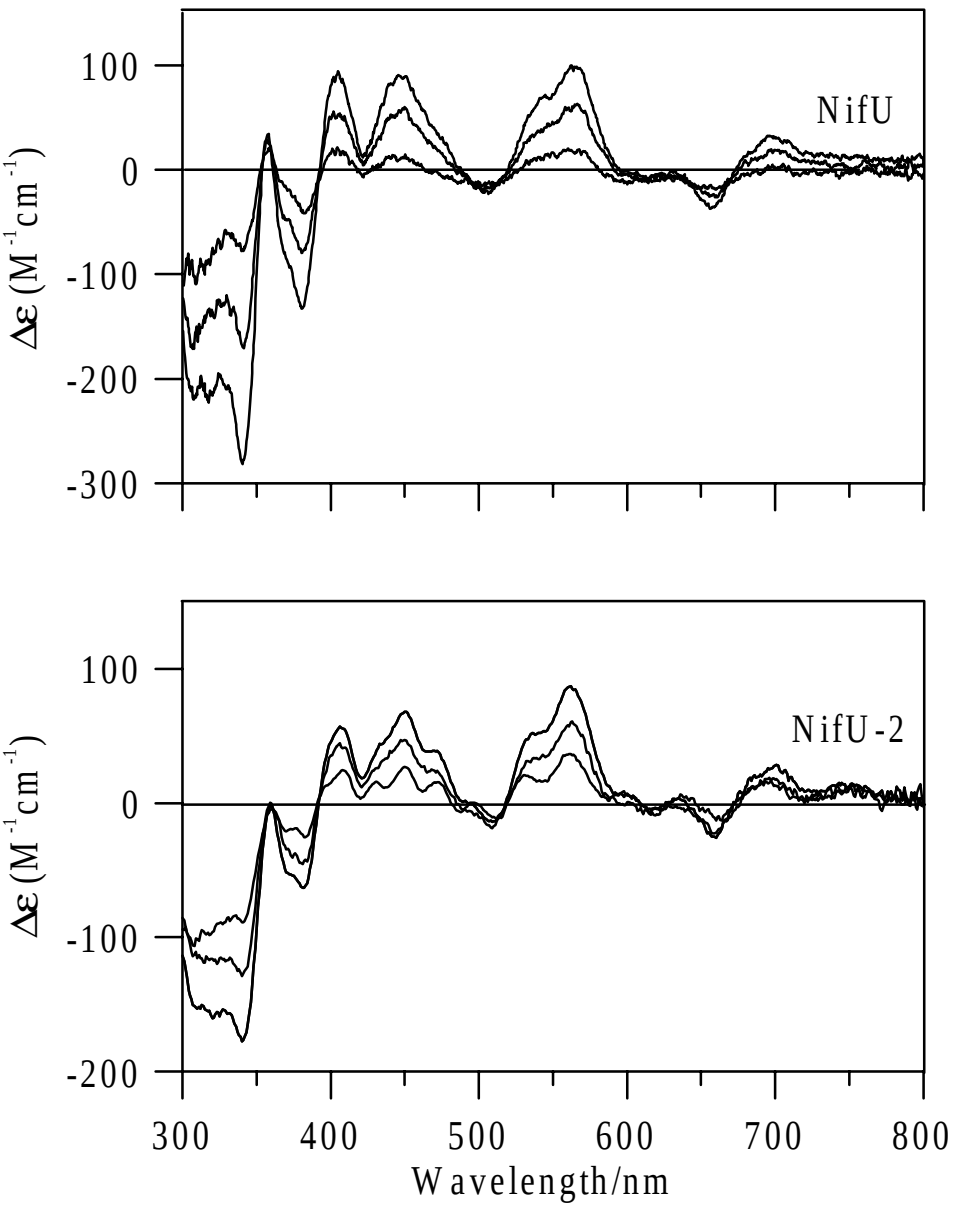
100
0
-100
-200
-300
Δε (M-1cm-1)
NifU
100
0
-100
-200
Δε (M-1cm-1)
NifU-2
300
400
500
600
700
800
Wavelength/nm

Figure3- 8. (A) Low temperature (2 °C) absorption spectra of ferric-bound forms of NifU and NifU-1. Upper panel: NifU (0.04 mM in 100 mM Tris-HCl buffer, pH 8) before (lower spectrum) and after (upper spectrum) incubation with a 1.2-fold stoichiometric excess of ferric citrate for 40 mins at 2 °C in a 1-cm pathlength cell. Middle panel: Difference spectrum of the spectra shown in the upper panel. Lower panel: NifU-1 (0.10 mM in100 mM Tris-HCl buffer, pH 8) after incubation with a 1.2-fold stoichiometric excess of ferric citrate NifU for 40 mins at 2 °C in a 1-cm pathlength cell. (B) Low temperature (2 °C) absorption spectra of ferric-bound forms of $Asp^{37}Ala$ NifU and wild-type NifU-1. Upper panel: $Asp^{37}Ala$ NifU (0.57 mM in 100 mM Tris-HCl buffer, pH 8) before (lower spectrum) and after (upper spectrum) incubation with a 1.2-fold stoichiometric excess of ferric citrate for 55 mins at 2 °C in a 1-mm pathlength cell. Middle panel: Difference spectrum of the spectra shown in the upper panel. Lower panel: As lower panel in A

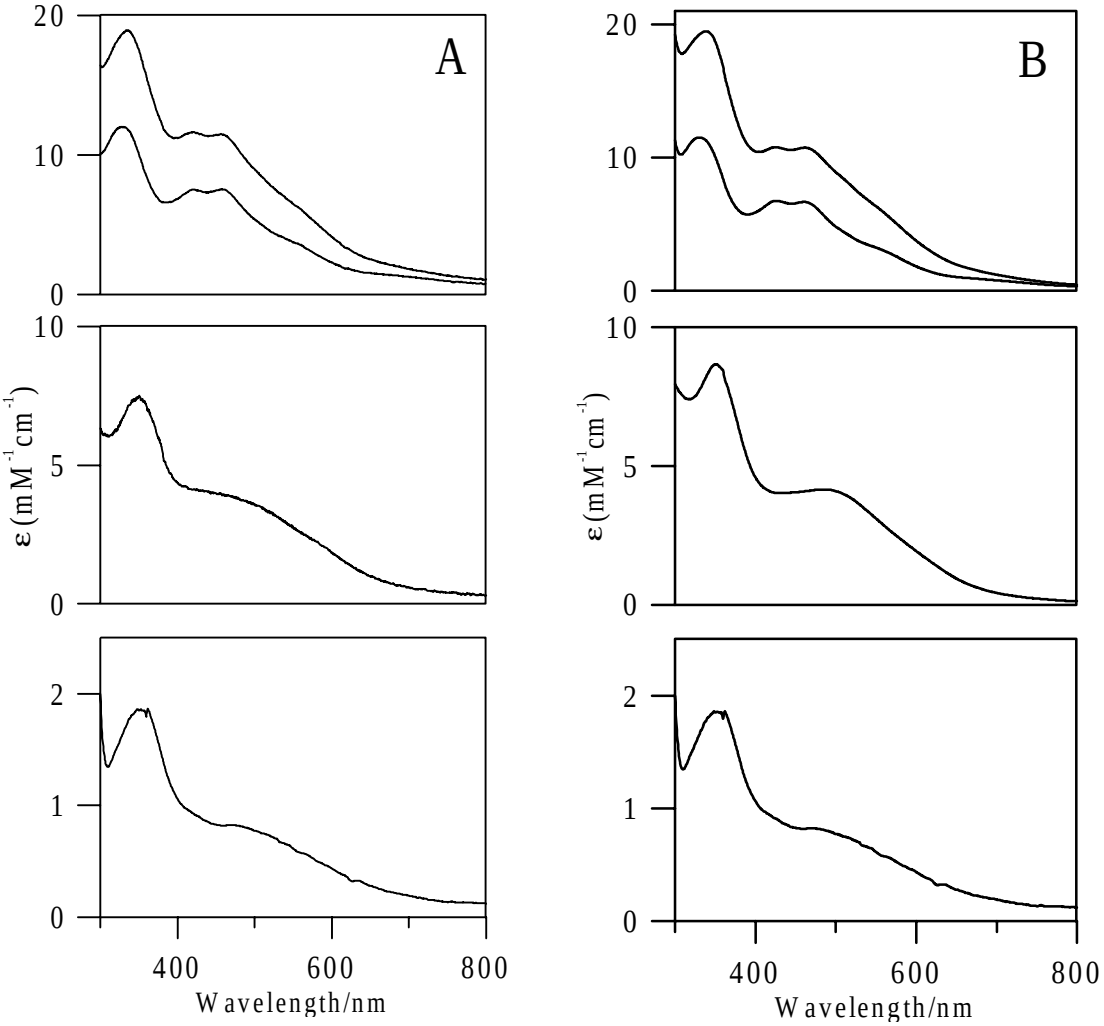
A
B
20
10
0
10
5
0
2
1
0
ε (mM-1cm-1)
400
600
800
Wavelength/nm

Figure 3-9. (A) Low temperature (18 K) resonance Raman spectra of ferric-bound forms of NifU and NifU-1. (a) NifU incubated with a 5-fold excess of ferric citrate at 2 °C for 60 mins. (b) NifU as isolated. (c) Difference spectrum (a) minus (b). (d) NifU-1 incubated with a 5-fold excess of ferric citrate at 2 °C for 60 mins. (B) Low temperature resonance Raman spectra of ferric-bound forms of $Asp^{37}Ala$ NifU and wild-type NifU-1. (a) $Asp^{37}Ala$ NifU incubated with a 5-fold excess of ferric citrate at 2 °C for 60 mins. (b) $Asp^{37}Ala$ NifU as isolated. (c) Difference spectrum (a) minus (b). (d) NifU-1 incubated with a 5-fold excess of ferric citrate at 2 °C for 60 mins. The spectra in panels A and B were collected on samples (~4 mM in 100 mM Tris-HCl buffer at pH 8) maintained at 18 K. Each spectrum was recorded using 496-nm excitation with 70-mW of laser power at the sample and is the sum of 40-50 scans. Each scan involved advancing the spectrometer in 1 cm^{-1} increments and photon counting for 2 s/point with 6 cm^{-1} resolution.

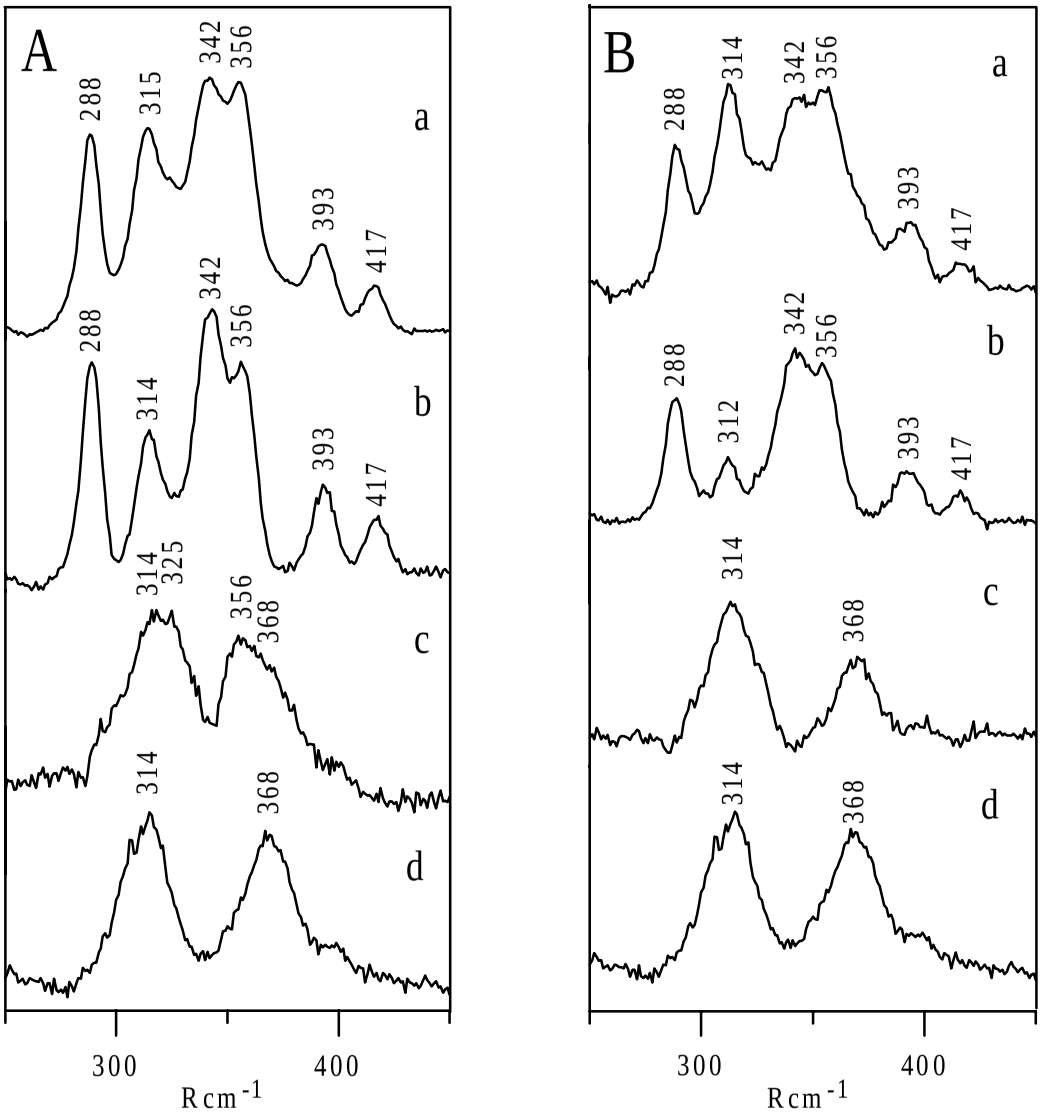
A
288
315
342
356
393
417
a
288
314
342
356
393
417
b
314
325
356
368
c
314
368
d
300
400
Rcm-1
B
288
314
342
356
393
417
a
288
312
342
356
393
417
b
314
368
c
314
368
d
300
400
Rcm-1

Chapter IV

NifS-directed assembly of a transient [2Fe-2S] cluster within the NifU protein[3]

[3] Pramvadee Yuvaniyama,[‡] Jeffrey N. Agar,[§] Valerie L. Cash [‡], Michael K. Johnson,[§] and Dennis R. Dean [‡], (2000) *Proc. Natl. Acad. Sci. U.S.A.* **97**, 599-604

[‡] Department of Biochemistry, Virginia Tech, Blacksburg, VA 24061-0346; and

[§] Department of Chemistry and Center for Metalloenzyme Studies, University of Georgia, Athens, GA 30602

Abstract

The NifS and NifU proteins from *Azotobacter vinelandii* are required for the full activation of nitrogenase. NifS is a homodimeric cysteine desulfurase that supplies the inorganic sulfide necessary for formation of the Fe-S clusters contained within the nitrogenase component proteins. NifU has been suggested to complement NifS either by mobilizing the Fe necessary for nitrogenase Fe-S cluster formation or by providing an intermediate Fe-S cluster assembly site. As isolated, the homodimeric NifU protein contains one $[2Fe\text{-}2S]^{2+,+}$ cluster per subunit, which is referred to as the permanent cluster. In this report, we show that NifU is able to interact with NifS and that a second, transient [2Fe-2S] cluster can be assembled within NifU *in vitro* when incubated in the presence of ferric ion, L-cysteine, and catalytic amounts of NifS. Approximately one transient [2Fe-2S] cluster is assembled per homodimer. The transient [2Fe-2S] cluster species is labile and rapidly released on reduction. We propose that transient [2Fe-2S] cluster units are formed on NifU and then released to supply the inorganic iron and sulfur necessary for maturation of the nitrogenase component proteins. The role of the permanent [2Fe-2S] clusters contained within NifU is not yet known, but they could have a redox function involving either the formation or release of transient [2Fe-2S] cluster units assembled on NifU. Because homologs to both NifU and NifS, respectively designated IscU and IscS, are found in non-nitrogen fixing organisms, it is possible that the function of NifU proposed here could represent a general mechanism for the maturation of Fe-S cluster-containing proteins.

Introduction

Iron-sulfur clusters are found in numerous proteins that have important redox, catalytic, or regulatory properties (for a recent review, see ref. 1). Moreover, Fe-S clusters are intimately involved in the respective functions of these proteins. For example, Fe-S clusters are known to act as electron carriers or environmental sensors or to be involved in substrate binding and activation. Advances in our understanding of the structures, organization, and reactivity of certain biologically relevant Fe-S clusters have involved determination of the spectroscopic and electronic properties of protein-bound Fe-S clusters, characterization of clusters chemically extruded from their polypeptide matrices, and preparation of synthetic Fe-S clusters. Until recently, however, the biological mechanism by which Fe-S clusters are formed has received scant attention. It was shown many years ago that Fe-S clusters could be spontaneously incorporated into apo-forms of certain ferredoxins by simply incubating them *in vitro* in a solution that contains iron and sulfide (2). However, considering the toxicity of free iron and sulfide, it is unlikely that protein-bound Fe-S clusters are spontaneously formed *in vivo* from free iron and sulfide. It is more likely that the iron and sulfur necessary for Fe-S cluster formation are delivered to the cluster assembly site by intermediate carrier proteins.

Previous work has led to the proposal that the NifU and NifS nitrogen fixation-specific gene products are involved in the acquisition of iron and sulfur necessary for the maturation of the two nitrogenase component proteins, both of which contain Fe-S clusters (3). It was shown that NifS is a pyridoxal phosphate-dependent L-cysteine desulfurase and that an enzyme-bound persulfide is an intermediate in that reaction (4, 5). Thus, NifS has been targeted as the source of inorganic sulfide necessary for nitrogenase Fe-S cluster formation. We have recently found that NifU is a modular protein with two distinct types of iron-binding sites (see Figure 1). One of these binding site types is located within the central third of the NifU primary sequence (6, 7) and binds a $[2Fe\text{-}2S]^{2+,+}$ cluster (one cluster binding site per subunit). The second type of site is a

labile mononuclear iron-binding site (7) located within the N-terminal third of the NifU primary sequence (one mononuclear site per subunit). Because the $[2Fe\text{-}2S]^{2+,+}$ clusters present in isolated NifU are tightly bound to the protein (6), the labile mononuclear site is the likely source of iron for nitrogenase Fe-S cluster assembly. If NifS and NifU do have complementary functions in the mobilization of sulfur and iron for nitrogenase Fe-S cluster assembly, several different pathways for this process can be considered. For example, NifS and NifU could either operate independently during Fe-S cluster formation or they could function together. If NifU and NifS function together, then iron and sulfur could be separately released from each of them during cluster assembly or an Fe-S cluster precursor could be preformed and then released. In the current work we have addressed these issues by asking whether NifU and NifS are able to form a macromolecular complex and whether a labile Fe-S cluster species can be formed on NifU.

Experimental Procedures

Plasmids and Strains. Construction of plasmids used for the heterologous expression of altered forms of NifU in *Escherichia coli* has been described (7). Plasmid pDB822 was used to express a full-length version of NifU for which the Cys^{137} residue is substituted by Ala. This form of NifU is designated NifU ($Cys^{137}Ala$). Plasmid pDB1041 was used to express a full-length version of NifU for which the Asp^{37} residue was substituted by Ala [designated NifU($Asp^{37}Ala$)]. Plasmid pDB937 was used to express a truncated form of NifU that includes the first 131 residues of NifU. This truncated form of NifU is designated NifU-1. Plasmid pDB1044 was obtained by the oligonucleotide-directed mutagenesis of pDB937. This plasmid expresses a form of NifU-1 that has the Asp^{37} residue substituted by Ala and is designated NifU-1 ($Asp^{37}Ala$). Figure 1 is a schematic representation of NifU and different forms of NifU used in the current work.

Biochemical Manipulations. The purification of NifS and altered forms of NifU was performed as previously described (4, 7). The optimized *in vitro* Fe-S cluster

biosynthetic system includes the following: 0.05 mM NifU-1 dimer (or other form of NifU-1 or NifU)/0.1 mM ferric ammonium citrate/5 mM β-mercaptoethanol/1 mM L-cysteine/1 μM NifS/0.1 M NaCl in a 25 mM Tris·HCl (pH 7.4) buffer. All volumes were 1.0 ml, and reactions were carried out anoxically in a septum-sealed cuvette under an Ar atmosphere. Protein samples were purified under Ar, and buffers used were extensively degassed and sparged with Ar before use. Anoxic conditions were maintained with a Schlenk apparatus and/or an anaerobic glovebox. Reactions were initiated by the addition of L-cysteine and were monitored by UV-visible spectroscopy as described below.

NifU and NifS complex formation was monitored by gel exclusion HPLC (Beckman System Gold) column chromatography with a Zorbax GF-250 column. Volumes of 100 μl containing 6 nmol of NifU or NifS (or 6 nmol of NifU plus 6 nmol of NifS) in a 25 mM Tris·HCl (pH 7.4) buffer containing 20 mM NaCl/1.0 mM DTT were injected onto the column. Samples that contained a mixture of NifU and NifS were preincubated at room temperature for 8 min before loading the column. For sample mixtures in which a molar excess of NifU or NifS was used, the sample contained approximately 6 nmol of one protein and 12 nmol of the other. Elution of the protein samples was monitored by visible A at 405 nm. Results obtained by using the Beckman System Gold HPLC were also independently confirmed with an Amersham-Pharmacia FPLC chromatography system fitted with a Superose 12 column.

Spectroscopic Methods. All sample concentrations are based on protein determinations and are expressed per NifU or NifU-1 monomer. UV-visible absorption spectra were recorded under anoxic conditions in septum-sealed 1-mm and 1-cm cuvettes, by using a Shimadzu 3101PC scanning spectrophotometer or a Cary diode array spectrophotometer. X-band (9.6 GHz) EPR spectra were recorded by using a Bruker ESP-300E EPR spectrometer equipped with a dual-mode ER-4116 cavity and an Oxford Instruments ESR-9 flow cryostat.

Resonance Raman spectra were recorded by using an Instruments SA (Edison, NJ) Ramanor U1000 spectrometer fitted with a cooled RCA 31034 photomultiplier tube with 90° scattering geometry and lines from a Coherent Radiation (Palo Alto, CA) Sabre10-W argon ion laser. Spectra were recorded digitally with photon-counting electronics, and the signal/noise ratio was improved by signal averaging multiple scans. Band positions were calibrated by using the excitation frequency and CCl4, and these positions are accurate to ±1 cm^{-1}. Samples consisted of 12-µl droplets of concentrated protein (2-4 mM) that were placed in a custom designed sample cell attached to the cold finger of an Air Products Displex model CSA-202E closed-cycle refrigerator. The sample temperature was maintained at 18 K during scanning to minimize laser-induced sample degradation. Bands caused by the frozen buffer solutions have been subtracted from all of the spectra shown in this work after normalization of lattice modes of ice centered at 229 cm^{-1}.

Results

NifU and NifS Complex Formation. That NifU and NifS do not form a tight complex was determined in two different ways. First, NifU was not found to copurify with NifS when NifS was isolated from crude extracts prepared from nitrogen-fixing *Azotobacter vinelandii* cells. Second, specific immunoprecipitation of either NifU or NifS from *A. vinelandii* crude extracts did not result in the coprecipitation of the complementary protein. However, NifU and NifS can form a transient complex because an equimolar mixture of NifU and NifS results in the appearance of a new peak during size-exclusion column chromatography when compared with individually chromatographed samples of either NifU or NifS (Figure 2). Calibration of the column and denaturing gel electrophoresis of the peak fraction of the NifU-NifS complex indicate formation of a heterotetrameric complex. When a twofold molar excess of NifU was mixed with NifS, a peak corresponding to the NifU-NifS complex and a peak corresponding to uncomplexed NifU could be resolved by gel exclusion chromatography.

The converse experiment involving the addition of a twofold molar excess of NifS also resulted in the appearance of two peaks during chromatography of the sample, one corresponding to NifS and the other corresponding to the NifU-NifS complex. The shoulder recognized in the NifU-NifS complex fraction shown in Figure 2 is reproducible and probably indicates that dissociation of the complex occurs during chromatography.

Experimental Rationale. In previous work we found that seven cysteines contained within NifU are required for its full *in vivo* function (7). Four of these cysteines (Cys^{137}, Cys^{139}, Cys^{172}, and Cys^{175}) are contained within a central segment of NifU and provide the ligands for the [2Fe-2S] cluster present in each monomer of the dimeric NifU protein as isolated. Because the [2Fe-2S] clusters contained within isolated NifU are tightly bound and cannot be released by chelating reagents, we refer to them as the permanent clusters and consider it unlikely that they represent precursors destined for assembly of the nitrogenase metalloclusters. We therefore became interested in whether a second, more labile cluster might be assembled elsewhere on NifU. The three other cysteines (Cys^{35}, Cys^{62}, and Cys^{106}) required for full *in vivo* NifU function were targeted as the most likely residues to participate in providing such an assembly site for formation of a transient cluster. The possibility for assembly of a second Fe-S cluster on NifU was also considered because we recently obtained evidence for the presence of one mononuclear Fe-binding site within each subunit of the NifU protein as isolated (7). Thus, we considered the possibility that binding of Fe at the mononuclear site could represent an intermediate stage in the assembly of a transient Fe-S cluster on NifU. Binding of Fe at the mononuclear site(s) requires residues Cys^{35}, Cys^{62}, and Cys^{106}.

Our ability to test whether a transient Fe-S cluster could be assembled on NifU was complicated by the presence of one permanent [2Fe-2S] cluster in each monomer of intact isolated NifU. This problem was circumvented in two different ways. First, a portion of NifU was recombinantly expressed and then isolated that corresponds only to the N-terminal third of the NifU coding sequence. This truncated form of NifU is referred

to as NifU-1, and it does not include those cysteines that provide the coordinating ligands to the permanent [2Fe-2S] cluster contained within full-length NifU. Thus, the isolated form of NifU-1, which is a homodimer, does not contain the permanent [2Fe-2S] clusters contained within full-length NifU (see Figure 1). Second, a full-length form of altered NifU that carries an alanine substitution for one of the 2Fe-2S cluster-coordinating residues (residue Cys^{137}) was also recombinantly produced and isolated. This altered NifU protein is referred to as NifU(Cys^{137}Ala) and also does not contain the permanent [2Fe-2S] cluster in its isolated form (Figure 1). Purified samples of NifU-1 and NifU (Cys^{137}Ala) were then used in experiments described below, which demonstrate that they can serve as scaffolds for NifS-catalyzed formation of $[2Fe\text{-}2S]^{2+}$ clusters.

NifU-1 and NifU(Ala^{137}) Can Serve as Scaffolds for Assembly of a $[2Fe\text{-}2S]^{2+}$ Cluster. It was possible to develop an optimized *in vitro* Fe-S cluster biosynthetic system that includes a 0.05 mM NifU-1 dimer or NifU (Cys^{137}Ala)/0.1 mM ferric ammonium citrate/5 mM β-mercaptoethanol/1 mM L-cysteine/1 μM NifS. In this biosynthetic system, NifS is present at only very low levels when compared with NifU-1 or NifU(Cys^{137}Ala). One reason for performing the biosynthetic assay in this way was to ensure that the pyridoxal-phosphate chromophore present in NifS would not interfere with the ability to detect Fe-S cluster formation by UV-visible absorption and resonance Raman spectroscopies. Also, by using only catalytic amounts of NifS, it was possible to monitor the time-dependent formation of Fe-S clusters. A typical experiment in which NifU-1 was used as a scaffold for Fe-S cluster assembly is shown in Figure 3A and B. These data show that there is a time-dependent assembly of a chromophoric species in NifU-1 that exhibits absorbance inflections at 325, 420, 465, and 550 nm (Figure 3A). This UV-visible absorption spectrum is characteristic of $[2Fe\text{-}2S]^{2+}$ cluster-containing proteins (8), although the absorption peaks are less well defined in our sample when compared with similar spectra from typical $[2Fe\text{-}2S]^{2+}$ cluster-containing proteins. The most likely explanation for the relatively featureless nature of the absorption spectrum is

that, once formed, the $[2Fe\text{-}2S]^{2+}$ cluster is relatively unstable at ambient temperature. This instability is manifested by a concomitant accumulation of a colloidal precipitate of iron sulfide that is responsible for the spectral inflections becoming increasingly less well defined upon incubation of the sample beyond about 200 min. A colloidal iron-sulfide precipitate also accumulates when NifU-1 is omitted from the reaction mixture, but this occurs at a much slower rate than the rate observed for Fe-S cluster biosynthesis in the complete system.

Figure 3B (curves a and b) shows the time dependence of [2Fe-2S] cluster assembly on the NifU-1 scaffold. These data also show that cluster formation is dependent on the concentration of NifS, with an approximate doubling in the rate of cluster formation when the amount of NifS in the reaction mixture is doubled. The results of control experiments presented in Figure 3B also show that an altered form of NifS, for which the active site Cys^{325} residue was substituted by alanine (5), is not active in cluster formation. Altered forms of NifU-1, in which any one of the three cysteine residues (Cys^{35}, Cys^{62}, and Cys^{106}) has been substituted by alanine, were also ineffective in cluster assembly. Finally, no [2Fe-2S] cluster formation occurred if any of the above-mentioned components of the biosynthetic mixture was omitted. When NifU(Cys^{137}Ala) was substituted for NifU-1 in the assembly mixture, a spectrum having a very similar line shape and intensity and the same absorbance maxima was observed (data not shown).

Isolation of an NifU-1 Variant That Contains a Stabilized $[2Fe\text{-}2S]^{2+}$ Cluster. The $[2Fe\text{-}2S]^{2+}$ cluster assembled onto NifU-1 or NifU(Cys^{137}Ala) is labile *in vitro*. For example, as judged by *A*420/*A*280 ratios, more than 50% of the cluster was lost when gel filtration was used to remove excess reagents. Such lability (also see below) was not unexpected considering that the proposed physiological function of the cluster is to supply the iron and sulfur necessary for nitrogenase metallocluster assembly. In other words, the transient [2Fe-2S] cluster must have a mechanism to escape from the NifU scaffold during the maturation of the nitrogenase component proteins and therefore

should not be tightly bound to NifU. During the course of our studies with altered forms of NifU-1 as an approach to examining the nature of the mononuclear iron-binding site, we fortuitously identified an altered form of NifU-1 that contains some $[2Fe\text{-}2S]^{2+}$ cluster in its isolated state (Figure 3C). This altered form of NifU-1 has the Asp^{37} residue substituted by alanine and is referred to as NifU-1 ($Asp^{37}Ala$). The isolated form of NifU-1 ($Asp^{37}Ala$) contained 0.15 Fe per monomer. Moreover, the $[2Fe\text{-}2S]^{2+}$ cluster contained within isolated NifU-1 ($Asp^{37}Ala$) is stable with no loss or change in the UV-visible spectrum even after incubation at ambient temperature for 12 h. Stabilization of an Fe-S cluster resulting from an amino acid substitution has precedence for the FNR protein from *E. coli*. In this case a variant form was identified that contains a more stable [4Fe-4S] cluster and is affected in signal transduction events dependent on cluster assembly and disassembly (9).

When NifU-1 ($Asp^{37}Ala$) was used as a scaffold for cluster assembly (Figure 3F), a threefold increase in visible absorption intensity over 200 min was observed. The resulting spectrum is characteristic of a biological $[2Fe\text{-}2S]^{2+}$ center and, in agreement with the Fe analyses of the isolated sample, the extinction coefficients (e.g., $A420 = 3.0$ mM^{-1} cm^{-1}) are indicative of approximately 0.5 clusters per monomer or 1.0 cluster per homodimer. This conclusion is based on the range of extinction coefficients for typical $[2Fe\text{-}2S]^{2+}$ proteins [$A420 = 6\text{-}11$ mM^{-1} cm^{-1} (8)]. Analogous biosynthetic cluster reconstitution experiments were also carried out with a full-length form of NifU for which the Asp^{37} residue is substituted by alanine [designated NifU($Asp^{37}Ala$)]. The resulting UV-visible absorption spectrum was indistinguishable from that of the starting spectrum originating from the permanent $[2Fe\text{-}2S]^{2+}$ clusters, except for a uniform 30% increase in absorption intensity in the 300- to 800-nm region. This result is consistent with the formation of about one additional $[2Fe\text{-}2S]^{2+}$ cluster per homodimer (data not shown). It should be noted that, in the biosynthetic system described here, only one ferric ion is added per each protein monomer. Consequently, no more than one $[2Fe\text{-}2S]^{2+}$

cluster could be formed per homodimer. Nevertheless, during the development of the biosynthetic system, we found that the addition of higher levels of ferric iron did not increase the amount of transient cluster accumulated when any of the various forms of NifU was used in the assembly cocktail. The main consequence of a twofold or fivefold increase in the ferric ammonium citrate concentration was to decrease the quality of the absorption data owing to an increase in the accumulation of colloidal iron sulfide.

Resonance Raman Evidence for Assembly of the Transient [2Fe-2S]$^{2+}$ Cluster. Resonance Raman spectroscopy was used to identify and further characterize the transient [2Fe-2S]$^{2+}$ clusters present in the various forms of NifU proteins investigated in this work. A comparison of the low-temperature resonance Raman spectra of the permanent [2Fe-2S]$^{2+,+}$ clusters in NifU and of the transient [2Fe-2S]$^{2+}$ assembled in NifU-1 by using 488-nm excitation is shown in Figure 4A and B. In both spectra, the pattern and frequency of bands in the Fe-S stretching region are uniquely indicative of [2Fe-2S]$^{2+}$ clusters (6, 10-12). The relative intensities of equivalent bands are remarkably similar for both clusters, but the frequencies are all up-shifted by 6-8 cm^{-1} for the transient [2Fe-2S]$^{2+}$ cluster in NifU-1 when compared with the permanent clusters in NifU. Hence, the vibrational assignments made for the permanent clusters in NifU (6) can be transferred directly to the transient cluster. Also, the relative intensities and frequencies of the bands in NifU-1 are almost identical to those of the [2Fe-2S]$^{2+}$ cluster in human ferrochelatase (ref. 12; Figure 4), which has recently been shown to have complete cysteinyl ligation by amino acid substitution (13) and crystallographic studies (H. A. Dailey, personal communication). This result strongly suggests that the cluster assembled on NifU-1 has complete cysteinyl ligation. Because there are only three cysteines available in each monomer, this situation indicates that the transient cluster is most likely bridged between the subunits. The higher Fe-S stretching frequencies for the transient cluster in NifU-1 compared with the permanent clusters in NifU indicate stronger Fe-S bonds for the transient structure. Thus, the lability of the transient cluster is more likely to

be a consequence of enhanced solvent accessibility resulting from its location at the subunit interface, rather than from an intrinsic thermodynamic instability.

Although the lability of the transient $[2Fe\text{-}2S]^{2+}$ cluster has thus far impeded our attempts to obtain resonance Raman spectra from reconstituted full-length NifU, the decreased lability in NifU ($Asp^{37}Ala$) has provided an opportunity to assess the resonance Raman spectrum of the cluster in a full-length version of NifU (Figure 5). The spectrum of the reconstituted form of NifU ($Asp^{37}Ala$) (Figure 5a) is clearly dominated by the permanent clusters of as-isolated NifU (Figure 5b). Nevertheless, the difference between the reconstituted and as-isolated data sets (Figure 5c) reveals a spectrum very similar to that of the reconstituted $[2Fe\text{-}2S]^{2+}$ cluster in NifU-1 ($Asp^{37}Ala$) (Figure 5d) and having approximately half the intensity of the permanent clusters. Because Fe-S stretching frequencies are very sensitive to minor perturbations in the cluster environment, this result indicates a negligible change in the transient cluster environment on removal of the C-terminal domain. Moreover, there is a close similarity in the resonance Raman spectra of the transient clusters reconstituted in NifU-1 (Figure 4b), NifU-1 ($Asp^{37}Ala$) (Figure 5d), and NifU ($Asp^{37}Ala$) (Figure 5c). The main differences among these species lie in the frequencies of the total symmetric predominantly Fe-S(Cys) modes assigned at 349, 337, and 340 cm^{-1} in NifU-1, NifU-1($Asp^{37}Ala$), and NifU($Asp^{37}Ala$), respectively. This variability is likely to originate from differences between the wild-type and $Asp^{37}Ala$ variant in terms of cysteinyl Fe-S-C-C dihedral angles and/or hydrogen bonding interactions involving cysteinyl-S atoms. An attractive possibility is that substitution of the Asp^{37} residue by alanine reduces cluster lability by decreasing solvent accessibility and that this feature is reflected in the resonance Raman as a result of perturbed hydrogen-bonding interactions involving the ligating cysteine S atoms. In summary, all of the resonance Raman spectra clearly demonstrate NifS-mediated assembly of a similar transient [2Fe-2S] cluster in a variety of different forms of NifU.

Release of the [2Fe-2S] Cluster on Its Reduction. UV-visible spectra and/or resonance Raman spectra of the Fe-S clusters formed in the biosynthetic system described here provides evidence for the catalytic formation of a labile $[2Fe\text{-}2S]^{2+}$ cluster within the NifU protein. Complementary spectroscopic evidence for this conclusion could not be obtained by using either electron paramagnetic resonance or variable-temperature magnetic circular dichroism spectroscopy, because of the extreme reductive lability of the cluster. For example, dithionite-mediated reduction of the transient $[2Fe\text{-}2S]^{2+}$ cluster resulted in an immediate, complete, and irreversible bleaching of the visible spectrum. Also, no paramagnetic form of the transient cluster could be trapped even by freezing the sample within 10 s after addition of a twofold excess of dithionite. The dithionite-reduced samples exhibited no $S = 1/2$ EPR signals over the temperature range 10-100 K and no temperature-dependent magnetic circular dichroism bands, suggesting that the $[2Fe\text{-}2S]^{+}$ form is unstable and degraded immediately on reduction. The lability of the transient [2Fe-2S] cluster on reduction was also shown by quantitative capture of the Fe^{2+} ion released during dithionite reduction by using the Fe^{2+}-chelating reagent α,α'-*N*-dipyridyl (data not shown).

Discussion

NifU contains two distinct types of iron-binding sites. In as-isolated NifU, one of these types of sites is occupied by a $[2Fe\text{-}2S]^{2+,+}$ cluster that we refer to as the permanent cluster (6). The other type of iron-binding site is a mononuclear site that is predominantly unoccupied in the as-isolated protein but can be filled *in vitro* by the addition of ferric ion (7). In the current work, we show that L-cysteine and catalytic amounts of NifS can be used to assemble an additional labile $[2Fe\text{-}2S]^{2+}$ cluster within a variety of different forms of the NifU protein. The lability of this cluster and the presence of the permanent clusters have so far prevented definitive identification of this transient cluster in full-length wild-type NifU. However, a combination of UV-visible absorption and resonance Raman studies has provided abundant evidence for the *in vitro* assembly of this cluster in samples

of NifU-1 and the NifU ($Cys^{137}Ala$) variant, neither of which contains the permanent clusters. Other evidence has been obtained with the NifU-1 ($Asp^{37}Ala$) and NifU ($Asp^{37}Ala$) variants, in which the transient cluster is less labile. The same three cysteine residues necessary for iron binding at the mononuclear site are also required for NifS-directed assembly of the transient [2Fe-2S] cluster (Figure 1). Although we cannot yet rule out the possibility that a set of conditions exists whereby one transient $[2Fe\text{-}2S]^{2+}$ cluster can be assembled within each subunit, the available data are consistent with a model in which ferric ions bound at the individual mononuclear sites are rearranged on donation of sulfur by NifS, to form a $[2Fe\text{-}2S]^{2+}$ cluster that is bridged between the two NifU subunits. Evidence supporting this mode of binding includes (i) the lability of the transient [2Fe-2S] cluster; (ii) the iron-binding stoichiometry at the mononuclear sites; (iii) a maximal UV-visible absorption intensity consistent with no more than one transient [2Fe-2S] cluster per NifU homodimer, and (iv) a resonance Raman spectrum that is interpreted in terms of four cysteine ligands, owing to its close correspondence to the spectrum of human ferrochelatase.

The lability of the transient cluster and its release from the polypeptide matrix on reduction is consistent with the hypothesis that the function of the transient cluster is to provide iron and sulfide necessary for the formation of the Fe-S cores of the nitrogenase metalloclusters. The role of the permanent [2Fe-2S] clusters contained within NifU is not yet known. However, the observed release of the transient cluster on reduction indicates that the role of the permanent clusters could be to provide reducing equivalents for that process. In this context we note that both irons contained in the NifU-bound transient cluster are in the ferric oxidation state and that previous work has shown that chemical reconstitution of Fe-S cluster-containing proteins is most effective when ferrous ions are used in the reconstitution system (2). Thus, reduction of the transient cluster might be important not only for its release but also for placing irons destined for nitrogenase metallocluster core formation in the appropriate oxidation state. It is also possible that

the permanent $[2Fe\text{-}2S]^{2+,+}$ clusters could have a redox function in the acquisition of iron for initial binding at the mononuclear sites. There is no *a priori* reason why the permanent clusters could not participate in all of these functions.

Genes encoding homologs to NifU and NifS are also located within the genomes of a wide variety of non-nitrogen fixing organisms (14). We have designated these as *isc* genes to indicate the proposed role of their products in the housekeeping function of general Fe-S cluster assembly. In line with this proposal the isc genes have been found to be essential for *A. vinelandii* viability (14). There is also mounting biochemical and genetic evidence from other laboratories that the *isc* gene products are involved in Fe-S cluster assembly in both prokaryotic (15) and eukaryotic (16-19) organisms. A comparison of the organization of the NifU protein and its proposed housekeeping counterpart, designated IscU, is relevant to the work described here. For example, the IscU protein is considerably truncated when compared with NifU, bearing sequence identity only to the N-terminal third of NifU. This portion of NifU corresponds to the NifU-1 fragment described in the present work. The NifU Cys^{35}, Cys^{62}, and Cys^{106} residues contained within this segment are also strictly conserved in all iscU gene products identified so far. In fact, the IscU primary sequence is among the most conserved sequence motifs in nature (20). The IscU protein does not contain a sequence corresponding to the permanent $[2Fe\text{-}2S]^{2+,+}$ cluster-binding domain present in NifU. However, there is another gene contained within the *isc* gene cluster whose product does harbor weak primary sequence identity when compared with the $[2Fe\text{-}2S]^{2+,+}$ cluster-binding region of NifU. This small ferredoxin has been purified and shown to contain a $[2Fe\text{-}2S]^{2+,+}$ cluster that is nearly identical in its spectroscopic and electronic properties when compared with the [2Fe-2S] clusters contained within as-isolated NifU (21, 22). Thus, a function analogous to that provided by the NifU permanent cluster might also be duplicated by this ferredoxin. It is interesting that a bacterial ferritin-associated $[2Fe\text{-}2S]^{2+,+}$ ferredoxin having the same spatial arrangement of

cluster-coordinating cysteines, as well as the same spectroscopic and electronic properties as the *isc*-specific ferredoxin, has also been identified in *E. coli* (23, 24). This observation has led to speculation that a function of the bacterial ferritin-associated ferredoxin could involve the release of iron from ferritin for Fe-S cluster assembly, a suggestion also in line with a possible role for the permanent clusters contained within NifU.

Although it is not yet known whether a [2Fe-2S] cluster can be assembled on IscU, both IscU and IscS from A. vinelandii have been recombinantly produced and isolated. IscS exhibits an L-cysteine desulfurase activity (14) similar to that demonstrated for NifS (4). Also, in preliminary work, IscS and IscU have been found to form a macromolecular complex similar to that described for NifS and NifU (our unpublished results). Despite these similarities the assembly of Fe-S clusters catalyzed by the Isc system might be considerably more complex than we have found so far for the Nif system. For example, there are heat-shock-cognate (Hsc) proteins encoded within bacterial genomes that have been suggested to have chaperone functions involving either the formation of Fe-S clusters or their insertion into various target proteins (13). Also, in *Saccharomyces cerevisiae*, certain Hsc proteins have already been implicated in the physiological assembly of Fe-S clusters (16, 18, 25). In contrast, there are no known *nif*-specific gene products homologous to the Hsc family of proteins.

Finally, there remain a number of important gaps in our understanding of the mobilization of the iron and sulfur required for maturation of Fe-S cluster-containing proteins. Although the current work demonstrates the *in vitro* ability of NifU to assemble a transient [2Fe-2S] cluster in the presence of NifS, whether this system functions by directly donating a [2Fe-2S] unit for *in vivo* cluster assembly still needs to be determined. If Fe-S clusters are assembled in this way, then there are fundamental issues concerning how the transient cluster is delivered to the target protein and how the [2Fe-2S] units might be assembled into higher-order clusters. In addition, it is not yet known how the

NifS-bound persulfide is physiologically released for assembly of the transient cluster. We believe that the Nif system will continue to provide a model for the biochemical-genetic approach to address these issues.

Acknowledgements

This work was supported by grants from the National Science Foundation (MCB9630127 to D.R.D.) and the National Institutes of Health (GM51962 to M.K.J.).

References

1. Beinert, H., Holm, R. H. & Münck, E. (1997) *Science* **277**, 653-659
2. Malkin, R. & Rabinowitz, J. (1966) *Biochem. Biophys. Res. Commun.* **23**, 822-827
3. Dean, D. R., Bolin, J. T. & Zheng, L. (1993) *J. Bacteriol.* **175**, 6737-6744
4. Zheng, L., White, R., Cash, V. L., Jack, R. F. & Dean, D. R. (1993) *Proc. Natl. Acad. Sci. U.S.A.* **90**, 2754-2758
5. Zheng, L., White, R. H. & Dean, D. R. (1994) *Biochemistry* **33**, 4714-4720
6. Fu, W., Jack, R. F., Morgan, T. V., Dean, D. R. & Johnson, M. K. (1994) *Biochemistry* **33**, 13455-13463
7. Agar, J. N., Yuvaniyama, P., Jack, R. F., Cash, V. L., Smith, A. D., Dean, D. R. & Johnson, M. K. (2000) *J. Biol. Inorg. Chem.* **5**, 166-177
8. Dailey, H. A., Finnegan, M. G. & Johnson, M. K. (1994) *Biochemistry* **33**, 303-407
9. Khoroshilova, N., Beinert, H. & Kiley, P. J. (1995) *Proc. Natl. Acad. U.S.A.* **92**, 2499-2503
10. Han, S., Czernuszewicz, R. S. & Spiro, T. G. (1989) *J. Am. Chem. Soc.* **111**, 3496-3504
11. Han, S., Czernuszewicz, R. S., Kimura, T., Adams, M. W. W. & Spiro, T. G. (1989) *J. Am. Chem. Soc.* **111**, 3505-3511
12. Crouse, B. R., Sellers, V. M., Finnegan, M. G., Dailey, H. A. & Johnson, M. K. (1996) *Biochemistry* **35**, 16222-16229
13. Sellers, V. M., Wang, K.-F., Johnson, M. K. & Dailey, H. A. (1998) *J. Biol. Chem.* **273**, 22311-22316
14. Zheng, L., Cash, V. L., Flint, D. H. & Dean, D. R. (1998) *J. Biol. Chem.* **273**, 13264-13272
15. Nakamura, M., Saeki, K. & Takahashi, Y. (1999) *J. Biochem.* **126**, 10-18

16. Kispal, G., Csere, P., Prohl, C. & Lill, R. (1999) *EMBO J.* **18**, 3981-3939

17. Schilke, B., Voisine, C., Beinert, H. & Craig, E. (1999) *Proc. Natl. Acad. Sci. U.S.A.* 96, 10206-10211

18. Strain, J., Lorenz, C. R., Bode, J., Garland, S., Smolen, G. A., Ta, D. T., Vickery, L. E. & Culotta, V. C. (1998) *J. Biol. Chem.* **273**, 31138-31144

19. Land, T. & Rouault, T. A. (1998) *Mol. Cell.* **2**, 807-815

20. Hwang, D. M., Dempsey, A., Tan, K.-T. & Liew, C.-C. (1996) *J. Mol. Evol.* **43**, 536-540

21. Jung, Y.-S., Gao-Sheridan, H. S., Christiansen, J., Dean, D. R. & Burgess, B. K. (1999) *J. Biol. Chem.* **45**, 32402-32410

22. Ta, D. T. & Vickery, L. E. (1992) *J. Biol. Chem.* **267**, 11120-11125

23. Andrews, S. C., Harrison, P. M. & Guest, J. R. (1989) *J. Bacteriol.* **171**, 3940-3947

24. Garg, R. P., Vargo, C. J., Cui, X. & Kurtz, D. M., Jr. (1996) *Biochemistry* **35**, 6297-6301

25. Silberg, J. J., Hoff, K. G. & Vickery, L. E. (1998) *J. Bacteriol.* **180**, 6617-6624

Figure 4- 1 Schematic representation of NifU and different forms of NifU. The uppermost line represents full-length NifU. Above the line are indicated the cysteine (C) and aspartate (D) residues relevant to the present work. The numerical residue positions are indicated below the line. Substituting residues present in altered forms of NifU or NifU-1 are indicated by a bold, underlined letter at the appropriate position. Dashed brackets at the top of thefigure indicate the respective mononuclear iron/transient [2Fe-2S] cluster domain and permanent [2Fe-2S] cluster domain within the NifU primary sequence.

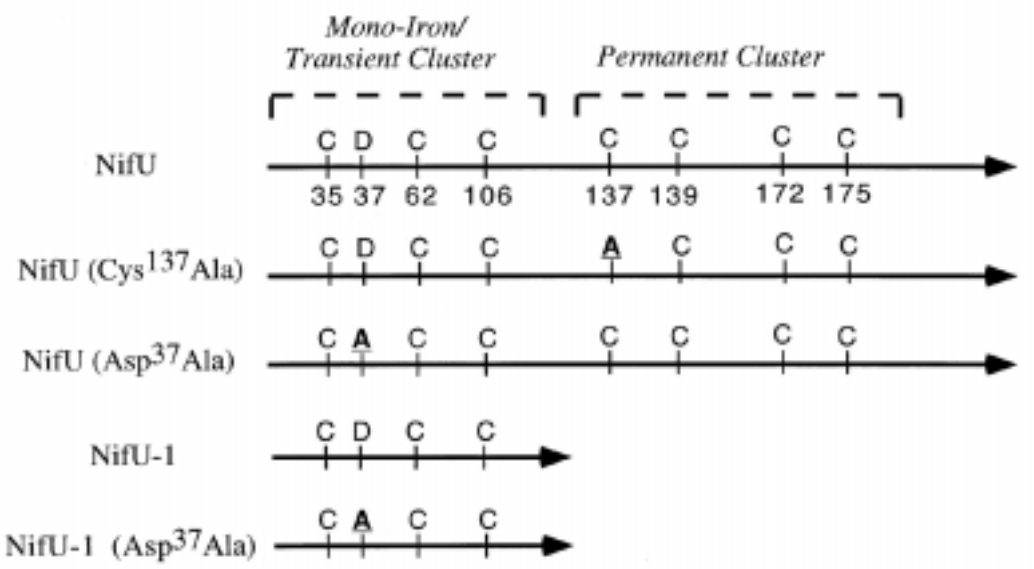
Mono-Iron/
Transient Cluster
Permanent Cluster
NifU
C D C C C C C C
35 37 62 106 137 139 172 175
NifU (Cys137Ala)
C D C C A C C C
NifU (Asp37Ala)
C A C C C C C C
NifU-1
C D C C
NifU-1 (Asp37Ala)
C A C C

Figure 4-2 Complex formation between NifU and NifS. The figure shows the elution profiles of NifS, NifU, or an equimolar mixture of NifU and NifS, by using size exclusion chromatography. Conditions used are described in Materials and Methods.

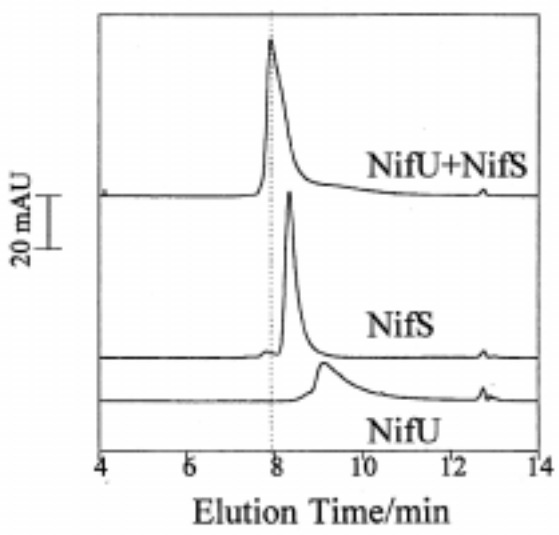
NifU+NifS
NifS
NifU
20 mAU
4
6
8
10
12
14
Elution Time/min

Figure 4-3 NifS-dependent *in vitro* Fe-S cluster assembly. (A) UV-visible spectrum of NifU-1 before *in vitro* Fe-S cluster assembly [before L-cysteine was added to initiate assembly (lower spectrum) and after 140 min of *in vitro* cluster assembly (upper spectrum)]. The post assembly spectrum shown in A is the maximum that could be obtained. (C) UV-visible spectrum of NifU-1(Asp^{37}Ala) before *in vitro* cluster assembly (lower spectrum) and after 80 min of *in vitro* Fe-S cluster assembly (upper spectrum). The post assembly spectrum shown in C represents approximately 60% of the maximum that could be obtained. (B) Time dependence of Fe-S cluster assembly as monitored by the change in extinction coefficient at 465 nm vs. time after initiation of the Fe-S cluster assembly reaction. The time dependence for cluster assembly shown in line a of panel B corresponds to the same sample shown in panel A. Line b of panel B shows cluster assembly under the same conditions as for line a, except that half of the amount of NifS was added to the assembly cocktail. Data shown in the lines labeled c are controls. One data set corresponds to conditions that are the same as for line a except that an altered form of NifS having the active-site Cys^{325} residue substituted by alanine was used. The other data set in C corresponds to conditions that are the same as used for line a, except that an altered form of NifU-1 having the Cys^{62} residue substituted for by alanine was used. Conditions for Fe-S cluster assembly are described in Materials and Methods.

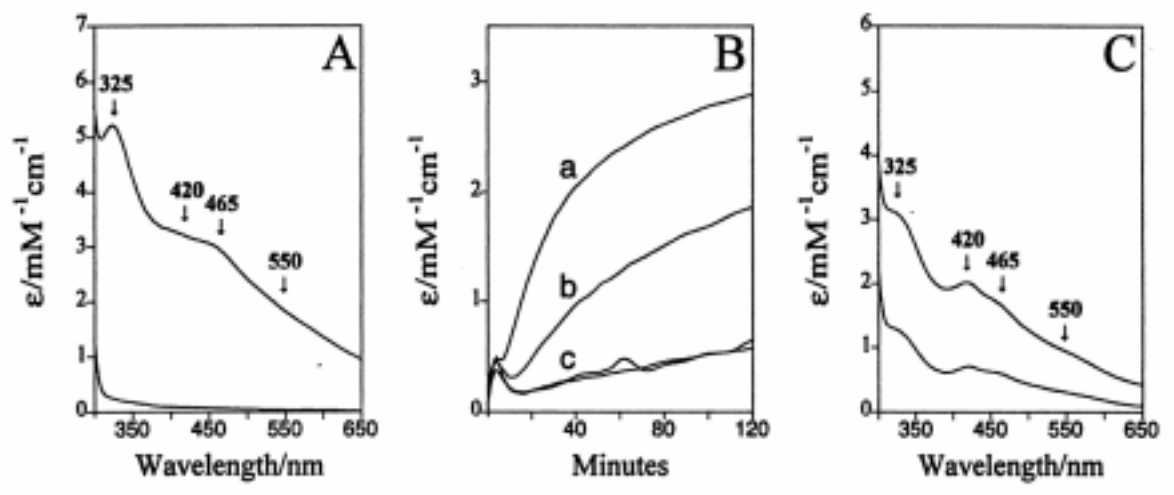
A
325
420
465
550
ε/mM⁻¹cm⁻¹
Wavelength/nm
B
a
b
c
Minutes
C
325
420
465
550
ε/mM⁻¹cm⁻¹
Wavelength/nm

Figure 4-4 Comparison of the low-temperature resonance Raman spectra of the $[2Fe\text{-}2S]^{2+}$ clusters in as-isolated NifU (a), reconstituted NifU-1 (b), and human ferrochelatase (c). All samples (2-4 mM in 100 mM Tris·HCl, pH 7.8, buffer) were in the form of concentrated frozen droplets maintained at 18 K. The spectra were recorded by using 488-nm excitation with 70-mW of laser power at the sample and are the sum of 19, 90, and 80 scans for a, b, and c, respectively. Each scan involved advancing the spectrometer in 1 cm^{-1} increments (0.5 cm^{-1} for c) and photon counting for 1 s/point with 6-cm^{-1} resolution.

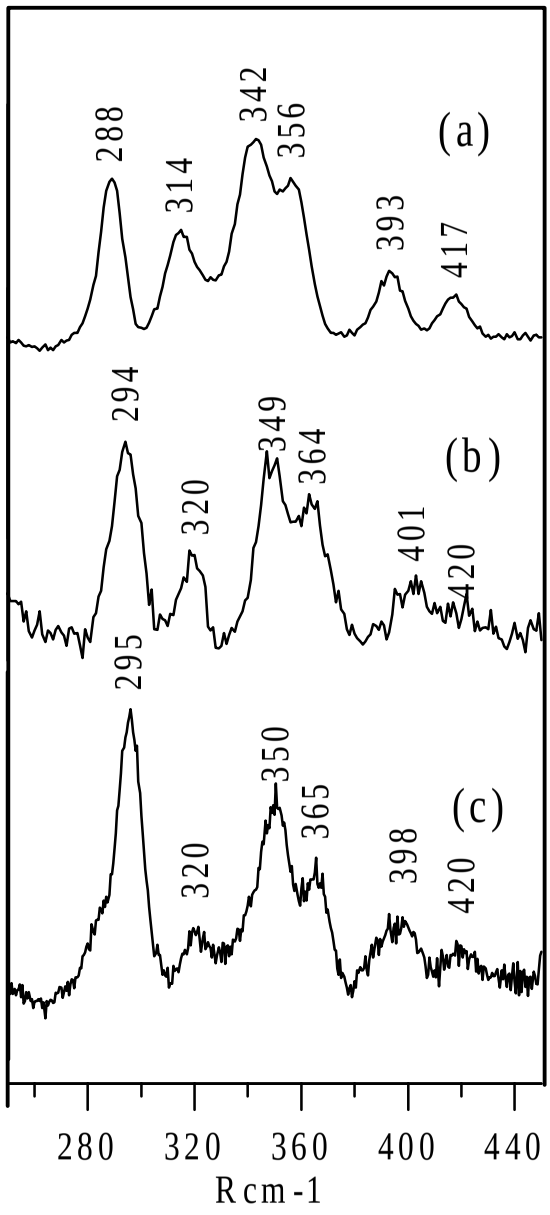
288
314
342
356
393
417
(a)
294
320
349
364
401
420
(b)
295
320
350
365
398
420
(c)
280
320
360
400
440
Rcm-1

Figure 4-5 Low-temperature resonance Raman spectra of transient $[2Fe\text{-}2S]^{2+}$ clusters. (a) NifU($Asp^{37}Ala$) after treatment by the cluster biosynthetic system; (b) as-isolated NifU($Asp^{37}Ala$); (c) difference spectrum (spectrum a minus spectrum b); (d) NifU-1($Asp^{37}Ala$) after treatment with the cluster biosynthetic system. The conditions used are the same as those described in Figure 4, and each spectrum is the sum of 33 scans.

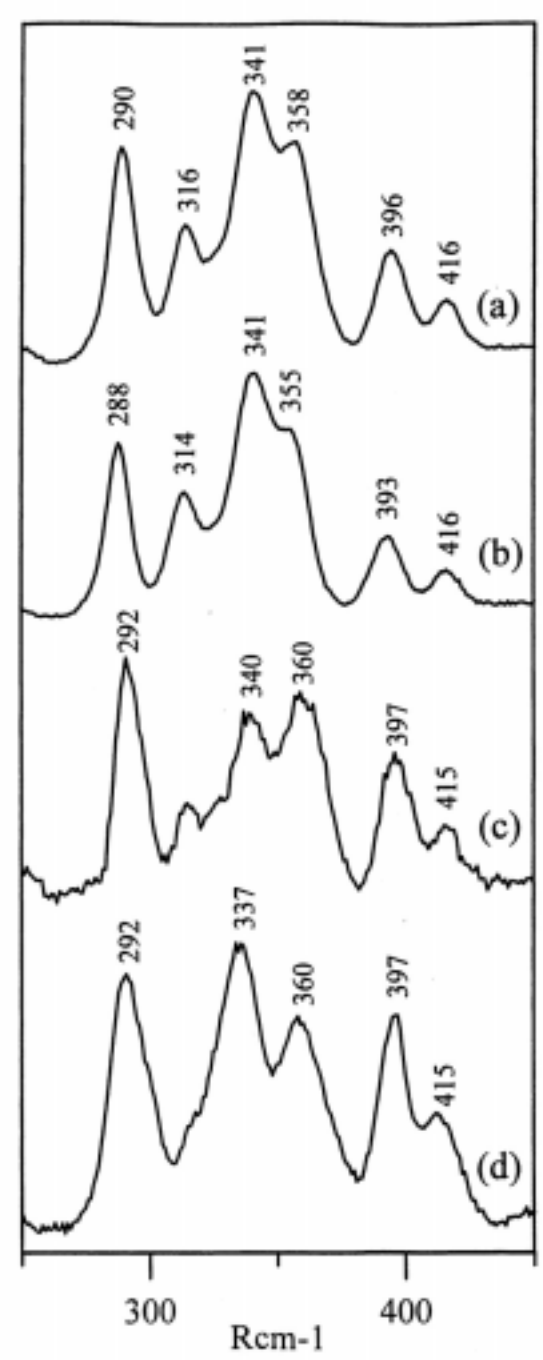
290
316
341
358
396
416
(a)
288
314
341
355
393
416
(b)
292
340
360
397
415
(c)
292
337
360
397
415
(d)
300
400
Rcm-1

Chapter V

Role of the IscU Protein in Iron-Sulfur Cluster Biosynthesis:

IscS-mediated assembly of a [Fe_2S_2] cluster in IscU[4]

[4] Jeffrey N. Agar[†], Limin Zheng,[‡], Valerie L. Cash[‡], Dennis R. Dean[‡], and Michael K. Johnson[†] (2000) *J. Am. Chem. Soc.* **122**, 2136-2137.[†] Department of Chemistry and Center for Metalloenzyme Studies, University of Georgia, Athens, GA 30602 and [‡] Department of Biochemistry, Virginia Tech, Blacksburg, VA 24061

Abstract: Iron-sulfur cluster biosynthesis in both prokaryotic and eukaryotic cells is known to be mediated by two highly conserved proteins, termed IscS and IscU in prokaryotes. The homodimeric IscS protein has been shown to be a cysteine desulfurase that catalyzes the reductive conversion of cysteine to alanine and sulfide. In this work, the combination of absorption and resonance Raman spectroscopies has been used to demonstrate IscS-mediated assembly of a reductively labile $[Fe_2S_2]^{2+}$ center in the homodimeric IscU protein. Analytical data and visible extinction coefficients indicate that up to one $[Fe_2S_2]^{2+}$ cluster can be assembled per IscU dimer. In addition, gel filtration and chemical cross-linking studies indicate the formation of a $\alpha_2\beta_2$ heterotetrameric complex between the IscU and IscS proteins. The results indicate a general mechanism for Fe-S cluster biosynthesis in which IscU provides a scaffold for IscS-mediated assembly of $[Fe_2(\mu_2\text{-}S)_2]$ core units.

Iron-sulfur clusters are ubiquitous in nature,[1] but the mechanisms for assembly and insertion of these centers in their cognate proteins are largely unknown. Recent genetic and biochemical studies point to a common mechanism, centered around two proteins termed IscS and IscU in prokaryotes,[2] that has been preserved for general Fe-S cluster biosynthesis in both prokaryotic and eukaryotic cells.[2,3] Functional and primary sequence homologs of IscS and IscU were first identified as the products of the nitrogen fixation *nifS* and *nifU* genes that specifically target the biosynthesis of the nitrogenase Fe-S clusters in *Azotobacter vinelandii*.[4] IscS is closely related to NifS and both have been shown to be homodimeric, pyridoxyl phosphate-dependent L-cysteine desulfurases, catalyzing the reductive conversion of cysteine to alanine and sulfide via an enzyme-bound persulfide intermediate.[2,5] The importance of IscU for Fe metabolism, in general, and Fe-S cluster biosynthesis, in particular, can be gauged by the fact that it is one of the most conserved sequence motifs in nature.[6] IscU has three conserved cysteine residues (Cys^{37}, Cys^{63}, and Cys^{106} in *A. vinelandii* and *E. coli* IscU)[2] and corresponds to the N-terminal third of NifU,[2,7] which has been overexpressed as a separate domain and termed NifU-1.[7b,8] These similarities, along with the observation that the *nif*-specific iron-sulfur cluster assembly operon is less complicated due to the absence of putative molecular chaperone genes, have led to our using the *nif*-specific pathway as a model for general biological iron-sulfur cluster assembly. Although we were successful in obtaining evidence for NifS-mediated assembly of a transient $[Fe_2S_2]^{2+}$ cluster within NifU,[8] the lability of this cluster and interference from the permanent $[Fe_2S_2]^{2+,+}$ cluster present in the central domain of NifU, impeded unambiguous characterization of this transient cluster in full-length NifU.[8] The involvement of IscU/IscS system in general Fe-S cluster biosynthesis and the lack of a permanent $[Fe_2S_2]$ cluster in IscU, clearly make this a more attractive system for investigating cluster assembly in IscU. Using purified *A. vinelandii* IscU and IscS, we report here the IscS-mediated assembly of a reductively labile $[Fe_2S_2]^{2+}$ cluster in IscU and evidence for the formation of a $\alpha_2\beta_2$ heterotetrameric complex

between the homodimeric IscU and IscS proteins. The results support a general mechanism for biological iron-sulfur cluster assembly in which IscU (or NifU) provides a scaffold for IscS (or NifS)-directed assembly of a reductively labile $[Fe_2S_2]$ cluster.

The initial evidence for the assembly of a $[Fe_2S_2]^{2+}$ cluster in *A. vinelandii* IscU was provided by UV-visible absorption spectroscopy, see Figure 1. Samples of IscU do not exhibit a visible chromophore as purified, but turn red over a period of 60 min on anaerobic treatment with catalytic amounts of IscS in the presence of excess L-cysteine and a stoichiometric amount of ferric ammonium citrate (based on the concentration of IscU monomer).[9] The resulting spectrum has bands centered at 320 nm, 410 nm, and 456 nm and a pronounced shoulder at 510 nm and is characteristic of a $[Fe_2S_2]^{2+}$ cluster.[10] Control experiments in the absence of IscU confirm that this chromophore is associated with the IscU protein (see inset in Figure 1) and the absorption intensity of this chromophore only increased for ferric concentrations up to one equivalent per IscU monomer (based on experiments with 0.5, 1.0, 2.0, and 8.0 equivalents of ferric ammonium citrate, data not shown). The maximal visible extinction coefficients, ε_{456} = 4.6 $mM^{-1}cm^{-1}$ and ε_{410} = 4.7 $mM^{-1}cm^{-1}$ are indicative of approximately one $[Fe_2S_2]^{2+}$ cluster per IscU dimer based on the published values for well-characterized 2Fe ferredoxins, ε_{460} = 6-10 $mM^{-1}cm^{-1}$ and ε_{420} = 8-11 $mM^{-1}cm^{-1}$.[10] In addition, the stoichiometry of one $[Fe_2S_2]^{2+}$ cluster per IscU dimer is supported by iron analyses and the A_{456}/A_{280} ratio. In contrast to NifU-1,[8] the $[Fe_2S_2]^{2+}$ cluster assembled in IscU stayed intact during brief exposure to excess EDTA (10-fold excess with respect to iron for < 5 mins) followed by anaerobic gel filtration and anion exchange chromatography to remove excess reagents. Samples of $[Fe_2S_2]$-containing IscU prepared using the above procedure with an 8-fold stoichiometric excess of ferric ion per IscU monomer for 3 hours and subjected to EDTA treatment followed by chromatographic repurification prior to analysis, yielded 1.0 ±0.1 Fe per IscU monomer (average of three determinations).[11] The resulting sample exhibited visible absorption characteristics identical to that shown in

Figure 1, with A_{456}/A_{280} = 0.20. This ratio is approximately half the value observed for 2Fe ferredoxins with similar numbers of UV-absorbing aromatic residues per monomeric unit and therefore indicative of one $[Fe_2S_2]^{2+}$ cluster per IscU dimer.[12]

Conclusive evidence that the chromophore assembled in IscU is a $[Fe_2S_2]^{2+}$ cluster was provided by resonance Raman spectroscopy, see Figure 2. The spectrum in the Fe-S stretching region is uniquely indicative of a $[Fe_2S_2]^{2+}$ center,[13] and the individual bands are readily assigned based on the isotope shifts and normal mode calculations reported for 2Fe ferredoxins and model complexes,[14] see Table 1. Although the Fe-S stretching modes of the $[Fe_2S_2]^{2+}$ cluster assembled in *A. vinelandii* IscU all occur at higher frequencies, compared to that assembled in *A. vinelandii* NifU-1 and the all-cysteinyl-ligated $[Fe_2S_2]^{2+}$ clusters present in as-purified samples of *A. vinelandii* NifU and human ferrochelatase, the relative intensities of individual modes using 488- and 457 nm excitation are strikingly similar in all four of these proteins.[7a,8,15] This strongly suggests analogous all-cysteine coordination environments for the $[Fe_2S_2]^{2+}$ centers in all four proteins with slightly stronger Fe-S(Cys) and Fe-S(bridging) bonds being responsible for the higher frequencies of the $[Fe_2S_2]^{2+}$ center in IscU.[16] Coordination by four cysteine residues requires the cluster to be bridging subunits in IscU and this is consistent with the cluster stoichiometry based on absorption and analytical data presented above.

The reductive lability of the $[Fe_2S_2]^{2+}$ cluster assembled in IscU was demonstrated by three distinct types of experiment. First, anaerobic reduction with stoichiometric dithionite resulted in complete and oxidatively irreversible bleaching of the visible absorption. Second, EPR studies gave no indication of the formation of a $S = 1/2$ $[Fe_2S_2]^{+}$ cluster on reduction, even in samples frozen within 2 seconds of dithionite addition. Third, the iron released on dithionite reduction was quantitatively accounted for using ferrous ion chelators such as ferrozine or α,α'-*N*-dipyridyl.

Evidence that IscS and IscU are able to interact with each other was obtained in two different ways. First, gel exclusion chromatography was used to show that an

equimolar mixture of isolated IscS dimer and isolated IscU dimer results in formation of a weakly bound $\alpha_2\beta_2$ heterotetramer (data not shown). Second, the thiol-specific cross-linking reagent dibromobimane could be used to cross-link one subunit of IscS to one subunit of IscU, see Figure 3. For chemical cross-linking experiments 0.06 µM IscS was mixed with 0.06 µM IscU in a final volume of 18 µl. After incubation at room temperature for 20 minutes, the cross-linking reaction was initiated by addition of 0.5 µl of a 20 mM solution of dibromobimane prepared in N,N´-dimethylformamide. The sample was incubated an additional 1.5 hours at room temperature then analyzed by denaturing polyacrylamide gel electrophoresis.[17] Controls included a sample that was not treated with dibromobimane and separate samples of IscS and IscU that were individually treated with dibrombimane. The results of these experiments are consistent with the hypothesis that persulfides catalytically formed on IscS[2] can be specifically transferred to IscU for cluster assembly through association of the two proteins.

The results indicate a general mechanism for Fe-S cluster biosynthesis in which IscU provides a scaffold for IscS-mediated assembly of $[Fe_2(\mu_2\text{-}S)_2]$ cores.[18] Structurally and electronically these units constitute the fundamental building blocks of biological $[Fe_2S_2]$, $[Fe_3S_4]$ and $[Fe_4S_4]$ centers.[1] Hence our current working hypothesis is that these units are transferred intact into apo-proteins. The Fe-S cluster biosynthesis gene cluster that is widely conserved in prokaryotes, encodes for several proteins whose functions are currently unknown, but are good candidates for mediating such transfer. The most likely candidates are the IscA protein that contains three conserved cysteine residues and the heat shock proteins HscA and HscB that bear sequence homology to the molecular chaperones.[2] Determining how the Fe^{3+} ion is acquired by IscU and how the $[Fe_2S_2]$ cores assembled in IscU are released and transferred into apo-proteins present fascinating challenges for future studies.

Acknowledgment. This research was supported by grants from the NSF (MCB9630127 to DRD) and NIH (GM51962 to MKJ) and an NSF Research Training Group Award to the Center for Metalloenzyme Studies (DBI-9413236)

References and Textural Footnotes:

(1) For recent reviews see: (a) Beinert, H.; Holm, R. H.; Münck, E. *Science* **1997**, *277*, 653-659. (b) Johnson, M. K. *Curr. Opin. Chem. Biol.* **1998**, *2*, 173-181. (c) Beinert, H.; Kiley, P. J. *Curr. Opin. Chem. Biol.* **1999**, *3*, 152-157.

(2) Zheng, L.; Cash, V. L.; Flint, D. H.; Dean, D. R. *J. Biol. Chem.* **1998**, *273*, 13264-13272.

(3) (a) Flint, D. H. *J. Biol. Chem.* **1996**, *271*, 16068-16074. (b) Nakamura, M.; Saeki, K.; Takahashi, Y. *J. Biochem.* **1999**, *126*, 10-18. (c) Schilke, B.; Voisine, C.; Beinert, H.; Craig, E. *Proc. Natl. Acad. Sci. U.S.A.* **1999**, *96*, 10206-10211. (d) Kispal, G.; Csere, P.; Prohl, C.; Lill, R. *EMBO J.* **1999**, *18*, 3981-3989.

(4) (a) Dean, D. R.; Bolin, J. T.; Zheng, L. *J. Bacteriol.* **1993**, *175*, 6737-6744. (b) Zheng, L.; Dean, D. R. *J. Biol. Chem.* **1994**, *269*, 18723-18726.

(5) (a) Zheng, L.; White, R. H.; Cash, V. L.; Jack, R. F.; Dean, D. R. *Proc. Natl. Acad. Sci.U.S.A.* **1993**, *90*, 2754-2758. (b) Zheng, L.; White, R. H.; Cash, V. L.; Dean, D. R. *Biochemistry* **1994**, *33*, 4714-4720.

(6) Hwang, D. M.; Dempsey, A.; Tan, K. T.; Liew, C. C. *J. Mol. Evol.* **1996**, *43*, 536-540.

(7) (a) Fu, W.; Jack, R. F.; Morgan, T. V.; Dean, D. R.; Johnson, M. K. *Biochemistry* **1994**, *33*, 13455-13463. (b) Agar, J. N.; Yuvaniyama, P.; Jack, R. F.; Cash, V. L.; Smith, A. D.; Dean, D. R.; Johnson, M. K. *JBIC, J. Biol. Inorg. Chem.* in press.

(8) Yuvaniyama, P.; Agar, J. N.; Cash, V. L.; Johnson, M. K.; Dean, D. R.. *Proc. Natl. Acad. Sci. U.S.A.* **2000**, *97*, 599-604.

(9) *A. vinelandii* IscS was heterologously produced in *Escherichia coli* and purified as previously described.[2] *A. vinelandii* IscU was similarly produced in *E. coli* and was purified anaerobically by ammonium sulfate fractionation followed by anion exchange chromatography using Pharmacia Q sepharose column chromatography.

Concentrations are based on protein determinations using the BCA method; Smith, P. K.; Krohn, R. L.; Hermanson, G. Y.; Mallia, A. K.; Gartner, F. H.; Provenzano, M. D.; Fujimoto, E. K.; Goeke, N. M.; Olson, B. J.; Klenk, D. C. Meth. Enzymol. **1985**, *226*, 199-232.

(10) Dailey, H. A.; Finnegan, M. G.; Johnson, M. K. *Biochemistry* **1994**, *33*, 403-407.

(11) Iron analyses were conducted colorimetrically on dithionite treated samples using the ferrous ion chelator α,α'-*N*-dipyridyl (ε_{520} = 8.4 $mM^{-1}cm^{-1}$).

(12) Chatelet, C.; Meyer, J. *JBIC, J. Biol. Inorg. Chem.* **1999**, *4*, 311-317.

(13) Spiro, T. G.; Czernuszewicz, R. S.; Han, S. In *Resonance Raman spectra of heme and metalloproteins*; Spiro, T. G., Ed.; John Wiley & Sons: New York, 1988; pp 523-554.

(14) (a) Han, S.; Czernuszewicz, R. S.; Kimura, T.; Adams, M. W. W.; Spiro, T. G. *J. Am. Chem. Soc.* **1989**, *111*, 3505-3511. (b) Han, S.; Czernuszewicz, R. S.; Spiro, T. G. *J. Am. Chem. Soc.* **1989**, *111*, 3496-3504. (c) Fu, W.; Drozdzewski, P. M.; Davies, M. D.; Sligar, S. G.; Johnson, M. K. *J. Biol. Chem.* **1992**, *267*, 15502-15510.

(15) Crouse, B.R.; Sellers, V.M.; Finnegan, M.G.; Dailey, H.A.; Johnson, M.K. *Biochemistry* **1996**, *35*, 16222-16229.

(16) The possibility that the anomalously high frequencies of the predominantly Fe-S^t stretching modes of the $[Fe_2S_2]^{2+}$ centers assembled in IscU and NifU-1 are a consequence of partial oxygenic ligation cannot be ruled out. Mutagenesis studies involving 2Fe ferredoxins indicate that the $A_g{}^t$ and $B_{3u}{}^t$ Fe-S stretching modes in the IscU and NifU-1 lie within the ranges established thus far for $[Fe_2S_2]^{2+}$ centers with one serinate ligand, i.e. 332-354 cm^{-1} and 289-302 cm^{-1}, respectively. Although the analytical data for the samples of IscU investigated in this work indicate that no more than one $[Fe_2S_2]$ cluster can be assembled per dimer, it is conceivable that the conditions have yet

to be found for assembly of one [Fe_2S_2] center in each subunit with three cysteine and one oxygenic ligand.

(17) Laemmli, U. K. *Nature* **1970**, *227*, 680-685.

(18) While this communication was in preparation, an alternative proposal for the mechanism of Fe-S cluster biosynthesis appeared in which the 2Fe ferredoxin (Fdx) encoded by the *fdx* gene in the bacterial Fe-S biosynthesis operon provides the "scaffold" for IscS-mediated cluster assembly; Takahashi, Y.; Nakamura, M. *J. Biochem.* **1999**, *126*, 917-926. We consider this alternative proposal to be unlikely in light of the evidence for IscS/IscU and NifS/NifU complex formation and NifS/IscS-mediated assembly of reductively labile [Fe_2S_2]$^{2+}$ clusters in NifU/IscU presented herein and in recently published studies of NifU.[8] Evidence has yet to be presented for the existence of a transient metal binding site in Fdx, in addition to the permanent [Fe_2S_2]$^{2+,+}$ cluster. If such a site does exist, our data is more consistent with a role in mobilizing Fe or Fe-S cluster fragments.

Table 5-4. Fe-S stretching frequencies (cm^{-1}) and assignments for the $[Fe_2S_2]^{2+}$ centers assembled in *A. vinelandii* IscU and NifU-1 and present in *A. vinelandii* NifU and human ferrochelatase.

Mode (D_{2h}) [a]	IscU	NifU-1 [b]	NifU[c]	Ferrochelatase[d]
B_{2u}^{b}	425	~420	417	420
A_g^{b}	406	401	393	398
B_{3u}^{b}	367	364	356	365
A_g^{t}	353	349	342	350
B_{1g}^{b}	328	320	314	320
B_{3u}^{t}	296	294	288	295

[a] Symmetry labels under idealized D_{2h} symmetry for a $Fe_2S_2^{b}S_4^{t}$ unit, where S^b and S^t indicate bridging and terminal (cysteinyl) S, respectively. The predominantly terminal B_{1u}^{t} and B_{2g}^{t} modes have not been assigned since they are generally not observed with 488 nm excitation. These modes are expected at similar frequencies since they differ only in the phasing of the asymmetric Fe-S^t stretches on opposite sides of the $Fe_2S_2^{b}$ core and may contribute to the broad bands assigned to the A_g^{t} mode.

[b] Taken from Yuvaniyama et al.[8]

[c] Taken from Fu et al.[7a]

[d] Taken from Crouse et al.[15]

Figure 5-1 IscS-mediated *in vitro* assembly of a $[Fe_2S_2]^{2+}$ cluster in IscU. UV-visible absorption spectrum of *A. vinelandii* IscU before (lower spectrum) and after 30 min of IscS-mediated cluster assembly (upper spectrum). Cluster biosynthesis was initiated by addition of 4 mM L-cysteine to 28 µM IscU in the presence of 0.4 µM IscS and 5 mM β-mercaptoethanol under strictly anaerobic conditions. The inset shows the time course monitored at 460 nm for reactions carried out in the presence (◆) and absence (✚) of IscU.

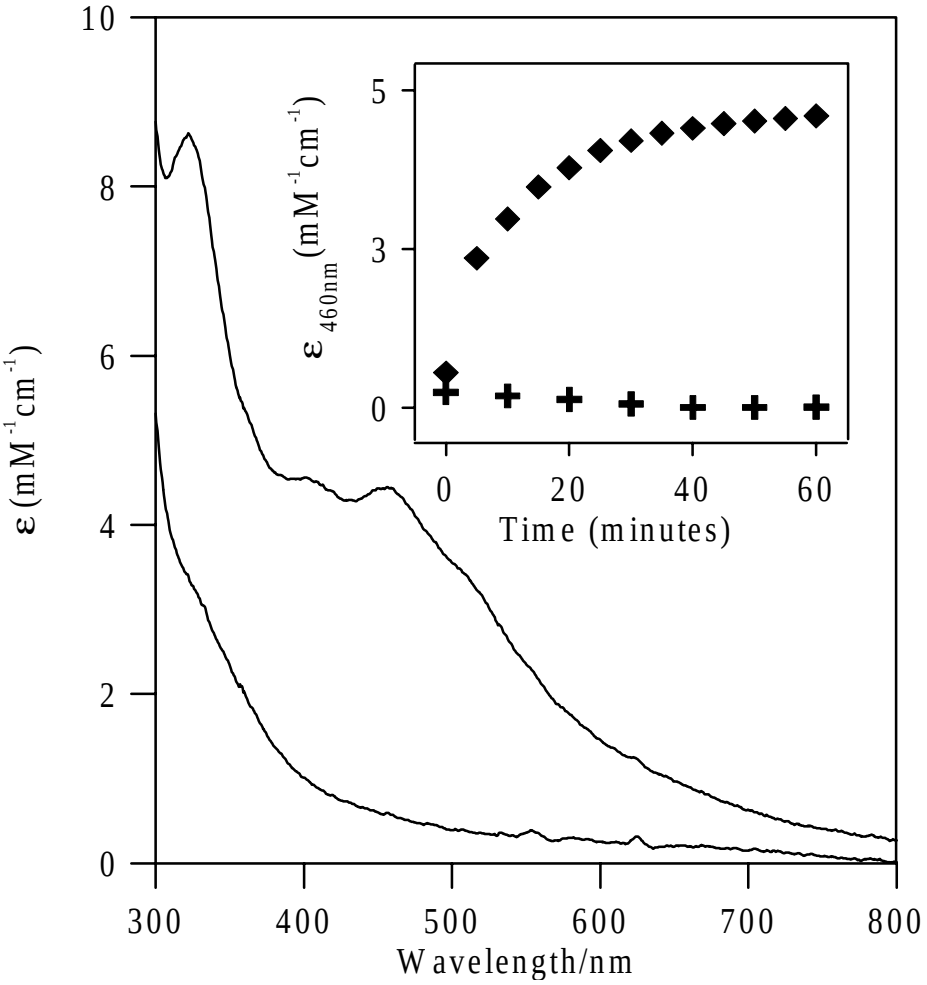
10
8
6
4
2
0
ε (mM-1cm-1)
300
400
500
600
700
800
Wavelength/nm
5
3
0
ε460nm (mM-1cm-1)
0
20
40
60
Time (minutes)

Figure 5-2 Low-temperature resonance Raman spectra of *A. vinelandii* IscU after IscS-mediated cluster assembly. The sample was prepared as described in Figure 1 with the reaction allowed to proceed for 3 hr before anaerobic centricon ultrafiltration to give a concentrated droplet, ~2 mM in monomer in 100 mM Tris-HCl buffer, that was frozen on the cold finger of a Displex unit at 18 K. The spectra were recorded using 488- and 457-nm excitation with 70-mW of laser power at the sample. Each spectrum is the sum of 40 scans, with each scan involving photon counting for 1 s at 1-cm^{-1} increments, with 6 cm^{-1} resolution. Bands due to lattice modes of the frozen buffer solution have been subtracted from both spectra.

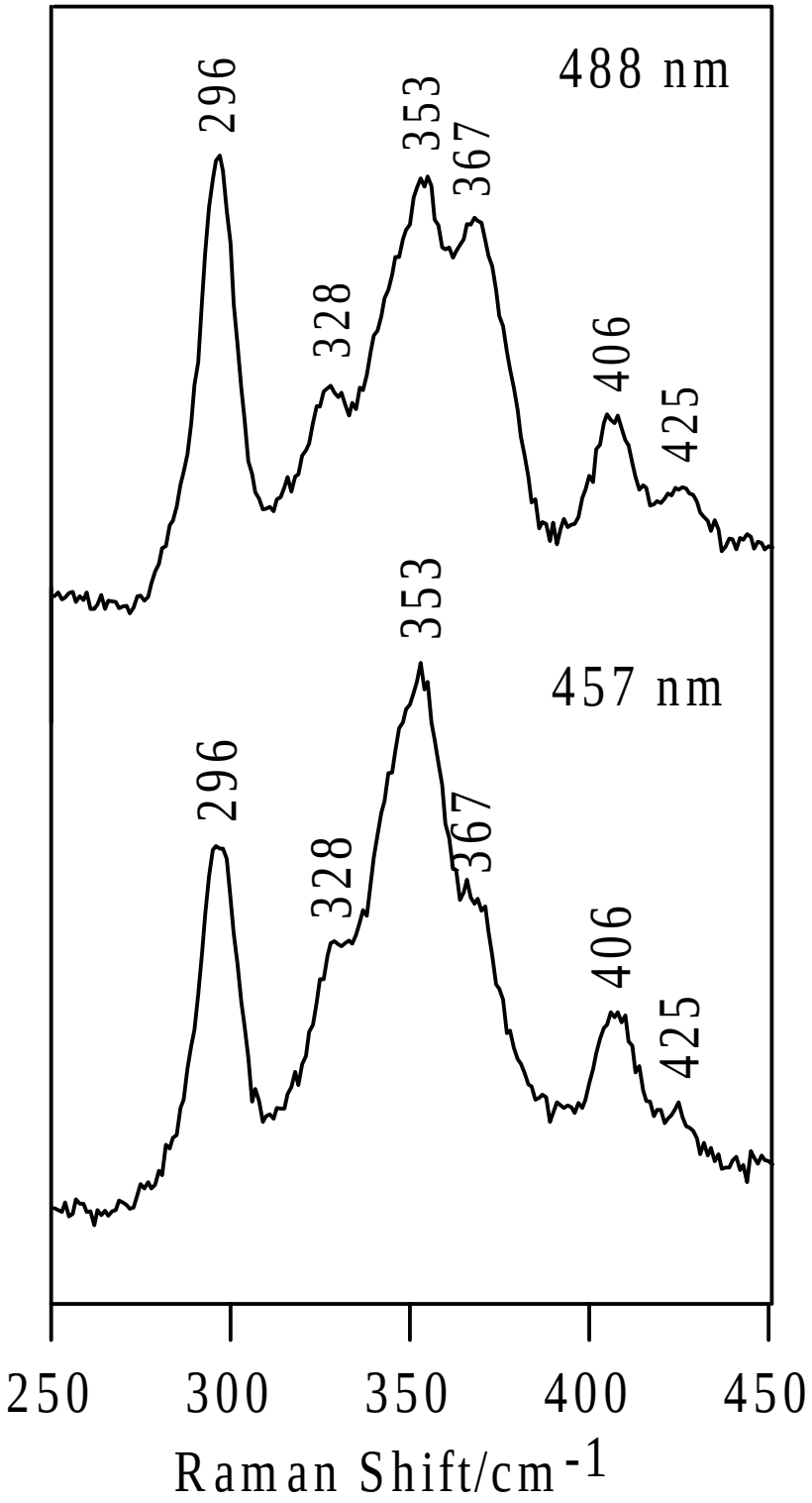
488 nm
296
328
353
367
406
425
457 nm
296
328
353
367
406
425
250
300
350
400
450
Raman Shift/cm-1

Figure 5-3 Denaturing polyacrylamide gel electrophoresis showing dibromobimane cross-linking of IscU and IscS. Lane 1, mixture of IscU and IscS with no added dibromobimane; Lane 2, purified IscS treated with dibromobimane; Lane 3, purified IscU treated with dibromobimane; Lane 4, mixture of IscU and IscS treated with dibromobimane. Lane M, molecular-weight markers: bovine serum albumin (66,200), ovalbumin (45,000), carbonic anhydrase (31,000), soybean trypsin inhibitor (21,500), lysozyme (14,400). The top arrow indicates the position of the IscU-IscS cross-linked heterodimer in Lane 4 and the lower arrow indicates the position of the IscU cross-linked dimer in Lane 3.

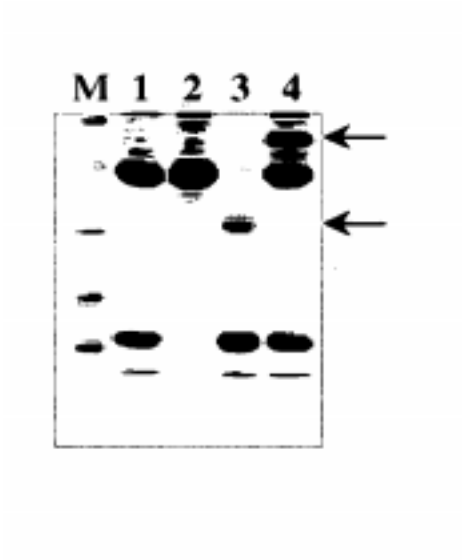
M 1 2 3 4

Chapter VI

IscU as a Scaffold for Iron-Sulfur Cluster Biosynthesis:

Sequential Assembly of [2Fe-2S] and [4Fe-4S] Clusters in IscU[5]

[5] Jeffrey N. Agar,[‡] Carsten Krebs,[§] Jeverson Frazzon,[||] Boi Hanh Huynh,[§] Dennis R. Dean,[||] and Michael K. Johnson,[‡] (2000) *Biochemistry* **in press,** [‡]*Department of Chemistry and Center for Metalloenzyme Studies, University of Georgia, Athens, GA 30602,* [||] *Department of Biochemistry, Virginia Tech, Blacksburg, VA 24061, and* [§] *Department of Physics, Emory University, Atlanta, Georgia 30322*

Abstract:

Iron-sulfur cluster biosynthesis in both prokaryotic and eukaryotic cells is known to be mediated by two highly conserved proteins, termed IscS and IscU in prokaryotes. The homodimeric IscS protein has been shown to be a cysteine desulfurase that catalyzes the reductive conversion of cysteine to alanine and sulfide. In this work, the time course of IscS-mediated Fe-S cluster assembly in IscU was monitored via anaerobic anion exchange chromatography. The nature and properties of the clusters assembled in discrete fractions were assessed via analytical studies together with absorption, resonance Raman and Mössbauer investigations. The results show sequential cluster assembly with the initial IscU product containing one $[2Fe\text{-}2S]^{2+}$cluster per dimer converting first to a form containing two $[2Fe\text{-}2S]^{2+}$ clusters per dimer and finally to a form that contains one $[4Fe\text{-}4S]^{2+}$ cluster per dimer. Both the $[2Fe\text{-}2S]^{2+}$ and $[4Fe\text{-}4S]^{2+}$ clusters in IscU are reductively labile and are degraded within minutes on being exposed to air. On the basis of sequence considerations and spectroscopic studies, the $[2Fe\text{-}2S]^{2+}$ clusters in IscU are shown to have incomplete cysteinyl ligation. In addition, the resonance Raman spectrum of the $[4Fe\text{-}4S]^{2+}$ cluster in IscU is best interpreted in terms of noncysteinyl ligation at a unique Fe site. The ability to assemble both $[2Fe\text{-}2S]^{2+}$ and $[4Fe\text{-}4S]^{2+}$ clusters in IscU supports the proposal that this ubiquitous protein provides a scaffold for IscS-mediated assembly of clusters that are subsequently used for maturation of apo Fe-S proteins.

INTRODUCTION

Iron-sulfur clusters are ubiquitous in nature and exhibit diverse functions which include mediating electron transport, providing the active sites of redox and nonredox enzymes, acting as sensors for regulatory processes, and generating organic radicals to initiate radical reactions (*1-4*). While the past two decades have witnessed a proliferation of data concerning the structure-function relationships of Fe-S clusters, the detailed mechanism of Fe-S cluster biosynthesis has remained elusive. Much of what is currently known stems from investigations into the function of specific genes involved with nitrogen fixation in *Azotobacter vinelandii*. Two gene products, NifS and NifU, have been extensively characterized and found to be essential for full activation and cluster assembly in both nitrogenase component proteins (*5-11*).

On the basis of sequence homology with the *nif* genes that specifically target nitrogenase Fe-S cluster biosynthesis, an *isc* (iron-sulfur cluster) gene cluster was identified in a wide range of nitrogen-fixing and non-nitrogen fixing prokaryotes and proposed to be responsible for general Fe-S cluster biosynthesis (*12*). Two of the nine *isc* genes, *iscS* and *iscU* , encode for homodimeric proteins whose sequences are homologous to NifS and NifU, respectively. Furthermore, in common with NifU and NifS (*11*), the gene products IscU and IscS have been shown to produce a heterotetrameric complex (*12*). IscS was purified from *Escherichia coli* and *A. vinelandii* and shown to be a pyridoxal phosphate-dependent L-cysteine desulfurase closely related to NifS (*13, 14*). Recently X-ray crystal structures of two members of this general class of enzyme have appeared (*15, 16*) and the active site structures are in good agreement with previous mechanistic proposals involving an active-site cysteine persulfide intermediate (*8*). IscU corresponds to the N-terminal domain of NifU and contains three conserved cysteine residues (Cys^{37}, Cys^{63} , and Cys^{106} in *A. vinelandii* and *E. coli* IscU (*13*)). In accord with the notion that Fe-S clusters are among the most ancient types of prosthetic group, the Isc proteins, in general, and IscU and IscS, in particular, have been

widely conserved throughout evolution. Indeed, IscU is widely considered to be one of the most conserved protein sequences in nature (*17*). Moreover, in the past two years, proteins homologous to the prokaryotic *iscS* and *iscU* gene products have been shown to be involved in Fe-S cluster assembly in eukaryotic organisms (*18-21*), on the basis of both biochemical and genetic evidence. Hence, understanding the function of the IscU and IscS proteins in prokaryotes is likely to provide insight into iron homeostasis and Fe-S cluster assembly in mitochondria, with potential relevance to iron-storage diseases and the control of cellular iron uptake.

The absence of a permanent [2Fe-2S] cluster in IscU and the enhanced stability of transient clusters assembled in IscU compared to the stability of those in NifU, make IscU an attractive system for investigating further the putative role of this proteins as a scaffold for Fe-S cluster biosynthesis. Support for this role has come from our recent studies which demonstrated IscS-mediated assembly of one reductively labile $[2Fe\text{-}2S]^{2+}$ cluster per dimer in *A. vinelandii* IscU (*12*). In the work presented here, we report a detailed investigation of the time course of IscS-mediated cluster assembly in *A. vinelandii* IscU using preparative FPLC to separate fractions and the combination of analytical, absorption, Mössbauer and resonance Raman studies to establish the number, type, and properties of clusters in discrete fractions.

MATERIALS AND METHODS

A. vinelandii IscS and IscU were heterologously produced in *E. coli* and purified as previously described (*12, 13*). IscS-mediated cluster assembly experiments, including time-based separation of discrete fractions using a Pharmacia FPLC system and the preparation of all spectroscopic samples, were carried out under rigorously anaerobic conditions inside a Vacuum Atmospheres glovebox under an Ar atmosphere (< 1 ppm O_2). Typical experiments involved initiating cluster biosynthesis by addition of 4 mM L-cysteine to a reaction mixture containing 100-400 µM IscU in the presence of 0.5-5.0 µM IscS, a 5-fold excess of freshly prepared ferric ammonium citrate (relative to the IscU

concentration) and 4 mM β-mercaptoethanol. The rate of cluster assembly was controlled by varying the IscU:IscS ratio, and ^{57}Fe-enriched ferric ammonium citrate (>95% enrichment) was used whenever Mössbauer samples were to be prepared. At selected time intervals, samples were loaded onto a an 8 mL mono-Q column (Pharmacia) and eluted with a shallow 0.1 to 0.4 M NaCl gradient. Individual fractions were concentrated and desalted via ultrafiltration prior to spectroscopic studies. All spectroscopic and cluster assembly studies were carried out in 50 mM Tris-HCl buffer, (pH 7.8). Concentrations are based on IscU monomer (MW = 13,742 for the apoprotein) and were assessed by protein determinations carried out after trichloroacetic acid precipitation and redissolution using the BCA method (*22*). Iron analyses were conducted colorimetrically on dithionite-treated samples using the ferrous ion chelator α,α′-*N*-dipyridyl (ε_{520} = 8.4 $mM^{-1}cm^{-1}$).

UV-visible absorption spectra were recorded under anaerobic conditions in septum-sealed 1 mm and 1 cm cuvettes, using a Shimadzu 3101PC scanning spectrophotometer fitted with a TCC-260 temperature controller. Resonance Raman spectra were recorded on droplets of frozen protein solutions at 17 K using an Instruments SA Ramanor U1000 scanning spectrometer fitted with a cooled RCA 31034 photomultiplier tube and lines from a Coherent Sabre 10-W argon ion laser. Mössbauer spectra in the presence of weak and strong applied magnetic fields were recorded using the previously described instrumentation (*23*) and specific experimental conditions are given in the figure legend. Analysis of the Mössbauer data was performed with the program WMOSS (WEB Research).

RESULTS

FPLC and UV-Visible Absorption Analysis of the Time Course of IscS-Mediated Cluster Assembly in IscU. Our previous studies on IscS-mediated cluster assembly in IscU under strictly anaerobic conditions revealed the progressive development of a $[2Fe2S]^{2+}$ chromophore over a period of approximately 1 h. These experiments involved

a reaction mixture comprising IscU with 0.5-8 equiv of ferric ammonium citrate, catalytic amounts of IscS (70:1 IscU:IscS ratio), and excess β-mercaptoethanol, and initiating the reaction by addition of excess L-cysteine. On the basis of visible extinction coefficients and Fe quantitation of EDTA-treated samples, it was concluded that one $[2Fe\text{-}2S]^{2+}$ cluster was assembled per IscU dimer under these conditions. However, monitoring cluster assembly in IscU by UV-visible absorption over longer time periods was impeded due to the concomitant formation of iron sulfides. Consequently a more detailed investigation of the time course of cluster assembly in IscU was undertaken using anaerobic FPLC with a mono-Q column and a 0.1 to 0.4 M NaCl gradient to separate fractions contained in samples taken from the reaction mixture at discrete time intervals. Mono-Q columns are capable of separating fractions with small conformation differences and have been shown to be effective in separating fractions of specific Fe-S proteins that differ in terms of cluster type or stoichiometry (*24*). The results of two sets of FPLC experiments in which protein absorbance at 280 nm was monitored at selected times during IscS-mediated cluster assembly in IscU are shown in Figure 1.

In the first FPLC experiment (Figure 1A), the IscU/IscS ratio was increased to 460:1 to slow the reaction and thereby afford temporal resolution of IscU species that cannot be observed in 1:1 mixtures. The level of the IscU apoprotein (fraction 1) that dominates prior to L-cysteine addition (0 h) progressively decreases as the reaction proceeds with a concomitant increase in the level of fraction 2 (2.5 h). No apoprotein is observed after 6.5 h, but a new fraction (fraction 3) starts to appear and is the dominant form of IscU after 7.5h. Iron and protein analyses indicated 1.2 and 1.9 Fe molecules/IscU monomer, for fractions 2 and 3, respectively. These values are likely to be an overestimate for fraction 2 and an underestimate for fraction 3 due to the difficulty in obtaining baseline separation of fractions 2 and 3. The UV-visible absorption spectra of fractions 2 and 3 are both characteristic of $[2Fe\text{-}2S]^{2+}$ centers (Figure 2), with the former corresponding to that reported previously for IscU samples containing one $[2Fe\text{-}2S]^{2+}$

cluster per IscU dimer (*12*). In accord with the Fe analyses, comparison of the visible extinction coefficients (ε_{456} = 5.8 $mM^{-1}cm^{-1}$ and 9.2 $mM^{-1}cm^{-1}$ for fractions 2 and 3, respectively) and the A_{456}/A_{280} ratios (0.31 and 0.44 for fractions 2 and 3, respectively) with well-characterized $[2Fe\text{-}2S]^{2+}$-containing proteins (*25*) (after correction of the 280 nm absorbance for the one W and four Y residues per IscU monomer), shows that fractions 2 and 3 as containing one and two $[2Fe\text{-}2S]^{2+}$ clusters per IscU dimer, respectively.

Because our previous studies showed that IscU samples containing one $[2Fe\text{-}2S]^{2+}$ cluster per IscU dimer were stable to EDTA treatment (*12*), fractions 2 and 3 were combined, treated with a 20-fold excess of EDTA for 10 min, and repurified by FPLC. The resulting sample contained only fraction 2 (Figure 1A), thereby providing homogeneous samples of IscU containing one $[2Fe\text{-}2S]^{2+}$ cluster per dimer for spectroscopic investigations. The absorption spectrum of the EDTA-treated sample (Figure 2) has an ε_{456} of 4.6 $mM^{-1}cm^{-1}$ and an A_{456}/A_{280} of 0.27, in good agreement with our previous results (*12*). We conclude that forms of IscU with two $[2Fe\text{-}2S]^{2+}$ clusters per dimer can be prepared, but that one cluster is readily removed by Fe chelators.

In the second FPLC experiment (Figure 1B), the IscU:IscS ratio was decreased from 460:1 to 28:1. Under these conditions, IscU containing two $[2Fe\text{-}2S]^{2+}$ clusters per dimer (fraction 3) is the dominant species after 2.5 h. However, over the next 10 h, the level of this fraction decreases with a concomitant increase in the level of a new fraction (fraction 4). The UV-visible absorption spectrum of fraction 4 (Figure 2) comprises a broad absorption centered at ~390 nm and is characteristic of a $[4Fe\text{-}4S]^{2+}$ cluster (*25*). Iron and protein analyses for fraction 4 revealed 1.9 Fe molecules/IscU monomer. Moreover, the visible extinction coefficient (ε_{390} = 7.4 $mM^{-1}cm^{-1}$) and the A_{390}/A_{280} ratio (0.34), when compared to those of well-characterized $[4Fe\text{-}4S]^{2+}$-containing proteins (*26, 27*) after correction for the number of 280-nm-absorbing W and Y residues in IscU, are indicative of one $[4Fe\text{-}4S]^{2+}$ cluster per IscU dimer. Subsequent FPLC experiments with a

1:1 IscU:IscS ratio showed that the IscS-mediated cluster assembly reaction proceeds rapidly to yield only the $[4Fe\text{-}4S]^{2+}$-containing fraction in less than 1 h.

UV-visible absorption studies showed that the Fe-S chromophores present in IscU fractions 2, 3 and 4 were irreversibly and completely degraded within minutes after exposure to air or immediately upon anaerobic addition of a 10-fold excess of dithionite. Moreover, EPR spectra of samples frozen within 2 s of dithionite addition did not reveal any resonances indicative of paramagnetic $[2Fe\text{-}2S]^{+}$ or $[4Fe\text{-}4S]^{+}$ clusters. Consequently, resonance Raman and Mössbauer studies were carried out to confirm cluster type and assess cluster ligation.

Resonance Raman Characterization of $[2Fe\text{-}2S]^{2+}$ Centers Assembled in IscU. The resonance Raman spectra of fractions 2 and 3 in the Fe-S stretching region (Figure 3) are identical within experimental error and indicative of $[2Fe\text{-}2S]^{2+}$ centers. Hence the two $[2Fe\text{-}2S]^{2+}$ clusters in fraction 3 and the single $[2Fe\text{-}2S]^{2+}$ cluster in fraction 2 must all have very similar environments. The spectra are in good agreement with those previously reported and assigned for $[2Fe\text{-}2S]^{2+}$-containing IscU using 457-nm excitation (*12*). The only significant differences compared to previously published spectra are decreased intensity, improved resolution, and 3-cm^{-1} downshifts for the bands in the 340-370 nm region. Since the IscU samples in these initial resonance Raman studies were used without chromatographic separation of discrete fractions, these differences are readily interpreted in terms of contributions from the $[4Fe\text{-}4S]^{2+}$-containing form of IscU (fraction 4).

As previously noted (*12*), the resonance Raman characteristics of the $[2Fe\text{-}2S]^{2+}$ center in IscU can be interpreted in terms of either complete cysteinyl ligation or partial noncysteinyl ligation. However, since the results presented herein show that two $[2Fe\text{-}2S]^{2+}$ clusters can be assembled per IscU dimer and each subunit contains only three cysteine residues, each cluster can maximally have three cysteine ligands. The frequencies of the A_g^t and B_{3u}^t predominantly Fe-S(Cys) stretching modes of biological $[2Fe\text{-}2S]^{2+}$

clusters generally provide an indication of cluster ligation (*28*). For the $[2Fe\text{-}2S]^{2+}$ cluster in IscU, these bands occur at anomalously high frequencies (356 and 296 cm^{-1}, respectively) compared to those of the all-cysteine-ligated $[2Fe\text{-}2S]^{2+}$ clusters in ferredoxins (281-291 and 326-340 cm^{-1}, respectively), but within the ranges established for $[2Fe\text{-}2S]^{2+}$ clusters with one serinate ligand introduced via site-directed mutagenesis (332-356 cm^{-1} and 289-302 cm^{-1}, respectively) (*28*). Currently, the only known exception is the all-cysteinyl-ligated $[2Fe\text{-}2S]^{2+}$ cluster in human ferrochelatase which has the A_g^t and $B_{3u}{}^t$ Fe-S(Cys) stretching modes at 350 and 295 cm^{-1}, respectively (*28*). In this case, the recent X-ray crystal structure indicates that the anomalous high frequencies of these modes are a consequence of dramatic differences in hydrogen-bonding interactions and cysteinyl Fe-S_γ-C_β-C_α dihedral angles compared to those of ferredoxins (*29*). The resonance Raman data provide only limited information about the number or nature of the noncysteinyl [2Fe-2S] cluster ligands in IscU. However, the Raman spectra argue against ligation by the side-chains of a histidyl and tyrosyl residues. On the basis of studies studies of a Rieske protein (*30*), histidyl ligation would be expected to decrease Fe-S(Cys) stretching frequencies due to the larger effective mass of the imidazole ring and the characteristic Fe^{3+}-tyrosinate vibrational modes (*31*) are not observed. Water/OH^-, serinate, aspartate, and glutamate are the best candidates for oxygenic ligation, although nitrogenic ligation from lysine or the N-terminal amino group cannot be ruled out.

Mössbauer Characterization of the $[2Fe\text{-}2S]^{2+}$ Centers Assembled in IscU. Direct evidence for at least partial noncysteinyl ligation at one of the Fe sites of the $[2Fe\text{-}2S]^{2+}$ clusters in IscU was provided by Mössbauer spectroscopy. Parts A and B of Figure 4 show the 4.2 K Mössbauer spectra recorded in the presence of a weak magnetic field of 50 mT for samples of IscS-reconstituted IscU corresponding to fractions 2 and 3, respectively. The fraction 2 sample corresponds to the EDTA-treated sample described above and characterized by FPLC and absorption in Figures 1 and 2, respectively. The fraction 3 sample contained some unresolved fraction 2 and FPLC analysis of the

concentrated sample used for Mössbauer analysis indicated ~60% of the two $[2Fe\text{-}2S]^{2+}$ clusters per dimer form (fraction 3), ~30% of the one $[2Fe\text{-}2S]^{2+}$ cluster per dimer form (fraction 2), and ~10% of the one $[4Fe\text{-}4S]^{2+}$ cluster per dimer form (fraction 4). The latter presumably formed during the concentration step. The Mössbauer spectra of both samples are very similar and comprise two partially resolved quadrupole doublets.

The spectrum of fraction 2 (Figure 4A) can be least-squares fitted with two quadrupole doublets of equal intensity, indicating the presence of two iron sites with equal concentration but different coordination environments. The results of the fits are plotted as a solid line overlaid with the experimental spectrum (Figure 4A). The parameters obtained for both Fe sites (Table 1) are typical for high-spin ferric ions. The smaller isomer shift, 0.26 mm/s, determined for site 1 is indicative of tetrahedral sulfur coordination (*32*), while the larger isomer shift, 0.32 mm/s, obtained for site 2 suggests the presence of non-sulfur ligands (*33*). The fact that these two high-spin ferric sites exhibit quadrupole-doublet spectra at 4.2 K suggests that either they are associated with an integer-spin system or their electronic relaxations are fast in comparison with the ^{57}Fe nuclear Larmor precession. The latter is rare for high-spin ferric ions at 4.2 K. To distinguish these two situations, we have recorded the spectrum of the fraction 2 at 4.2 K in a parallel applied field of 4 T (Figure 4D). The solid line plotted over the experimental spectrum is a theoretical simulation using the parameters determined for the two doublets and assuming diamagnetism. The agreement between the simulation and experiment indicates that the two iron sites are indeed associated with a diamagnetic system. For the all-ferric Fe-S clusters, diamagnetism is unique to the $[2Fe\text{-}2S]^{2+}$ cluster, of which the two ferric ions are antiferromagnetically coupled to form a diamagnetic ground state (*34*). Consequently, the Mössbauer data presented above confirm that the EDTA-treated IscU sample contains only $[2Fe\text{-}2S]^{2+}$ clusters and indicate the presence of noncysteinyl ligation at one of the iron sites. The only crystallographically defined biological $[2Fe\text{-}2S]^{2+}$ center with noncysteinyl ligation that has been characterized by Mössbauer

spectroscopy is the Rieske protein which has two histidyl ligands on one Fe site (*33*, *35*). Within experimental uncertainties, the Mössbauer parameters obtained for the $[2Fe\text{-}2S]^{2+}$ cluster in IscU are identical to those of the $[2Fe\text{-}2S]^{2+}$ cluster of the Rieske protein (*33*). However, the Mossbauer parameters for the noncysteinyl ligated site are not expected to be sensitive to O or N ligation. Hence, although the resonance Raman data and the lack of two conserved histidine residues in IscU (*13*) argue strongly against a histidyl-ligated Rieske-type center, the Mössbauer data dictate one or two noncysteinyl ligands at one Fe site of the $[2Fe\text{-}2S]^{2+}$ cluster in IscU.

Comparison of panels A and B of Figure 4 shows that the Mössbauer spectra of the forms of IscU with one and two $[2Fe\text{-}2S]^{2+}$ clusters per dimer are the same within experimental error. The only significant difference in the Mössbauer spectra of these samples is a shoulder at ~ 1 mm/s in the predominantly fraction 3 sample (Figure 4B). The position of this shoulder coincides with that of the high-energy line of the $[4Fe\text{-}4S]^{2+}$ cluster that is present in fraction 4 (Figure 4C, see below). Therefore, in accord with the FPLC data, analysis of the Mössbauer spectrum indicates that approximately 10% of the iron absorption can be attributed to a $[4Fe\text{-}4S]^{2+}$ cluster that must have formed during concentration of the sample. The dashed line plotted in Figure 4B is the spectrum of the $[4Fe\text{-}4S]^{2+}$ cluster in fraction 4 normalized to 10% absorption of the experimental spectrum. Removal of this contribution of the $[4Fe\text{-}4S]^{2+}$ cluster from the raw data yielded a spectrum that can be fitted with two quadrupole doublets of equal intensity. Within experimental errors, the parameters obtained from the fit (listed in Table 1) are identical to those of the $[2Fe\text{-}2S]^{2+}$ cluster in fraction 2. The solid line plotted over spectrum B is generated by addition of the $[4Fe\text{-}4S]^{2+}$ spectrum (10%) to the least-squares fit of the $[2Fe\text{-}2S]^{2+}$ spectrum.

Resonance Raman Characterization of the $[4Fe\text{-}4S]^{2+}$ Center Assembled in IscU. Both resonance Raman and Mössbauer studies confirm the characterization of fraction 4 as a homogeneous $[4Fe\text{-}4S]^{2+}$-containing form of IscU. The resonance Raman spectrum

(Figure 3) is uniquely indicative of a $[4Fe\text{-}4S]^{2+}$ center (*36*) and is dominated by the totally symmetric breathing mode of the [4Fe-4S] core at 343 cm^{-1}. Since the resonance enhancement of the Fe-S stretching modes in the Raman spectra of $[2Fe\text{-}2S]^{2+}$ centers is approximately 5-fold greater than for $[4Fe\text{-}4S]^{2+}$ clusters with 457-nm excitation (*36*), the absence of bands indicative of the $[2Fe\text{-}2S]^{2+}$ centers in IscU, shows that fraction 4 is a homogeneous $[4Fe\text{-}4S]^{2+}$-containing form of IscU. Moreover, all the observed bands can be rationally assigned by direct analogy with the detailed vibrational assignments that have been made for model complexes and ferredoxins on the basis of extensive isotope shift data and normal mode calculations (*36*, *37*). The frequency of the totally symmetric breathing mode of the [4Fe-4S] core has been found to be a useful indicator of coordination by a noncysteinyl ligand at a unique Fe site of a $[4Fe\text{-}4S]^{2+}$ cluster (*27*, *38*). The currently observed ranges are 333-339 cm^{-1} for complete cysteinyl ligation and 340-343 cm^{-1} for clusters with OH^-, serinate, or aspartate ligation at a unique Fe site (*27*). By this criterion, the single $[4Fe\text{-}4S]^{2+}$ cluster in IscU is likely to have noncysteinyl ligation at one Fe site, and therefore could be located exclusively within one subunit or bridging subunits using ligands from both subunits.

Mössbauer Characterization of the $[4Fe\text{-}4S]^{2+}$ Center Assembled in IscU The Mössbauer spectrum of fraction 4 recorded at 4.2 K in a parallel magnetic field of 50 mT exhibits a slightly asymmetric quadrupole doublet (Figure 4C). The solid line plotted over the data is the result of a least-squares fit to the data assuming two unresolved quadrupole doublets of equal intensity. The parameters obtained are listed in Table 1 and are typical for $[4Fe\text{-}4S]^{2+}$ clusters (*34*, *39*, *40*). Studies of $[4Fe\text{-}4S]^{2+}$ model compounds with tetrahedral coordinate Fe sites having mixed terminal ligands (thiophenolate and/or phenolate) indicate that the Mössbauer parameters are relatively insensitive to the nature of the ligand type (*41*). Figure 4E shows a spectrum of this sample recorded at 4.2 K in a parallel field of 4 T. The solid line plotted over the experimental spectrum is a theoretical simulation using the parameters obtained from the least-squares fit of the weak-field

spectrum and assuming diamagnetism. The agreement between the experiment and simulation indicates that the cluster has a diamagnetic ground state as expected for a $[4Fe\text{-}4S]^{2+}$ cluster.

DISCUSSION

Our working hypothesis for Fe-S cluster biosynthesis is that the IscU protein provides a scaffold for IscS-directed assembly of clusters that can be inserted intact into apo forms of Fe-S cluster-containing proteins, possibly via other associated carrier proteins (*11, 12*). While intact cluster transfer from IscU has yet to be demonstrated, this hypothesis is further supported by the ability of IscU to accommodate both $[2Fe\text{-}2S]^{2+}$ and $[4Fe\text{-}4S]^{2+}$ clusters as evidenced by the UV-visible absorption, resonance Raman, and Mössbauer studies presented herein. Moreover, it is clear that IscS-mediated cluster assembly in IscU proceeds in sequential steps involving well-defined forms of IscU containing one $[2Fe\text{-}2S]^{2+}$ cluster per dimer, two $[2Fe\text{-}2S]^{2+}$ clusters per dimer, and one $[4Fe\text{-}4S]^{2+}$ cluster per dimer. The rates at which these individual species appear are critically dependent on the IscU:IscS ratio, and the reaction proceeds rapidly to yield the $[4Fe\text{-}4S]^{2+}$ cluster form in less than 1 h when a 1:1 IscU:IscS ratio is used. IscU and IscS have been shown to form a 1:1 complex (*12*). However, it is clearly premature to draw any conclusions concerning which of the cluster-containing forms of IscU that can be produced *in vitro*, are physiologically relevant.

The $[2Fe\text{-}2S]^{2+}$ clusters in both the one- and two- $[2Fe\text{-}2S]^{2+}$cluster-containing forms of IscU have been shown by the combination of UV-visible absorption, resonance Raman, and Mössbauer spectroscopies to have very similar protein environments with at least one and possibly two oxygen (nontyrosyl) or nitrogen (nonhistidyl) ligands at one Fe site. Since IscU has three conserved cysteine residues, each subunit can therefore accommodate one $[2Fe\text{-}2S]^{2+}$ cluster. However, the possibility that both $[2Fe\text{-}2S]^{2+}$ clusters bridge subunits cannot be excluded at this stage, and the observation that one of the two $[2Fe\text{-}2S]^{2+}$ clusters is selectively removed by EDTA treatment clearly merits

further investigation. The ligation and subunit location of the $[4Fe\text{-}4S]^{2+}$ cluster in IscU are less well defined. The resonance Raman properties are best interpreted in terms of three cysteinyl ligands and one oxygenic ligand, but the possibility of complete cysteinyl ligation with anomalous Fe-S vibrational frequencies resulting from differences in H-bonding and/or Fe-S_γ-C_β-C_α dihedral angles compared to those of other biological $[4Fe\text{-}4S]^{2+}$ centers, cannot be ruled out. In either case, the single $[4Fe\text{-}4S]^{2+}$ cluster in IscU could be located within one subunit or bridging between subunits.

The results also offer some insight into the mechanism of assembly of a [4Fe-4S] cluster in IscU. The conversion of the form of IscU containing two $[2Fe\text{-}2S]^{2+}$ clusters per dimer to the form containing one $[4Fe\text{-}4S]^{2+}$ cluster per dimer occurs in the absence of apoprotein and without an increase in the level of the apoprotein fraction (fraction 1) or the one- $[2Fe\text{-}2S]^{2+}$cluster-containing fraction (fraction 2). Furthermore, it is not accompanied by the appearance of an IscU fraction containing one $[2Fe\text{-}2S]^{2+}$ and one $[4Fe\text{-}4S]^{2+}$ cluster or two $[4Fe\text{-}4S]^{2+}$ clusters. These observations argue against mechanisms for $[4Fe\text{-}4S]^{2+}$ cluster assembly involving degradation of $[2Fe\text{-}2S]^{2+}$ clusters and reassembly of a $[4Fe\text{-}4S]^{2+}$ cluster in apo IscU or building onto individual $[2Fe\text{-}2S]^{2+}$ clusters. Rather, the data are most consistent with a concerted [4Fe-4S] cluster assembly process with reductive conversion of two $[2Fe\text{-}2S]^{2+}$ clusters to one $[4Fe\text{-}4S]^{2+}$ cluster. Reductive coupling of two $[2Fe\text{-}2S]^{2+}$ clusters has long been known to be a viable approach for synthesizing $[4Fe\text{-}4S]^{2+}$ clusters in aprotic media (*42*). The work presented here provides the first evidence that this type of chemistry might be used in a general pathway of $[4Fe\text{-}4S]^{2+}$ cluster biosynthesis.

ACKNOWLEDGMENTS

We thank Chad Williamson for technical help in the purification of proteins and Marly Eidsness in the BioXpress Laboratory at the University of Georgia for providing the mono-Q column and for advice on separating protein fractions. This work was supported by the National Science Foundation (MCB9630127 to D.R.D.), the National

Institutes of Health (GM51962 to M.K.J. and GM47295 to B.H.H), and by a National Science Foundation Research Training Group Award to the Center for Metalloenzyme Studies (DBI9413236)

REFERENCES

1. Beinert, H., Holm, R. H., and Münck, E. (1997) *Science 277*, 653-659.
2. Johnson, M. K. (1998) *Curr. Opin. Chem. Biol. 2*, 173-181.
3. Beinert, H., and Kiley, P. J. (1999) *Curr. Opin. Chem. Biol. 3*, 152-157.
4. Beinert, H. (2000) *J. Biol. Inorg. Chem.* 5, 2-15.
5. Dean, D. R., Bolin, J. T., and Zheng, L. (1993) *J. Bacteriol. 1756*, 6737-6744.
6. Zheng, L., and Dean, D. R. (1994) *J. Biol. Chem. 269*, 18723-18726.
7. Zheng, L., White, R. H., Cash, V. L., Jack, R. F., and Dean, D. R. (1993) *Proc. Natl. Acad. Sci. U.S.A. 90*, 2754-2758.
8. Zheng, L., White, R. H., Cash, V. L., and Dean, D. R. (1994) *Biochemistry 33*, 4714-4720.
9. Fu, W., Jack, R. F., Morgan, T. V., Dean, D. R., and Johnson, M. K. (1994) *Biochemistry 33*, 13455-13463.
10. Agar, J. N., Yuvaniyama, P., Jack, R. F., Cash, V. L., Smith, A. D., Dean, D. R., and Johnson, M. K. (2000) *J. Biol. Inorg. Chem. 5*, 167-177.
11. Yuvaniyama, P., Agar, J. N., Cash, V. L., Johnson, M. K., and Dean, D. R. (2000) *Proc. Natl. Acad. Sci. U.S.A. 97*, 599-604.
12. Agar, J. N., Zheng, L., Cash, V. L., Dean, D. R., and Johnson, M. K. (2000) *J. Am. Chem. Soc. 122*, 2136-2137.
13. Zheng, L., Cash, V. L., Flint, D. H., and Dean, D. R. (1998) *J. Biol. Chem. 273*, 13264-13272.
14. Flint, D. H. (1996) *J. Biol. Chem. 271*, 16068-16074.
15. Fujii, T., Maeda, M., Mihara, H., Kurihara, T., Esaki, N., and Hata, Y. (2000) *Biochemistry 39*, 1263-1273.

16. Kaiser, J. T., Clausen, T., Bourenkow, G. P., Bartunik, H.-D., Steinbacher, S., and Huber, R. (2000) *J. Mol. Biol. 297*, 451-464.

17. Hwang, D. M., Dempsey, A., Tan, K. T., and Liew, C. C. (1996) *J. Mol. Evol. 43*, 536-540.

18. Kispal, G., Csere, P., Prohl, C., and Lill, R. (1999) *EMBO J. 18*, 3981-3989.

19. Schilke, B., Voisine, C., Beinert, H., and Craig, E. (1999) *Proc. Natl. Acad. Sci. U.S.A. 96*, 10206-10211.

20. Strain, J., Lorenz, C. R., Bode, J., Garland, S., Smolen, G. A., Ta, D. T., Vickery, L. E., and Culotta, V. C. (1998) *J. Biol. Chem. 273*, 31138-31144.

21. Land, T., and Rouault, T. A. (1998) *Mol. Cell 2*, 807-815.

22. Smith, P. K., Krohn, R. L., Hermanson, G. T., Mallia, A. K., Gartner, F. H., Provenzano, M. D., Fujimoto, E. K., Goeke, N. M., Olson, B. J., and Klenk, D. C. (1985) *Methods Enzymol. 226*, 199-232.

23. Ravi, N., Bollinger, J. M., Jr., Huynh, B. H., Stubbe, J., and Edmondson, D. E. (1994) *J. Am. Chem. Soc. 116*, 8007-14.

24. Fawcett, S. E. J., Davis, D., Breton, J. L., Thomson, A. J., and Armstrong, F. A. (1998) *Biochem. J. 335*, 357-368.

25. Dailey, H. A., Finnegan, M. G., and Johnson, M. K. (1994) *Biochemistry 33*, 403-407.

26. Johnson, M. K., Robinson, A. E., and Thomson, A. J. (1982) in *Iron-Sulfur Proteins* (Spiro, T. G., Ed) pp 367-406, Wiley-Interscience, New York.

27. Brereton, P. S., Duderstadt, R. E., Staples, C. S., Johnson, M. K., and Adams, M. W. W. (1999) *Biochemistry 38*, 10594-10605.

28. Crouse, B. R., Sellers, V. M., Finnegan, M. G., Dailey, H. A., and Johnson, M. K. (1996) *Biochemistry 35*, 16222-16229.

29. Wu, C.-K., Dailey, H. A., Rose, J. P., Burden, A., and Wang, B.-C. (2000) *Nature Struct. Biol.*, (in press).

30. Kuila, D., Schoonover, J. R., Dyer, R. B., Batie, C. T., Ballou, D. P., Fee, J. A., and Woodruff, W. H. (1992) *Biochim. Biophys. Acta 1140*, 175-183.

31. Que, L., Jr. (1988) in *Biological Applications of Raman Spectroscopy. Vol. 3: Resonance Raman Spectra of Heme and Metalloproteins* (Spiro, T. G., Ed.) pp 491-521, Wiley-Interscience, New York.

32. Yoo, S. J., Angove, H. C., Burgess, B. K., Hendrich, M. P., and Münck, E. (1999) *J. Am. Chem. Soc. 121*, 2534-2545.

33. Fee, J. A., Findling, K. L., Yoshida, T., Hille, R., Tarr, G. E., Hearshen, D. O., Dunham, W. R., Day, E. P., Kent, T. A., and Münck, E. (1984) *J. Biol. Chem. 259*, 124-133.

34. Trautwein, A. X., Bill, E., Bominaar, E. L., and Winkler, H. (1991) *Struct. Bonding 78*, 1-95.

35. Iwata, S., Saynovits, S., Link, T. A., and Michel, H.(1996) *Structure 4*, 567-579.

36. Spiro, T. G., Czernuszewicz, R. S., and Han, S. (1988) in *Biological Applications of Raman Spectroscopy. Vol. 3: Resonance Raman Spectra of Heme and Metalloproteins* (Spiro, T. G., Ed.) pp 523-554, Wiley-Interscience, New York.

37. Czernuszewicz, R. S., Macor, K. A., Johnson, M. K., Gewirth, A., and Spiro, T. G. (1987) *J. Am. Chem. Soc. 109*, 7178-7187.

38. Conover, R. C., Kowal, A. T., Fu, W., Park, J.-B., Aono, S., Adams, M. W. W., and Johnson, M. K. (1990) *J. Biol. Chem. 265*, 8533-8541.

39. Middleton, P., Dickson, D. P. E., Johnson, C. E., and Rush, J. D. (1978) *Eur. J. Biochem. 88*, 135-41.

40. Middleton, P., Dickson, D. P. E., Johnson, C. E., and Rush, J. D. (1980) *Eur. J. Biochem. 104*, 289-96.

41. Kanatzidis, M. G., Baenziger, N. C., Coucouvanis, D., Simopoulos, A., and Kostikas, A (1984) *J. Am. Chem. Soc. 106*, 4500-4511.

42. Hagen, K. S., Reynolds, J. G. and Holm, R. H. (1981) *J. Am. Chem. Soc. 103*, 4054-4063.

Table 6-4 Mössbauer parameters at 4.2 K for the Fe-S clusters assembled in IscU

sample	cluster type	fe site	δ (mm/s)	ΔE_Q (mm/s)	η
fraction 2 [a]	$[2Fe\text{-}2S]^{2+}$	1	0.26 ± 0.03	0.64 ± 0.05	1.0
		2	0.32 ± 0.03	0.91 ± 0.05	0.7
fractions 2 & 3 [b]	$[2Fe\text{-}2S]^{2+}$	1	0.27 ± 0.02	0.66 ± 0.04	1.0
		2	0.32 ± 0.02	0.94 ± 0.04	0.7
fraction 4	$[4Fe\text{-}4S]^{2+}$	pair 1[c]	0.44 ± 0.02	0.98 ± 0.04	0.3
		pair 2[c]	0.45 ± 0.02	1.23 ± 0.04	0.7

[a] Homogeneous fraction 2 prepared by EDTA treatment of a combined sample of fractions 2 and 3 described in the text

[b] On the basis of FPLC and Mössbauer analysis of this sample fractions 3, 2, and 4 contribute 71, 18, and 11% to the total Mössbauer absorption, respectively. See the text for further details.

[c] $[4Fe\text{-}4S]^{2+}$ clusters may be considered to comprise of two valence-delocalized Fe(II)Fe(III) pairs.

Figure 6-1 Anaerobic FPLC analysis of the reaction mixture during IscS-mediated cluster assembly in IscU. Samples taken at selected time intervals after addition of 4 mM L-cysteine to the reaction mixture were loaded on a mono-Q column, eluted with a 0.1-0.4 M NaCl gradient and monitored by absorption at 280 nm. Each trace is aligned in a stack plot based on the conductivity of the eluting fraction. A. Reaction mixture: 370 µM IscU, 0.8 µM IscS, 1.85 mM ferric ammonium citrate and 4 mM β-mercaptoethanol. Conductivity range:156-193 mM NaCl. The trace labeled EDTA-treated corresponds to a sample in which fractions 2 and 3 were combined and treated with a 20-fold excess of EDTA for 10 min before being reloaded on to the column. B. Reaction mixture: 140 µM IscU, 5.0 µM IscS, 0.7 mM ferric ammonium citrate and 4 mM β-mercaptoethanol. Conductivity range: 131-350 mM NaCl.

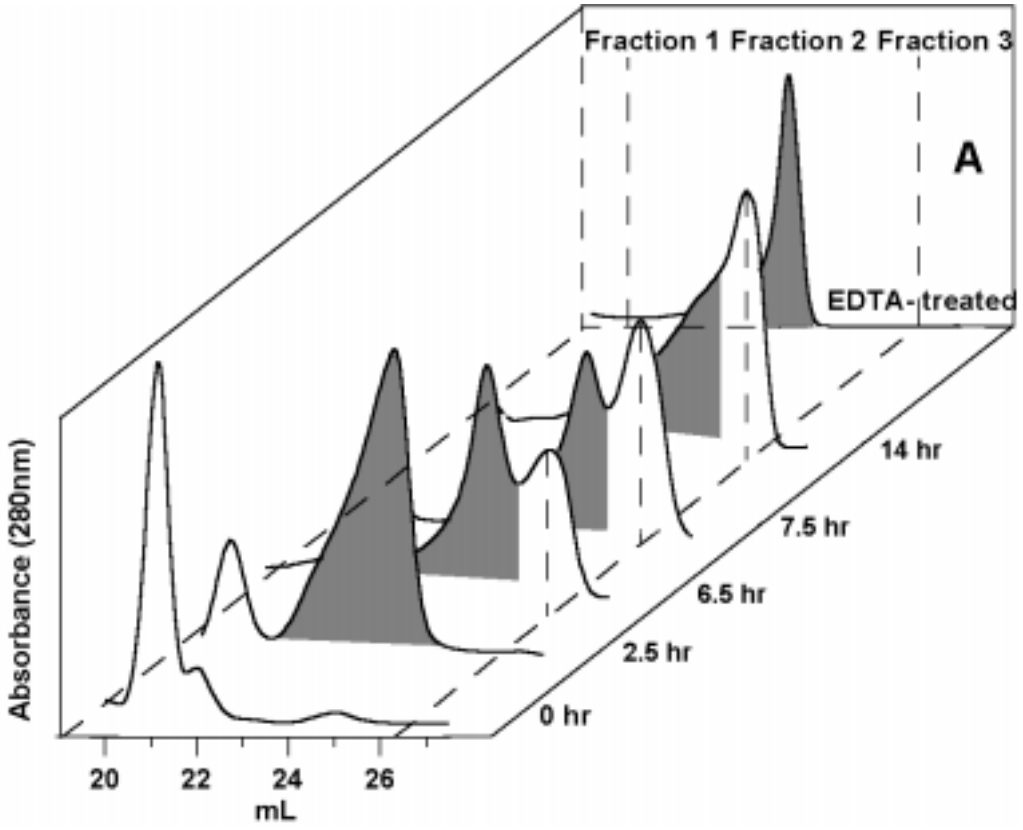
Fraction 1 Fraction 2 Fraction 3
A
EDTA-treated
14 hr
7.5 hr
6.5 hr
2.5 hr
0 hr
Absorbance (280nm)
20
22
24
26
mL

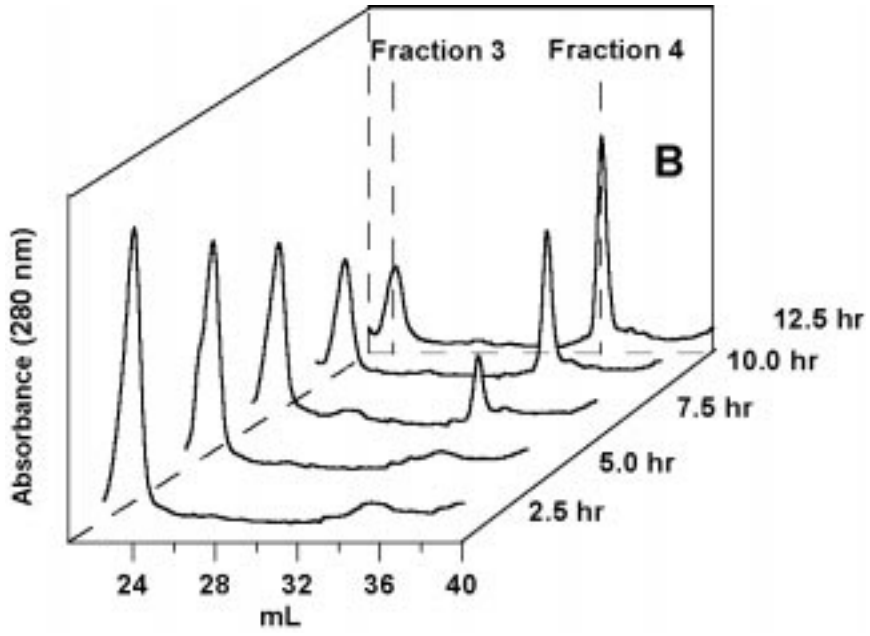
Fraction 3
Fraction 4
B
12.5 hr
10.0 hr
7.5 hr
5.0 hr
2.5 hr
Absorbance (280 nm)
24
28
32
36
40
mL

FIGURE 6-2 UV-visible absorption spectra of Fe-S cluster-containing IscU samples. *Upper panel*: fraction 2 (dash line); fraction 3 (thick line); EDTA-treated (thin line). *Lower panel*: Fraction 4. The samples used are defined in Figure 1.

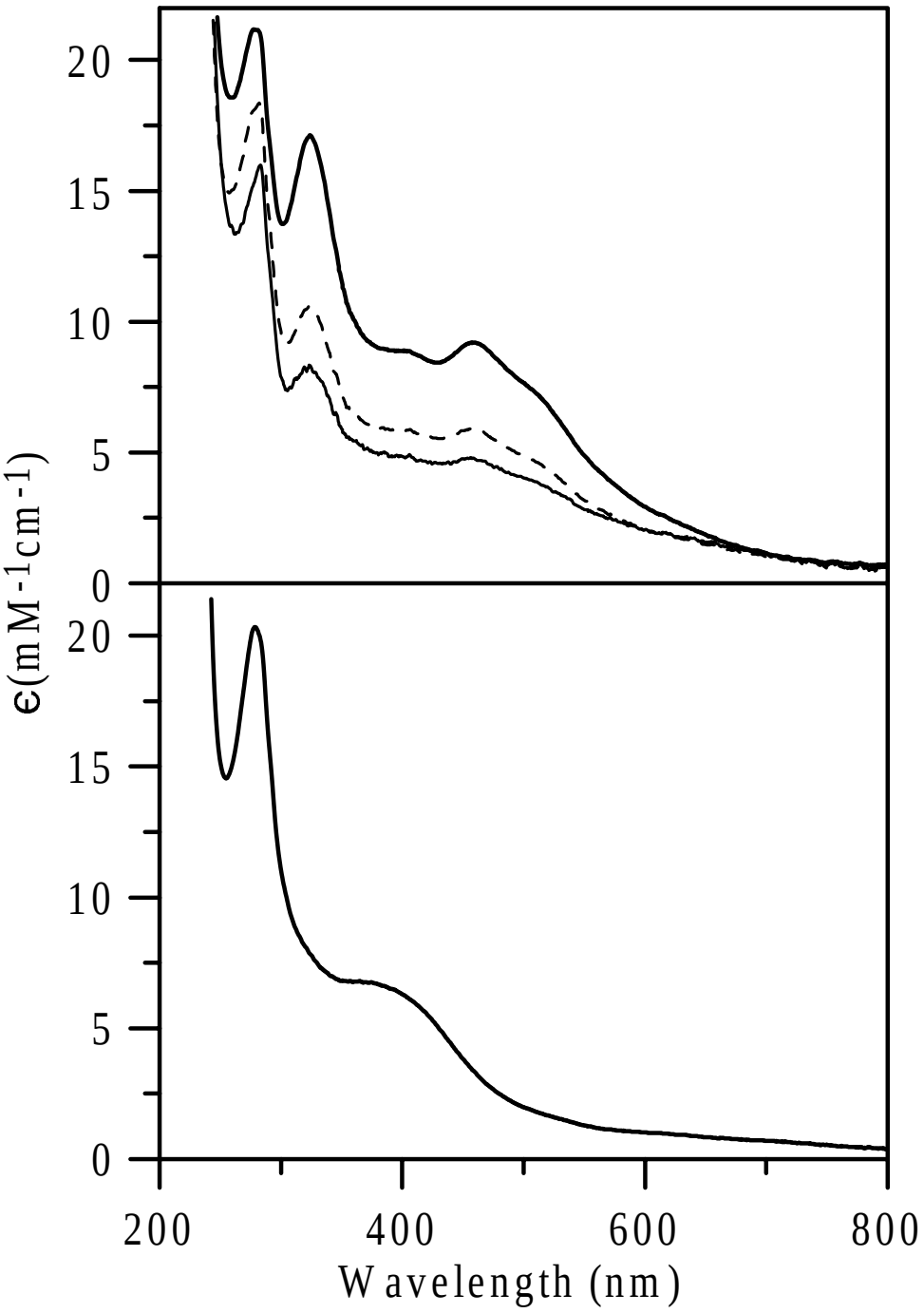
20
15
10
5
0
20
15
10
5
0
ϵ(mM-1cm-1)
200
400
600
800
Wavelength (nm)

FIGURE 6-3 Low-temperature resonance Raman spectra of Fe-S cluster-containing IscU samples. The samples corresponding to fractions 2, 3, and 4 are defined in Figure 1 and were concentrated to ~ 2 mM in IscU monomer prior to freezing a 10 µl droplet on the cold finger of a Displex unit at 17 K. The spectra were recorded using 457-nm excitation with 100-mW of laser power at the sample. Each spectrum is the sum of 100 scans, with each scan involving photon counting for 1 s at 1-cm^{-1} increments, with 6 cm^{-1} resolution. Bands due to lattice modes of the frozen buffer solution have been subtracted from all spectra.

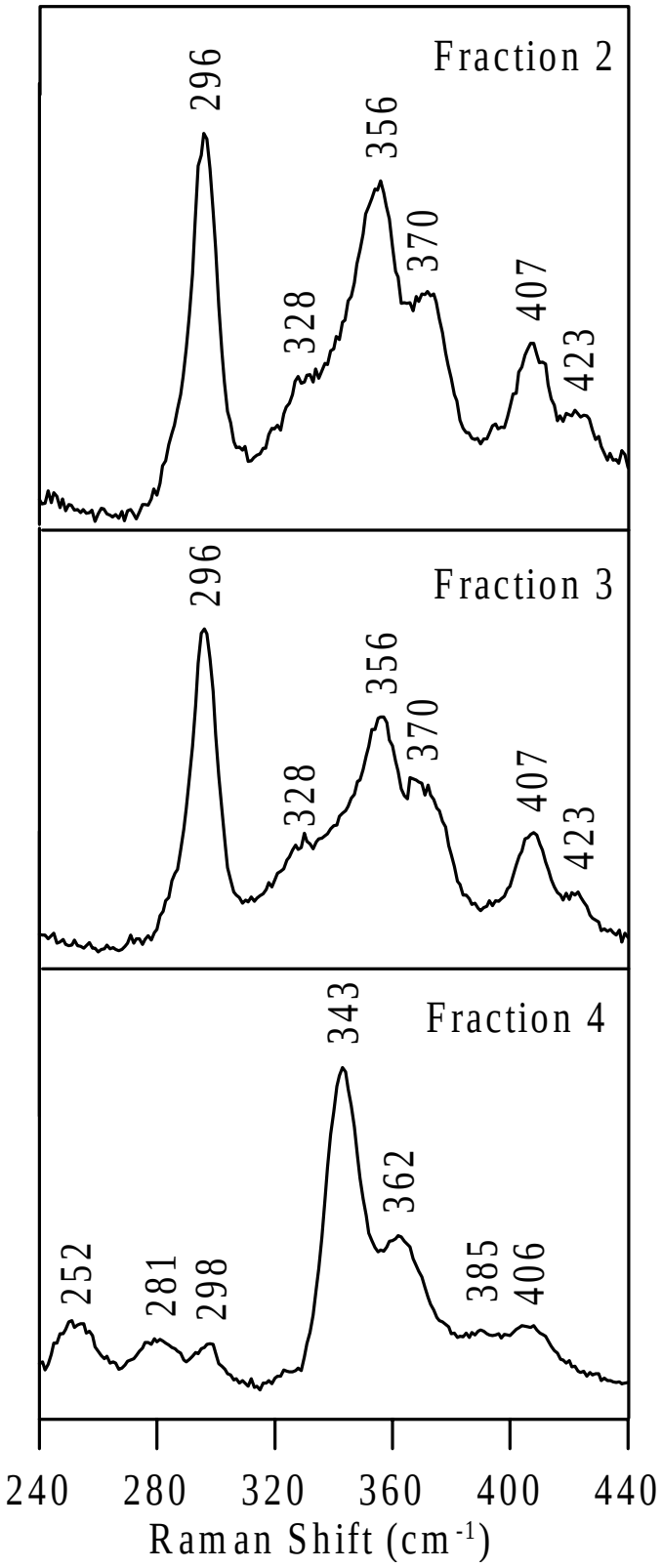
Fraction 2
296
328
356
370
407
423
Fraction 3
296
328
356
370
407
423
Fraction 4
252
281
298
343
362
385
406
240
280
320
360
400
440
Raman Shift (cm-1)

FIGURE 6-4 Mössbauer spectra of Fe-S cluster-containing IscU samples: EDTA-treated (A and D), non-EDTA-treated (B), and fraction 4 (C and E). The spectra were recorded at 4.2 K in a field of 50 mT (A, B, and C) or 4 T (D and E) applied parallel to the γ-beam. The dash line in B is spectrum C normalized to 10% of the total absorption area of spectrum B. The solid lines are either least-squares fits or theoretical simulations that have been described in text.

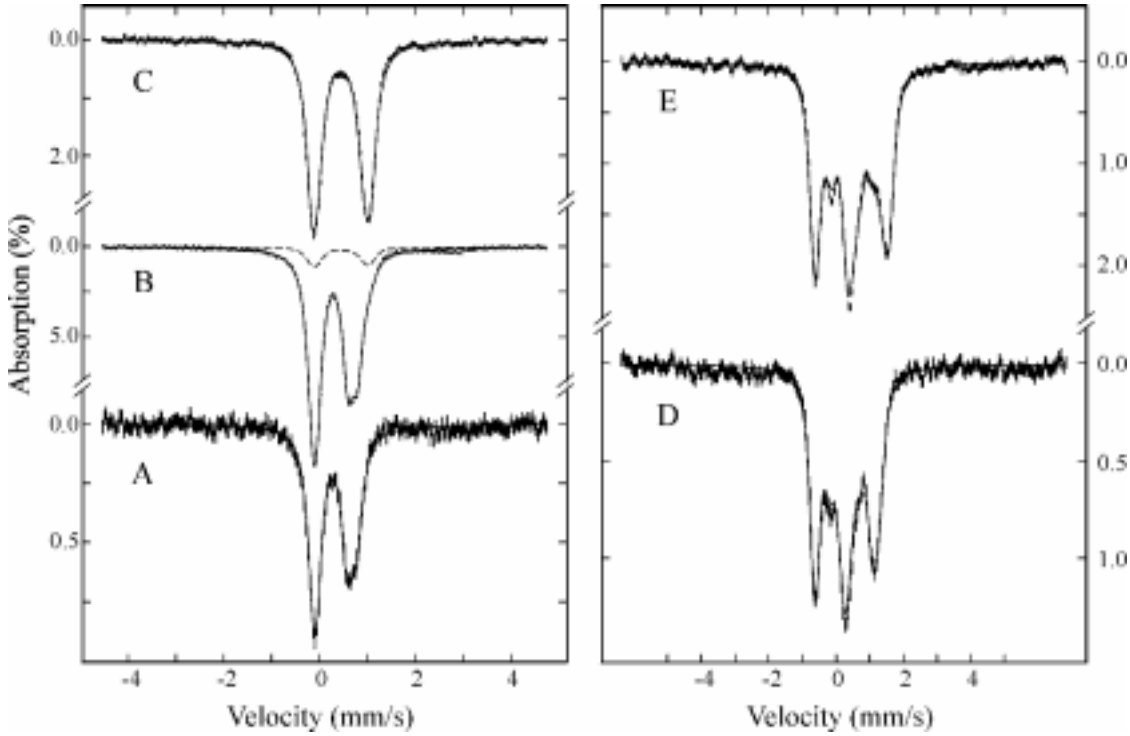
Absorption (%)
0.0
2.0
0.0
5.0
0.0
0.5
C
B
A
-4
-2
0
2
4
Velocity (mm/s)
E
D
0.0
1.0
2.0
0.0
0.5
1.0
-4
-2
0
2
4
Velocity (mm/s)

Chapter VII

Conclusions and Future Work:

The papers presented herein provide evidence that two proteins, NifU and IscU, are capable of assembling Fe-S clusters with properties that separate them from hitherto characterized clusters. The properties of oxidative and reductive lability, as well as the propensity of the $[Fe_2S_2]^{2+}$ clusters to reductively couple, forming $[Fe_4S_4]^{2+}$ clusters, are consistent with clusters which are built not for the purpose of serving in redox or catalytic roles, but to be transferred. *In vivo* evidence which supports the *in vitro* cluster assembly findings was presented for D37A NifU-1, where a $[Fe_2S_2]^{2+}$ cluster is present in the as-purified protein. NifEN was shown to be an $\alpha 2\beta 2$ heterotetramer which contains two, subunit bridging, $[Fe_4S_4]^{2+,1+}$ clusters per heterotetramer.

Both IscU and NifU are capable of serving as scaffolds for the assembly of transient cluster, and future experiments must assess the physiological significance of this ability. The transfer of an intact cluster from IscU or NifU and into another protein is of utmost importance in this regard. It has long been known that model Fe-S clusters can undergo ligand substitution reactions in which stoichiometric loss of one ligand occurs concomitant to the gain of another ligand (70). Any *intact* cluster transfer between IscU and another protein must involve a similar mechanism. The fact that IscU $[Fe_2S_2]$ cluster is released reductively, taken together with the mechanistic requirement for the substitution of IscU cysteines with those of an apoprotein, lead to the prospect of reduction mediated, ligand exchange as the mechanism of iron-sulfur cluster transfer. If such a process occurs, the noncysteinyl IscU cluster ligands identified in chapter V are surely significant, and would tend to have a decreased affinity towards ferrous, as opposed to ferric iron. Indeed, Lippard has synthesized a bridged di-iron complex, albeit without sulfur ligands, in which the μ-oxo bridges fall apart upon reduction (140). A reversible, reduction based, 12Å translocation of iron from a site with oxygenic ligands to a site with softer nitrogen ligands

has also been characterized (141) Assessing whether a cluster is transferred intact, or as the result of breakdown of the cluster into its components followed by reassembly into an apoprotein (142), will be a daunting task. Attempts will be made to fully load IscU and NifU with isotopically labeled iron-sulfur clusters, and then to transfer clusters in a solution with excess, natural abundance iron. This process can be monitored by using radioactive ^{55}Fe, or by using ^{57}Fe in conjunction with Mössbauer. Creating and characterizing an Fe-S cluster bound form of *wildtype* NifU, has yet to be achieved and is a necessary step if NifU is to be used as a cluster done. Mössbauer studies of a cluster-bound form of NifU are now underway.

Whole-cell Mössbauer studies of overexpressed IscU or NifU may also provide insight into physiological intermediates and will be pursued. The structures, obtained either by crystallography or NMR are also fundamental to understanding these proteins, and will be the focus of future study. The development of a kinetic assay of cluster assembly upon IscU, should provide valuable insight into the mechanism of the reactions of iron, cysteine, IscU, and IscS. Finally, the mutation of conserved amino acids, an integral part of any structure function study, began with the D37A mutant described in chapter III, and must continue.

Although NifU and IscU are both involved in the process of Fe-S cluster assembly and share considerable homology, these proteins may not function in exactly the same way. In *A. vinelandii*, NifU is responsible for the assembly of the higher nuclearity P-cluster and $[Fe_4S_4]^{2+,1+}$ cluster of the nitrogenase component proteins(113;129). The *isc* genes in contrast, have been shown to aid in the formation of $[Fe_2S_2]^{2+,1+}$ clusters in a number of different ferredoxins(143;144), and can also aid in the formation of the higher nuclearity nitrogenase clusters (111;115). Furthermore, NifU and NifU-1 can bind Fe(III) in a stable, rubredoxin-like environment at low temperatures, whilst IscU cannot. Mössbauer studies of the Fe-S cluster(s) formed upon NifU should provide valuable insight into the nature and ligands of the clusters formed upon NifU.

After IscS and IscU, there remain four genes that are in the *isc* operon which do not have obvious homology to characterized proteins or a known function. The genes products of *orf1*, *orf2*, *orf3*, and *iscA* remain to be characterized, and will provide a fascinating area of study. Orf2 has a DNA binding motif, and enough cysteines to assemble a regulatory Fe-S cluster, as with the iron-regulator proteins (31;145). In future publications, this gene will be referred to as *IscR*, to denote its involvement in the regulatory process. Assessing the role of the putative iron-sulfur cluster in the regulatory process will be an active area of research.

Further studies with NifEN will parallel those presented for IscU and NifU, by trapping and characterizing FeMoCofactor assembly intermediates upon NifEN. Unlike the *isc* proteins, which can assemble clusters into a variety of apoproteins, NifEN has only one, very specific task- to aid in the maturation, and perhaps insertion, of the nitrogenase FeMo cofactor. The parallels and differences in the specific and non-specific Fe-S cluster assembly proteins will provide an interesting area of research.

References for **conclusions and future** work are on pages 12-25.